Superfluides fermioniques

Xavier Leyronas

HAL Id: tel-00371713

https://theses.hal.science/tel-00371713

Submitted on 30 Mar 2009

Université Pierre et Marie Curie

Laboratoire de Physique Statistique
Département de Physique
de l'Ecole Normale Supérieure

Superfluides fermioniques

Thèse d'Habilitation à diriger des recherches
de l'Université Pierre et Marie Curie

présentée par
Xavier LEYRONAS

Soutenance le 23 Septembre 2008 devant le jury composé de :

Prof. Claude ASLANGUL	Président
Prof. Roland COMBESCOT	Invité
Prof. Stefano GIORGINI	Examinateur
Dr. Thierry JOLICOEUR	Rapporteur
Dr. Peter SCHUCK	Rapporteur
Prof. Giancarlo STRINATI	Rapporteur

CURRICULUM VITAE
LEYRONAS Xavier
né le 31 Mars 1969

Situation familiale : vit en concubinage, deux enfants

Fonction : depuis le 1er Septembre 1999 :
Maître de Conférences à l'Université Pierre et Marie Curie (Paris VI), 28eme section.

Laboratoire de recherche : Laboratoire de Physique Statistique ,
Ecole Normale Supérieure, 24 rue Lhomond , 75231 Paris Cedex 05.
Equipe : théorie de la matière condensée.

Titres universitaires :
Docteur de l'Université Pierre et Marie Curie en Physique, 6 Janvier 1997.

Titre de la thèse : *Longueur de London et symétrie du paramètre d'ordre dans les cuprates supraconducteurs : aspects théoriques.*

Directeur de thèse : Roland COMBESCOT.

Formation et diplômes :
Septembre 1997-Septembre 1999 : séjour Post-doctoral à l'Université de Leyde, dans le groupe de Carlo BEENAKKER.

Avril 1997-Juillet 1997 : Séjour Post-doctoral à l'Université de Bayreuth, en collaboration avec Dierk RAINER.

Juin 1993 : D.E.A de Physique Quantique de l'Université Paris VI, mention Bien.

Février 1992-Juillet 1992 : Stage de Magistère au département de Physique de l'Ohio State University. Responsable : A. EPSTEIN.

Sujet : *Absorption de la lumière photo-induite dans des polymères.*

1992 : Maîtrise de Physique au Magistère Interuniversitaire de Physique (MIP).

1991 : Licence de Physique au Magistère Interuniversitaire de Physique

1990-1994 : Elève de l'Ecole Normale Supérieure, option Physique

Participation à des conférences avec et sans communication scientifique :

Octobre 1993 : GDR CNRS "Supraconducteurs", Chichilianne

26-28 Septembre 1994 : GDR CNRS *Supraconducteurs*, Colloque *" Interaction des supraconducteurs avec le champ électromagnétique"*, Nice. Présentation orale. Titre : profondeur de pénétration du champ magnétique en couplage fort.

Janvier 1995 : GDR CNRS "Supraconducteurs et fermions corrélés", Les Arcs

Juin 1995 : GDR CNRS *Fermions corrélés*, Aussois. Présentation d'un poster. Titre : Couplage entre plans et chaînes dans $YBa_2Cu_3O_7$: une solution possible pour la symétrie du paramètre d'ordre.

Septembre 1996 : GDR CNRS "Supraconducteurs", Caen

7-14 Août 1996 : *XXI International Conference on Low Temperature Physics in Prague.* Présentation d'un poster. Titre : Impurity effect on T_c in the coupled Plane-Chain model $YBa_2Cu_3O_7$.

25-31 Octobre 1997 : "Strong Interaction in Quantum Dots", Israël.

Décember 1997 : Conférence Wetenschappelijke Vergadering Werkgemeenschap voor de Gecondenseerde Materie, Veldoven, Pays-Bas.

Mai 1998 : Conférence TMR "Phase-Coherent Dynamics in Hybrid Nanostructures", Ioannina, Grèce. Présentation orale. Titre : Non-Cayley tree model for quasiparticle decay in a quantum dot.

Décembre 1998 : Conférence Wetenschappelijke Vergadering Werkgemeenschap voor de Gecondenseerde Materie, Veldoven, Pays-Bas, présentation d'un poster. Titre : quasiparticle lifetime in a quantum dot.

Janvier 1999 Conférence "Quantum Physics at mesoscopic scale", les Arcs. Présentation orale. Titre : Non-Cayley tree model for quasiparticle decay in a quantum dot.

Mars 2001 : Journées de la matière condensée-Paris Centre
Séminaire "Le rapport gap sur température critique dans les supraconducteurs "ondes d".

Août 2002 : Low Temperature Physics 23- Hiroshima (Japon)
Présentation du poster "Equation of state from hydrodynamic modes in dense trapped ultracold gases"

Mars 2004 : Workshop on ultracold Fermi gases, Levico (Italie)
Présentation du poster : "Momentum distribution of a gas of ultracold interacting fermions"

Septembre 2005 : ESF Research Conference on Bose Einstein Condensation, San Feliu de Guixols (Espagne) Présentation de deux posters :
"Equation of state and collective frequencies of a trapped Fermi gas along the BEC-unitarity crossover"
"Bound states of three and four resonantly interacting particles"

Juillet 2006 : 15th International Laser Physics Workshop (LPHYS'06), Lausanne, Suisse
Présentation orale. Titre : "Exact diagrammatic approach for dimer-dimer scattering and bound states of three and four resonantly interacting particles"

Juillet 2007 : 14th Confererence "Recent Progress in Many Body Theory", Barcelone, Espagne.
Présentation du poster : "Superfluid equation of state of dilute composite bosons"

Juillet 2008 : 17th International Laser Physics Worshop (LPHYS'08), Trondheim, Norvège
Présentation orale. Titre : "Superfluid equation of state of dilute composite bosons or how to include 3 and 4-body problem in the *many*body problem"

Juillet 2008 : Workshop on supersolids, Les Treilles, Tourtour, France
Présentation orale. Titre : "Superfluid equation of state of dilute composite bosons or how to include 3 and 4-body problem in the *many*body problem"

Séminaires :

– Janvier 1996 : Journées de Physique Statistique
– Décembre 1996 : Laboratoire de Physique des Solides, Orsay,
  Séminaire : Couplage Plan-Chaîne dans $YBCO$.
– Mars 1997 : visite de Laboratoires aux Etats-Unis. Séminaires :
  5 Mars : Université d'Urbana Champaign
  6 Mars : Université de Northwestern à Evanston
  7 Mars : Laboratoire National à Argonne
  11 Mars : Université de Rochester
– Avril 1997 : séminaire au Laboratoire de Physique de Bayreuth (Bavière).
– Mai 1997 : séminaire à l'Instituut Lorentz, Leyde (Pays-Bas).
– Juin 1997 : séminaire à l'Université d'Augsburg (Bavière).
– Janvier 1999 Séminaire au Laboratoire de Physique Statistique de l'Ecole Normale Supérieure, Paris. Titre : durée de vie d'un électron dans une boîte quantique.
– Mars 1999 Séminaire au Laboratoire de Physique Théorique et Modèles Statistiques, Orsay. Titre : durée de vie d'un électron dans une boîte quantique.
– Mars 2001 : Journées de la matière condensée-Paris Centre
  Séminaire "Le rapport gap sur température critique dans les supraconducteurs "ondes d".
– Octobre 2003 "Modes hydrodynamiques dans les gaz ultrafroids"
  Séminaire du Laboratoire de Physique Statistique de l'Ecole Normale Supérieure, Paris.
– Septembre 2004 : Journées du Laboratoire de Physique Statistique de l'ENS
  Présentation orale courte (10 minutes) :
  Titre : "Modes collectifs dans le crossover condensat de Bose / superfluide BCS"
– Octobre 2005 "Condensats de molécules et superfluides BCS dans les gaz fermioniques ultrafroids"
  Séminaire du Laboratoire de Physique Statistique de l'Ecole Normale Supérieure, Paris.
– Décembre 2005 "Condensats de molécules et superfluides BCS dans les gaz fermioniques ultrafroids"
  Séminaire théorique du vendredi, maison des Magistères, Grenoble.
– Janvier 2006 "Condensats de dimères dilués"
  Journées de Physique Statistique, Paris
– Septembre 2007 "Condensats de dimères dilués"
  Séminaire théorie de la matière condensée de l'ENS.
– Juin 2008 : Journées du Laboratoire de Physique Statistique de l'ENS
  Présentation orale (30 minutes) :
  Titre : "L'activité théorie de la matière condensée au LPS "

Liste des publications :

Articles :

1. R. Combescot and X. Leyronas
   Coupling between Planes and Chains in $YBa_2Cu_3O_7$:
   A Possible Solution for the Order Parameter Controversy
   Phys. Rev. Lett. **75** (1995) 3732-3735.

2. X. Leyronas and R. Combescot
   London penetration depth of strongly coupled superconductors : Low-temperature
   behavior
   Phys. Rev. B **54** (1996) 3482-3488.

3. R. Combescot and X. Leyronas
   Plane-Chain coupling in $YBa_2Cu_3O_7$:
   Impurity effect on the critical temperature
   Phys. Rev. B **54** (1996) 4320-4330.

4. X. Leyronas and R. Combescot
   Plane-Chain coupling in $YBa_2Cu_3O_7$:
   Temperature dependence of the Penetration Depth
   Physica C 290 (1997) 215-228

5. X. Leyronas, J. Tworzydło and C. W. J. Beenakker
   Non-Cayley tree model for quasiparticle decay
   in a quantum dot.
   Phys. Rev. Lett. **82**, 4894 (1999)

6. X. Leyronas, P. G. Silvestrov and C. W. J. Beenakker
   Scaling at the chaos threshold for interacting electrons
   in a quantum dot.
   Phys. Rev. Lett. **84**, 3414 (2000)

7. R. Combescot and X. Leyronas
   A simple theory for high Δ/T_c ratio in d-wave superconductors
   Eur. Phys. J. B **23**, 159-163 (2001)

8. X. Leyronas and M. Combescot
   Quantum wells, wires and dots with finite barrier :
   analytical expressions for the bound states
   Solid State Communications 119 (2001) 631-635

9. R. Combescot and X. Leyronas
Hydrodynamic modes in dense trapped ultracold gases
Phys. Rev. Lett. **89** 190405 (2002)

10. M. Combescot, X.Leyronas and C. Tanguy
On the N-exciton normalization factor
Eur. Phys. J. B **31**, 17-24 (2003).

11. J. N. Fuchs, X. Leyronas and R. Combescot
Hydrodynamic modes of a 1*D trapped Bose gas*
Phys. Rev. A **68**, 043610 (2003)

12. X. Leyronas and R. Combescot
Instability of a trapped ultracold Fermi gas with attractive interactions : quantum effects
Eur. Phys. J. D **31**, 493-497 (2004)

13. R. Combescot and X. Leyronas
Comment on "Collective excitations of a degenerate gas at the BEC-BCS crossover"
Phys. Rev. Lett. **93**, 138901 (2004)

14. R. Combescot and X. Leyronas
Axial collective excitations of a degenerate Fermi gas in the BEC to unitarity crossover
Eur. Phys. Lett., **68** 762-768 (2004)

15. G.E. Astrakharchik, R. Combescot, X. Leyronas and S. Stringari
Equation of state and collective frequencies of a trapped Fermi gas along the BEC-unitarity crossover Phys. Rev. Lett. **95**, 030404 (2005).

16. I.V. Brodsky, A. V. Klaptsov, M. Yu Kagan, R. Combescot and X. Leyronas
Bound states of three and four resonantly interacting particles JETP Letters vol. 82, issue 5 , page 306-311 (2005) [cond-mat/0507240]

17. R. Combescot, X. Leyronas, M.Yu. Kagan
Self-consistent theory for molecular instabilities in a normal degenerate Fermi gas in the BEC-BCS crossover Phys. Rev. A. **73**, 023618 (2006) [cond-mat/0507636]

18. I.V. Brodsky, A. V. Klaptsov, M. Yu Kagan, R. Combescot and X. Leyronas
Exact diagrammatic approach for dimer-dimer scattering and bound states of three and four resonantly interacting particles Phys. Rev. A **73**, 032724 (2006)

19. X. Leyronas and R. Combescot
Superfluid equation of state of dilute composite bosons Phys. Rev. Lett. **99**, 170402 (2007)

20. C. Mora, X. Leyronas and N. Regnault
Current noise through a Kondo quantum dot in a SU(N) Fermi liquid state, Phys. Rev. Lett. **100**, 036604 (2008).

21. R. Combescot and X. Leyronas *Superfluid equation of state of cold fermionic gases in the Bose-Einstein regime* Phys. Rev. A **78**, 053621 (2008)

Compte-rendus de conférences :

1. X. Leyronas, R. Combescot
   Low temperature penetration depth of strongly coupled superconductors
   Proceeding et article sélectionné pour la 21eme Conférence Internationale sur la Physique des Basses Temperatures
   Prague $8-14$ Août 1996.

2. R. Combescot and X. Leyronas
   Impurity effect on T_c in the coupled plane-chain model of $YBa_2Cu_3O_7$
   Proceeding pour la 21eme Conférence Internationale sur la Physique des Basses Temperatures, Prague $8-14$ Août 1996.

3. X. Leyronas and R. Combescot
   Equation of state from hydrodynamic modes in dense trapped ultracold gases
   Physica B 329-333 (2003) 32-33 (Proceeding de la conférence "Low Temperature Physics 23" Hiroshima, Japon, Août 2002).

4. M. Yu. Kagan,I. V. Brodsky, A. V. Klaptsov, R. Combescot, and X. Leyronas, Composite fermions and bosons in ultracold quantum gases, in Quantum Liquids and Crystals, Low Temperature Solid State Physics, volume 1 of Russian LT-XXXIV, page 209, Sochi, 2006 (en russe)

5. I. V. Brodsky, M. Yu. Kagan, A. V. Klaptsov, D. V. Efremov, R. Combescot, and X. Leyronas, Composite fermions and quarters in optical dipole traps and in high-T c superconductors, in AIP Proceedings of LT24 conference in Orlando, v. 850, p. 39 (2006) Florida, 2006.

6. M. Yu. Kagan, A. V. Klaptsov, I. V. Brodsky, R. Combescot, and X. Leyronas, Bound states of three and four particles in ultracold gasses and high-T C superconductors, in 2-nd International Conference on Fundamental Problems of High Temperature Superconductivity, edited by Yu.V. Kopaev, page 15, 2006 (en russe).

7. I.V. Brodsky, A. V. Klaptsov, M. Yu Kagan, R. Combescot and X. Leyronas
   Four -particle problem using Feynman diagrams, Laser Physics 2007, Vol. 17, No. 3, pp. 1-4. Proceedings pour la Conférence "15th International Laser Physics workshop (LPHYS'06)", 24-28 Juillet 2006 Lausanne, Suisse.

8. X. Leyronas and R. Combescot
   Superfluid equation of state of dilute composite bosons o how to include 3 and 4-body problem in the manybody problem, Laser Physics 2009, Vol. XX, No. XX, pp. XX-XX. Proceedings pour la Conférence "17th International Laser Physics workshop (LPHYS'08)", 30 Juin-4 Juillet 2008 Trondheim, Norvège.

Fonctions d'intérêt collectif :

– 2001 - 2002 ; 2002 - 2003 ; 2003 -2004 :
  membre titulaire de la commission de spécialistes de l'Université Pierre et Marie
  Curie, 28e section.
– Depuis Décembre 2007 : correspondant communication du LPS avec le CNRS et
  l'Université Pierre et Marie Curie (Paris 6)

Encadrements de stages :

– 2005-Stage de M2, parcours de physique quantique
  spécialité : concepts fondamentaux de la physique
  Stagiaire : Rémi Avriller
  Titre : "*Amplitudes de diffusion dans un gaz de fermions ultrafroids*"
– 2007-Stage de M2, parcours de physique quantique
  spécialité : concepts fondamentaux de la physique
  Stagiaire : Sébastien Giraud
  Titre : "*Gaz de fermions ultrafroids fortement polarisés*"
– 2007-Stage de M2, parcours de physique théorique des systèmes complexes,
  spécialité : systèmes dynamiques et statistiques de la matière complexe
  Stagiaire : Florent Alzetto
  Titre : "*Stability and critical temperature of a fermionic gas in the BEC-BCS crossover*"

Co-direction de thèses :

depuis Septembre 2007 (avec Roland Combescot) :
– Florent Alzetto
– Sébastien Giraud

Liste des collaborateurs :

– R. Combescot
– C. W. J. Beenakker
– J. Tworzydło
– P. G. Silvestrov
– M. Combescot
– C. Tanguy
– J. N. Fuchs
– G.E. Astrakharchik
– S. Stringari
– I.V. Brodsky
– A. V. Klaptsov
– M. Yu Kagan
– C. Mora
– N. Regnault

Activités d'enseignement :

Depuis septembre 1999 : Maître de Conférences à l'Université Pierre et Marie Curie :

2008 - 2009 :

Premier semestre :
– cours (2/3) et TD (1/3) Master 2, spécialité "Concepts fondamentaux de la Physique", parcours de Physique Quantique "Effets des interactions en matière condensée" (14 + 6h)
– Travaux dirigés et travaux pratiques Licence 2, "Thermodynamique" (58h)

Second semestre :
– Travaux dirigés de Master 1 "Propriétés physiques des milieux continus" (20*h*)
– Travaux dirigés et travaux pratiques Licence 2, "Champs électrique et magnétique, induction" (68 h)

2007 - 2008 :

Allègement d'1/3 de service en vue de la soutenance d'Habilitation à Diriger des Recherches

Premier semestre :
– Travaux dirigés et travaux pratiques Licence 2, "Thermodynamique" (58h)

Second semestre :
– Travaux dirigés et travaux pratiques Licence 2, "Champs électrique et magnétique, induction" (68 h)

2006 - 2007 :

Premier semestre :
Accueil en délégation CNRS

Second semestre :
– Travaux dirigés "Atomes et molécules" Master 1, Parcours Physique Générale (36 heures)
– Travaux dirigés "Physique des solides" Master 1, Parcours Physique Fondamentale (18 heures)
– Travaux dirigés et travaux pratiques Licence 2, "Champs électrique et magnétique, induction" (48 heures)

2005 - 2006 :

Premier semestre :
– Travaux dirigés de "Physique Quantique et Applications" Master 1, Parcours Physique Générale (32 heures)
– Travaux dirigés et travaux pratiques Licence 2, "Ondes mécaniques et lumineuses" (60 heures)

Second semestre :
– Travaux dirigés "Atomes et molécules" Master 1, Parcours Physique Générale (36 heures)
– Travaux dirigés "Physique des solides" Master 1, Parcours Physique Fondamentale (18 heures)
– Travaux dirigés et travaux pratiques Licence 2, "Champs électrique et magnétique, induction" (48 heures)

2004 - 2005 :

– Travaux dirigés de Mécanique Quantique Master 1, Parcours Physique Générale
– Travaux dirigés et travaux pratiques Licence 2, "Ondes mécaniques et lumineuses"

– Travaux dirigés "Atomes et molécules" Master 1, Parcours Physique Générale
– Travaux dirigés et travaux pratiques Licence 2, "Champs électrique et magnétique, induction"

2003 - 2004 :
– Travaux dirigés de Mécanique Quantique Master 1, Parcours Physique Générale
– Travaux dirigés et travaux pratiques Licence 2, Ondes mécaniques et lumineuses
– Travaux dirigés "Atomes et molécules" Master 1, Parcours Physique Générale

2002 - 2003 :
– Travaux dirigés de Mécanique Quantique en Maîtrise de Physique Fondamentale
– Travaux dirigés de Physique Atomique en Maîtrise de Physique et nouvelles Technologies
– Travaux dirigés et travaux pratiques en DEUG SCM12 (Physique 2)

2001 - 2002 :
– Travaux dirigés de Physique Atomique en Maîtrise de Physique et nouvelles Technologies
– Travaux dirigés de Physique Quantique en Licence de Physique Fondamentale
– Travaux dirigés et travaux pratiques en DEUG SCM12 (Physique 2)

2000 - 2001 :
– Cours et travaux dirigés de Mécanique Quantique en Maîtrise de Physique Fondamentale (section Travailleurs)
– Travaux dirigés de Mécanique Quantique en Maîtrise de Physique Fondamentale
– Travaux dirigés en DEUG SCM12 (Physique 2)

1999 - 2000 :
– Cours et travaux dirigés de Physique Quantique en Licence de Physique Fondamentale, section Travailleurs (cours du soir)
– Travaux dirigés et travaux pratiques (Physique 1) en DEUG Science de la Matière première année (section SCM12).

1994-1997 :
Allocataire Moniteur Normalien à l'Ecole Normale Supérieure de Paris.
– Cours et travaux pratiques de programmation en FORTRAN pour les élèves de Licence du MIP. Encadrement des projets numériques.
– 1996 : Sessions d'initiation au courrier électronique, à UNIX, Netscape et Latex pour les étudiants de première année de l'Ecole Normale Supérieure.
– 1995-1997 : Projets expérimentaux :
– 1995-1997 : absorption et luminescence dans les semi-conducteurs.
– 1995 : Interféromètre de Mach-Zehnder.
– 1995-1996 : Responsable de la bibliothèque du magistère de Physique Interuniversitaire (MIP).

Préambule :

Ce mémoire présente mon activité de recherche. Tous mes travaux ont porté sur la théorie de la matière condensée : supraconducteurs, physique mésoscopique, excitons ou gaz ultrafroids. Ces systèmes sont très différents dans leur réalité expérimentale. Un de leur point commun est qu'il s'agit très souvent de fermions en interaction dans un régime "dégénéré" où la statistique de Fermi est importante. Ainsi, les électrons des supraconducteurs s'attirent et peuvent s'apparier pour former des paires de Cooper (Chapitre 1), les électrons des boîtes quantiques acquiert une durée de vie finie du fait de leur interaction (Chapitre 2). Les atomes fermioniques de ^6Li peuvent former des molécules diatomiques de taille variable (Chapitre 4). Dans le Chapitre 5, on s'intéresse aux excitons, "molécules" formées par l'interaction entre particule et trou de semiconducteurs. Dans ce même chapître est abordé un travail sur l'effet Kondo dans les systèmes mésoscopiques. Ici, c'est l'"impureté magnétique" (en fait une boîte quantique ou un nanotube de carbone) qui induit une interaction locale entre électrons.

Le premier chapitre est ainsi consacré à nos travaux sur les supraconducteurs à hautes températures critiques et présente des calculs de profondeur de pénétration du champ magnétique en théorie de couplage fort, ainsi que le modèle "plan-chaînes" de cuivre-oxygène. Le deuxième chapitre traite lui de mes travaux de physique mésoscopique, effectués lors de mon séjour postdoctoral à Leyde aux Pays-Bas.

Dans les troisième et quatrième chapitres, nous quittons la physique de la matière condensée traditionnelle pour les gaz ultrafroids. Il y est question d'une part de l'étude des modes collectifs dans ces systèmes et d'autre part du phénomène fascinant qu'est la transition "BEC-BCS". Le cinquième chapitre est consacré aux "autres travaux" : excitons et effet Kondo dans les systèmes mésoscopiques.

Mes projets de recherche à court et moyen terme sont ensuite exposés dans le dernier chapitre. Ils portent d'une part sur des prolongements prometteurs de nos travaux où intervient les problèmes à quelques corps (sections 4.2 et 4.3), et d'autre part sur le problème de mélanges de gaz ultrafroids, un domaine certainement prometteur.

Table des matières

Chapitre 1

Supraconducteurs

1.1 Profondeur de pénétration et théorie de couplage fort

Durant ma thèse, j'ai tout d'abord travaillé sur la théorie de couplage fort de la supraconductivité (théorie d'Eliashberg). Plus précisément j'ai étudié le comportement basse température de la profondeur de pénétration du champ magnétique, quantité qui est reliée à la densité de superfluide. Le comportement à basse température renseigne sur la population thermique des excitations de basse énergie. Expérimentalement, il avait été observé des dépendances quadratique et linéaire en température dans le supraconducteur à haute température critique $YBa_2Cu_3O_7$. Ceci ne pouvait s'expliquer par la théorie de couplage faible BCS en "onde s". J'ai donc étudié si on pouvait l'expliquer par la théorie de couplage fort.

Cette théorie décrit la supraconductivité dans un système où l'interaction attractive entre électrons, qui peut être forte, est médiée par des phonons. Elle tient compte d'une durée de vie finie des excitations et de la population thermique des phonons. J'ai fait une étude systématique du comportement basse température de la densité superfluide dans le cadre de la théorie d'Eliashberg. J'ai aussi étudié les cas limites. Pour un large domaine de paramètres, il est possible de reproduire des lois de puissance, avec parfois une très bonne précision. Il est possible de reproduire une dépendance quadratique en température pour des paramètres raisonnables, mais cela est impossible pour une dépendance linéaire. Cette forte dépendance en température est due à la présence de phonons basses fréquences, qui se comportent comme des diffuseurs quasi-élasiques, dont le nombre varie avec la température (publication n°2).

A titre d'exemple, la Fig.1.1 montre la dépendance en température de l'inverse du carré de la profondeur de pénétration du champ magnétique (à un facteur près la densité superfluide) pour différents paramètres théoriques, dans la limite où il y a des phonons de très basses fréquences. La courbe en caractère gras est très similaire aux résultats expérimentaux du groupe de W. Hardy [1].
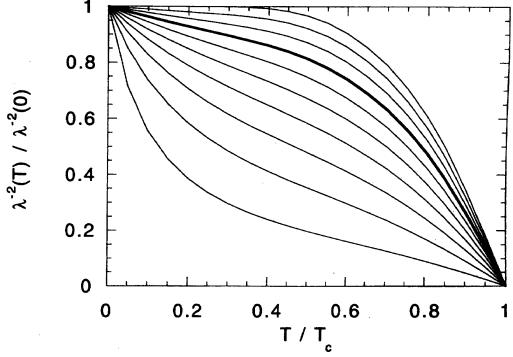
FIG. 1.1 – Fraction superfluide pour différents paramètres, dans notre théorie de couplage fort. La courbe en trait gras ressemble aux résultats expérimentaux du groupe de W. Hardy.

1.2   Modèle Plans-Chaînes pour $YBa_2Cu_3O_7$

La deuxième partie de ma thèse fut consacrée à l'étude d'un modèle couplant Plans et Chaînes de Cuivre-Oxygène dans $YBa_2Cu_3O_7$. Ce modèle fut motivé par l'existence de plusieurs expériences contradictoires concernant la forme du paramètre d'ordre ("gap") dans ce composé. Un premier groupe d'expériences (effet tunnel, profondeur de pénétration) a montré l'existence d'excitations de basse énergie. En particulier, la dépendance linéaire en température de la profondeur de pénétration est en accord avec l'existence de noeuds pour le paramètre d'ordre. Un deuxième type d'expériences, utilisant l'effet Josephson, a montré un changement de signe du paramètre d'ordre entre les axes a et b. Ces deux types d'expériences sont en accord avec un paramètre d'ordre de type "onde d". Pourtant, des expériences d'effet tunnel selon l'axe c entre $YBCO$ et le Pb ont montré un courant Josephson continu non nul, en contradiction avec le résultat prédit par les ondes d.

Nous avons proposé, avec R. Combescot, un modèle proposant une solution possible à ces expériences contradictoires (publication $n°1$). Ce modèle prend en compte deux types de couplages entre les Plans et les Chaînes de Cuivre-Oxygène. Le premier type de couplage est l'hybridation entre ces deux systèmes, qui correspond à la possibilité pour un électron de sauter de plans à chaîne (voir Fig.1.2).

Le deuxième type de couplage est une interaction d'appariement répulsive qui entraîne que les paramètres d'ordre des Plans et des Chaînes (supposés isotropes) sont de signe opposés.

Ainsi, grâce à l'hybridation, lorsqu'on se déplace sur la Surface de Fermi, on va continûment d'une région où l'électron se situe plutôt dans les Plans à une situation où il est plutôt dans les Chaînes. Ceci est indiqué sur la Fig.1.3, où les "lignes de Fermi" sont représentées dans la première zone de Brillouin $[-\pi, \pi] \times [-\pi, \pi]$. Le changement de signe implique par continuité que le paramètre d'ordre s'annule sur un même morceau de la Surface de Fermi, ce qui est représenté par des ronds noirs sur la Fig.1.3. Ce changement de signe et les lignes de noeuds (à trois dimensions), avec la possibilité d'un paramètre d'ordre de valeur moyenne non nulle, fournit une explication possible aux expériences

6
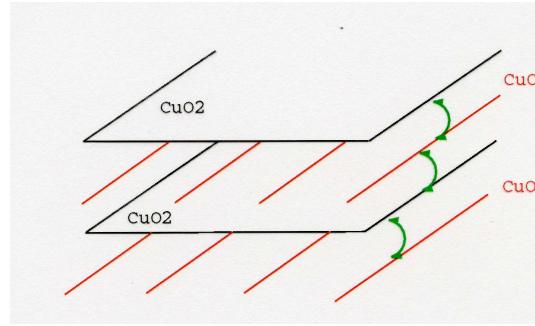
FIG. 1.2 –
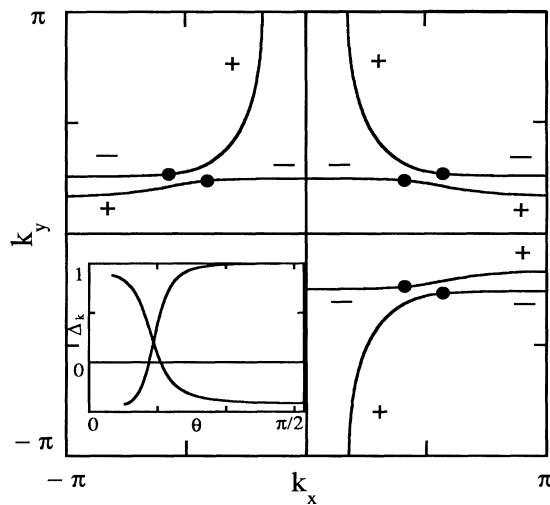
FIG. 1.3 – Surface de Fermi dans la première zone de Brillouin. Les signes $\pm$ indiquent les signes du paramètre d'ordre sur les différents morceaux de la surface de Fermi. Les ronds noirs donnent la position des noeuds. L'insert montre la variation du paramètre d'ordre sur les deux morceaux de la surface de Fermi, en fonction de l'angle polaire θ.

contradictoires décrites plus haut (publication $n°1$). J'ai étudié dans le cadre de ce modèle l'influence des impuretés sur la température critique (publication $n°3$), ainsi que les profondeurs de pénétration du champ magnétique dans les trois directions cristallographiques (publication $n°4$).

1.3 Rapport gap sur température critique dans les supraconducteurs à haute température critique

Après mon recrutement, en Septembre 1999, à l'Université Pierre et Marie Curie au sein du LPS, j'ai, dans un premier temps, travaillé en collaboration avec Roland Combescot, sur le problème du rapport gap sur température critique (T_c) dans les cuprates supraconducteurs. Ce dernier est anormalement grand (de l'ordre de 6 à 10) alors que la théorie BCS prédit une valeur maximale autour de 2. Nous avons alors étudié un modèle de supraconducteur en "onde d" dans lequel des phonons (qui existent dans les cuprates) ont pour effet de diminuer à la fois le gap (à température nulle) et T_c. L'idée, confirmée par des calculs numériques, est que le gap et T_c diminuent en présence de phonons, mais T_c plus fortement que le gap, puisque l'effet des phonons est plus important à la température de la transition supraconductrice T_c (ils sont peuplés thermiquement) qu'à température nulle (publication $n°7$). Sur la Fig.1.4, le rapport gap sur température critique est porté en fonction de la constante de couplage électron-bosons, pour différentes valeurs de l'énergie des bosons Ω. On voit ainsi que l'on peut augmenter significativement le rapport gap sur T_c.
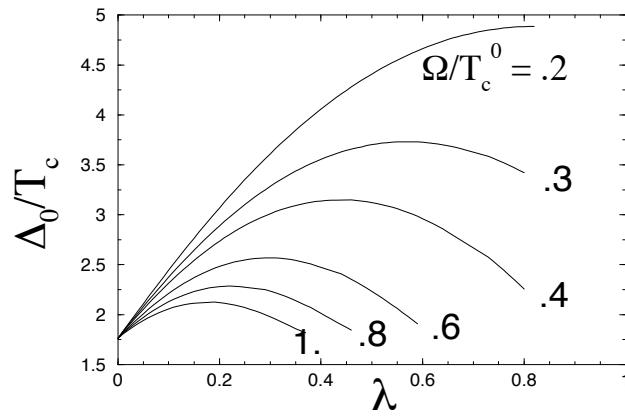

FIG. 1.4 – Rapport du gap sur la température critique Δ_0/T_C en fonction de la constante de couplage λ pour différentes fréquences bosoniques Ω.

Chapitre 2

Physique mésoscopique

2.1 Durée de vie d'une quasiparticle dans un boîte quantique

Durant mon séjour postdoctoral à l'Université de Leyde, j'ai travaillé, en collaboration avec Carlo Beenakker et Jakub Tworzydło, sur un modèle décrivant l'interaction d'électrons dans un boîte quantique. Le problème qui nous intéressait est celui de la durée de vie d'une quasi-particule dans un boîte quantique, c'est à dire la durée de vie d'un état initial avec un électron occupant un niveau au dessus du niveau de Fermi, ou un trou occupant un niveau au dessous du niveau de Fermi.

En effet, à cause des interactions avec les électrons au dessous du niveau de Fermi, l'électron introduit dans le matériau va se désintégrer en des états contenant deux électrons et un trou, puis trois électrons et deux trous, etc... La particule injectée acquiert ainsi une *durée de vie finie.*

La quantité physique qui permet d'observer ce phénomène est la densité spectrale qui va donner le poids des différents états propres vers lesquels la particule introduite va transiter. S'il n'y avait pas d'interaction entre les particules, l'état initial serait un état stationnaire, et la densité spectrale aurait un pic infiniment étroit, à l'énergie du niveau sans interaction auquel la particule se trouve. En revanche, les interactions induisent une durée de vie de la quasiparticule qui se traduit par l'élargissement de ce pic avec une largeur donnée par l'inverse de la durée de vie de la quasiparticule, qui est la "largeur" du niveau considéré.

Une des particularités des boîtes quantiques est que ce sont des objets si petits que l'espacement entre niveaux d'énergie sans interaction, Δ, ne peut pas être considéré comme infiniment faible. Ainsi, il a été possible de résoudre expérimentalement différents niveaux, lorsque la largeur est plus petite que Δ [2].

Peu avant le début de mon séjour postdoctoral [3], il avait été avancé qu'en dessous d'une certaine énergie, une quasiparticule introduite dans une boîte quantique pourrait avoir une *durée de vie infinie.* Ceci se traduirait par le fait que la densité d'états ne présenterait que quelques pics infiniment étroits, seuls quelques états propres ayant un recouvrement appréciable avec l'état initial. Pour obtenir ce résultat, les auteurs de [3] ont fait l'analogie entre ce problème et le problème de la localisation d'Anderson sur le réseau de Bethe, aussi appelé arbre de Cayley . Dans cette approche, l'espace de Hilbert

des états sans interaction couplés par l'interaction à l'état initial, est considéré comme un réseau de Bethe sur lequel des sites sont couplés entre eux par des termes de sauts. Cette analogie est illustrée Fig.2.1. Un électron au dessus du niveau de Fermi (état $|1\,j\rangle$) est couplé à des états à 3 particules (2 électrons +1 trou), eux-mêmes couplés à des états à 5 particules (3 électrons +2 trous), etc ... En faisant l'hypothèse de l'absence de boucles dans ce réseau, on retrouve la structure d'arbre de Cayley. Dans le langage du modèle
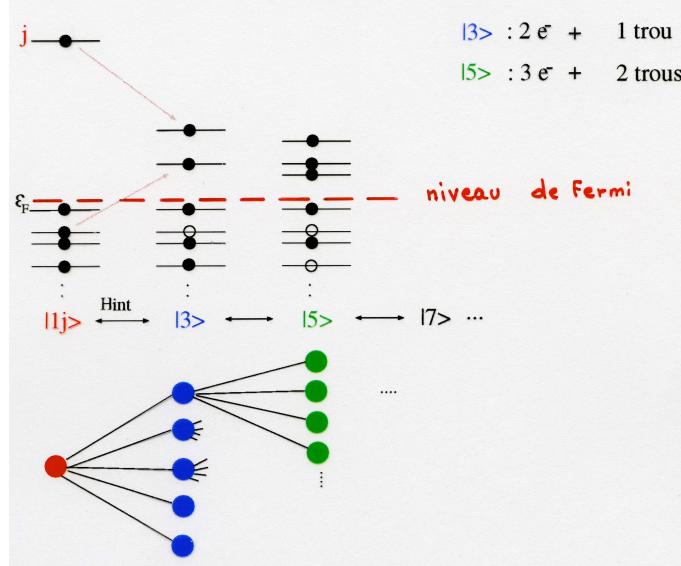

FIG. 2.1 – La désintégration de l'électron initialement au dessus du niveau de Fermi en créant des paires particules-trous rappelle la structure de l'arbre de Cayley.

d'Anderson, le désordre sur site vient du fait que l'énergie sans interaction de chacun des sites a des fluctuations d'ordre Δ. On sait par ailleurs que le problème de la localisation d'Anderson sur le réseau de Bethe présente une transition de localisation : lorsque les fluctuations d'énergie sont plus grandes qu'un seuil, tous les états propres sont localisés. En dessous de ce seuil, les états sont étendus sur tout le réseau. Dans le cas localisé, la particule va ainsi avoir une durée de vie infinie, dans le cas contraire, elle aura une durée de vie finie.

Nous avons voulu reconsidérer ce problème, à l'aide d'un modèle particulier d'inter-action à deux corps, le modèle en couche. Ce modèle ne couple que les états qui ont une différence d'énergie de l'ordre de Δ. L'idée de notre approche est la suivante : un électron va se désintégrer en deux électrons et un trou, qui eux-même vont se désintégrer en deux électrons et un trou, etc... Nous avons donc fait l'approximation que la "self-energy" d'un état à deux électrons et un trou, qui décrit la durée de vie de cet état, est la somme des self-energies des deux électrons et du trou. On aboutit alors à des équations que l'on ré-soud numériquement. Nous avons de plus effectué des calculs numériques exacts, pour des systèmes avec quelques particules, afin de tester notre approximation. Pour caractériser quantitativement ce changement de régime, nous avons calculé le taux de participation inverse, qui est fini dans le cas d'une situation localisée, et nul dans le cas d'une situation délocalisé.

Nos résultats indiquent l'existence d'une transition de délocalisation douce, en accord

qualitatif avec les auteurs de [2], qui prédisent la transition abrupte de l'arbre de Cayley. Ainsi, en augmentant le désordre (i.e. Δ), nous trouvons que l'on passe d'une situation où la quasiparticule a une durée de vie infinie (la densité d'états est constituée de quelques pics infiniment fins), à une situation où la quasiparticule a une durée de vie finie (la densité d'états est une fonction régulière avec une largeur donnée par l'inverse de la durée de vie). Ces deux cas sont illustrés sur la Fig.2.2, par nos calculs numériques (algorithme de Lanczos).
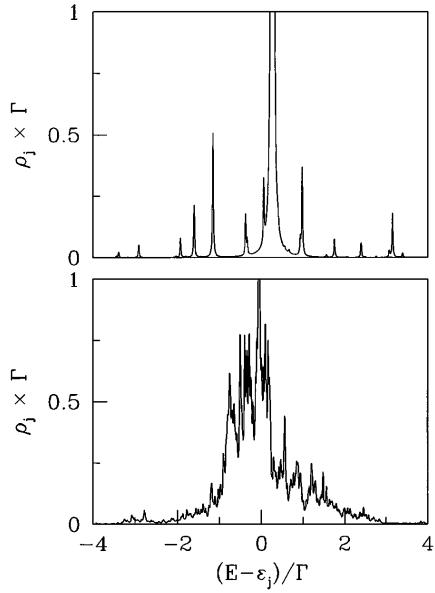
FIG. 2.2 – Haut : densité spectrale présentant quelques pics infiniment fins (durée de vie "infinie"). Bas : densité spectrale avec une largeur finie (durée de vie finie).

2.2 Seuil de chaos pour des électrons en interaction dans une boîte quantique

Lors de mon séjour post-doctoral à Leiden, j'ai continué à travailler sur le problème d'électrons en interaction dans une boîte quantique (publication $n°6$) à l'aide du même modèle "en couche". La question que nous nous sommes posée est la suivante : est-il possible qu'il y ait délocalisation sans chaos total ? Si oui, y a-t-il une transition entre ces deux régimes et quel est le paramètre qui gouverne cette transition ? J'ai effectué des calculs numériques de diagonalisation exacte afin de déterminer le nombre typique de déterminants de Slater (états propres sans interaction) qui contribuent à un état propre de l'hamiltonien avec interaction. Le chaos correspond à une situation où les interactions "mélangent complètement" (on peut préciser cette notion) les déterminants de Slater, alors que dans une situation délocalisée, un grand nombre de déterminants de Slater (mais pas tous) participent à un état propre. Nous avons pu mettre en évidence ces deux régimes, ainsi que la possibilité d'une transition abrupte lorsque le nombre de particules

devient grand. Les calculs numériques sont en accord avec une théorie proposée par P. G. Silvestrov, qui est co-auteur de la publication $n°6$.

Chapitre 3

Modes collectifs dans les gaz ultrafroids

Depuis 2001, j'ai réorienté mon activité de recherche vers l'étude des gaz ultrafroids, sujet très dynamique, en particulier au Laboratoire Kastler-Brossel du département de Physique de l'ENS. Mon travail a tout d'abord porté sur l'étude des modes collectifs dans ces systèmes. Par la suite, il s'est orienté vers des théories plus "microscopiques", décrites dans les chapitres suivants.

3.1 Effondrement de fermions ultrafroids et modes hydrodynamiques :

J'ai ainsi en premier lieu travaillé sur l'observation possible d'un effondrement ("collapse") du gaz de fermions ultrafroids sous l'effet de ses interactions attractives lorsque le gaz devient suffisamment dense. Nous avons plus spécifiquement étudié ce phénomène dans le cas particulier d'une situation inhomogène comme on la trouve expérimentalement, puisque ces gaz se trouvent en général dans un piège harmonique. Nous avons obtenu que la densité critique (au centre du piège) n'est que faiblement modifiée par cette inhomogénéité (publication $n°12$). Ce travail a motivé l'étude qui suit des modes hydrodynamiques qui peuvent être un signe précurseur à l'effondrement, comme c'est le cas dans un condensat de Bose avec des interactions attractives [4].

L'étude des modes collectifs d'oscillation est un outil expérimental particulièrement pratique pour sonder les gaz ultrafroids [5]. D'une part, ils fournissent une information in situ sur le gaz, sans nécessairement ouvrir le piège afin de faire des mesures de temps de vol. Du point de vue théorique, ils sont également importants, car ils correspondent aux excitations élémentaires de basse énergie et grande longueur d'onde. Pour l'étude de ces modes, les équations de l'hydrodynamique permettent d'étudier des systèmes en interaction forte, alors que la plupart des approches microscopiques se restreignent au régime de couplage faible. Les équations de l'hydrodynamique du gaz sont alors[1] (nous

---

[1] On retrouve l'équation d'Euler habitiuelle avec la pression P en utilisant l'identité thermodynamique $\partial P/\partial n = n\,\partial\mu/\partial n$.

nous restreindrons à la limite de température nulle)

$$\partial_t n + \nabla \cdot (n\mathbf{v}) = 0 \qquad (3.1)$$

$$m\frac{d\mathbf{v}}{dt} = -\nabla(\mu(n) + V) \qquad (3.2)$$

où $\mu(n)$ est le potentiel chimique du gaz à la densité n; $\mathbf{v}$ le champ de vitesse et V le potentiel de piégeage extérieur. Si on suppose par exemple un piège harmonique isotrope de pulsation Ω

$$V(r) = \frac{1}{2}m\Omega^2 r^2$$

alors la fréquence d'un mode propre de pulsation rapportée à la pulsation du piège ω/Ω ne dépend plus que de $\mu(n)$, que nous qualifierons d'*équation d'état*.

3.1.1 Modèles exactement solubles

En manipulant de manière générale les équations pour les modes (publication n°9), obtenues par linéarisation des équations 3.1 et 3.2, on peut trouver une famille d'équation d'état à deux paramètres (α, p) pour laquelle les modes sont déterminés exactement. Si l'on note $\bar{\mu} = \mu(n)/\mu(n(\mathbf{0}))$ et $\bar{n} = n(\mathbf{r})/n(\mathbf{0})$, le modèle "$\alpha - p$" correspond à

$$\bar{\mu} = 1 - (1 - \bar{n}^{1/p})^{2/\alpha} \qquad (3.3)$$

Dans le cas d'une symétrie sphérique où, comme en mécanique quantique, les nombres quantiques l et m_l sont de "bons nombres quantiques", on trouve pour les fréquences des modes du modèle $\alpha - p$

$$\frac{\omega^2}{\Omega^2} = l + \frac{\alpha}{p}n\left(n + p + \frac{2l+1}{\alpha}\right) \qquad (3.4)$$

où le "nombre quantique principal" n peut valoir $0, 1, \cdots$. On peut de plus définir une autre classe de modèle "quasi-polynomiaux" définis à l'aide de plus de paramètres, et qui sont "quasi-analytiques" dans le sens où la résolution numérique associée est triviale (publication n°9).

Le principe de la méthode est le suivant : on détermine les paramètres (2 ou 3 en pratique) qui reproduisent au plus près une équation d'état donnée. On en déduit alors l'ensemble du spectre, par exemple pour le modèle $\alpha - p$ via l'Eq.3.4. Nous avons appliqué cette méthode au calcul des modes dans le cas d'une équation d'état pour un gaz de fermions de spin $1/2$ en interaction attractive, dans l'approximation du champ moyen. Le modèle $\alpha - p$ donne déjà de très bons résultats avec une erreur relative de quelques pourcents. Lorsqu'on raffine à l'aide du modèle quasipolynomial, ou bien en traitant en perturbation la différence entre l'équation d'état exacte et le modèle $\alpha - p$, l'erreur relative chute à quelques pour-milles.

3.1.2 Première application : le gaz de Bose $1D$

Nous avons appliqué la méthode à une situation physique plus intéressante et qui trouve des réalisations expérimentales : le gaz de Bose à une dimension (publication n°11).

En pratique, les gaz de Bose $1D$ sont réalisés en piégeant des condensats de Bose-Einstein dans des pièges très allongés dans la direction z (et donc très "serrés" dans les deux autres directions transverses). On considère ainsi un piège harmonique de symétrie axiale, dont la pulsation radiale $\omega_\perp$ est très grande devant la pulsation axiale $\omega_z \ll \omega_\perp$. Lorsque la longueur d'oscillateur radiale $a_\perp = \sqrt{\hbar/m\omega_\perp}$ est très grande devant la longueur de diffusion a, on peut montrer [6] que la longueur de diffusion effective $1D$ est donnée par $a_1 = a_\perp^2/a$. Nous avons montré dans la publication $n°11$ que l'on retrouve les équations de l'hydrodynamique $1D$ à partir de celles à $3D$. La densité $n_1(z)$ est simplement obtenue en moyennant radialement la densité tri-dimensionnelle.

Concernant le gaz de Bose $1D$, les auteurs de la Ref.[7] ont montré l'existence de deux domaines :

- un domaine "haute densité" où le gaz est décrit microscopiquement par l'équation de Gross-Pitaïevskii.
- un domaine "basse densité" où tous les atomes sont dans l'état fondamental de l'oscillateur harmonique. Le modèle microscopique est celui de Lieb-Liniger, exactement soluble par l'ansatz de Bethe [8].

Associés à ces deux domaines, correspondent des cas limites simples pour l'équation d'état $1D$ et donc pour les fréquences de modes propres. Nous considérons le mode de fréquence la plus basse et nous noterons $\nu^2 = \omega^2/\omega_z^2$. Dans le cas "haute densité", si $n_1(0)a \gg 1$, le condensat est beaucoup plus large que l'état fondamental de l'oscillateur harmonique. On peut négliger le terme d'énergie cinétique de l'équation de Gross-Pitaïevskii (approximation de Thomas Fermi). On trouve : $\mu(n_1) = 2\hbar\omega_\perp(a\,n_1)^{1/2}$ et $\nu^2 = 5/2$. Si $n_1(0)a \ll 1$ et $n_1(0)a_1 \gg 1$, les degrés de liberté radiaux sont gelés et la taille radiale tend vers $a_\perp$. C'est le régime "champ moyen $1D$", où l'on a $\mu = 2\hbar\omega_\perp\,an_1$ et $\nu^2 = 3$. Enfin, si $n_1(0)a_1 \ll 1$, le système est un gaz de bosons impénétrables (gaz de Tonks-Girardeau). Le potentiel chimique est donné par $\mu = \frac{\hbar^2}{2m}(\pi n_1)^2$ et $\nu^2 = 4$. La figure 3.1 montre comment $\nu^2 = \omega^2/\omega_z^2$ évolue en fonction de la densité. Les paliers aux valeurs $5/2, 3$ et 4 sont pour les cas limites mentionnés. Les différents symboles (croix, cercles et losanges) indiquent les différents modèles utilisés pour le calcul de la fréquence. On voit ainsi l'excellente précision de la méthode, puisque, le modèle $\alpha - p$ mis à part, les autres méthodes sont en très bon accord.
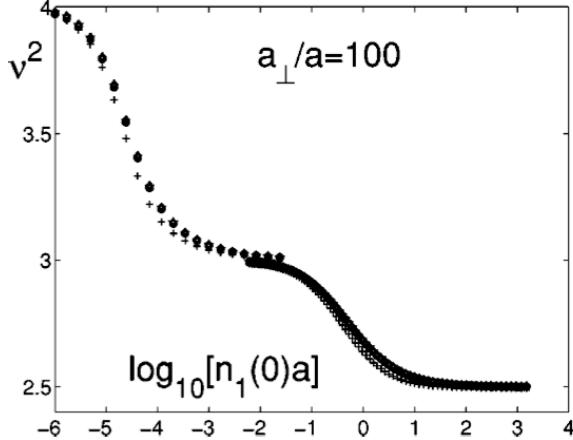
Fig. 3.1 – Mode de compression le plus bas pour la gaz de Bose $1D$ piégé ($a_\perp/a = 100$). Le carré de la fréquence $\nu^2 = \omega^2/\omega_z^2$ est porté en fonction de $\log_{10}[n_1(0)\,a]$. Les croix ($+$) correspondent au modèle $\alpha - p$; les cercles ($\bigcirc$) au modèle quasipolynomial ; et les losanges ($\Diamond$) au modèle quasipolynomial corrigé. A cette échelle, tous les symboles tombent les uns sur les autres, sauf les croix.

3.2   Deuxième application : mode de compression et équation d'état dans le crossover limite unitaire-limite BEC

En 2003, il a été observé (et prédit) la formation de molécules constituées de deux atomes fermioniques. La molécule formée étant essentiellement un boson, des condensats moléculaires ont été observés par la suite [9]. Puis, des mesures très précises de fréquences de modes propres ont été menées [10]. Nous avons appliqué notre approche à ces expériences (publications $n°13$, 14). Par la suite, en collaboration avec Sandro Stringari et son étudiant Grigory Astrakharchik (Université de Trente, Italie), cette étude a été poursuivie (publication $n°15$). Le phénomène étudié était le crossover BEC-BCS, qui sera expliqué dans le chapitre 4. Nous verrons alors que l'interaction entre atomes est caractérisé par la longueur de diffusion a. Nous nous restreignons ici au cas $a > 0$. Si $a \to 0_+$, cela correspond à la limite BEC d'un condensat de molécules. La limite $a \to +\infty$ est appelée "limite unitaire".

Dans la publication $n°15$, nous avons comparé quantitativement notre méthode de calcul de fréquence de mode à une autre méthode dite de "changement d'échelle". Dans cette approche, on suppose qu'à chaque instant, le profile de densité $n(\mathbf{r}, t)$ est obtenu à partir du profil à l'équilibre $n_0(\mathbf{r})$ via un changement d'échelle :

$$n(\mathbf{r}, t) \;=\; \gamma(t)\, n_0(a_1(t)x_1,\, a_2(t)x_2,\, a_3(t)x_3) \tag{3.5}$$

avec $\gamma(t) = \Pi_i a_i(t)$ afin de conserver le nombre total de particules, et on a noté x_1 pour x, par exemple. L'analyse montre qu'il n'y a alors qu'un seul paramètre sans dimension

Γ qui intervient

$$\Gamma \;=\; \frac{3}{2}\frac{\langle n\frac{\partial \mu}{\partial n}\rangle}{\langle V_{oh}\rangle} - 1 \tag{3.6}$$

On a supposé un piège harmonique $V_{oh}(\mathbf{r}) = \sum_i 1/2\, m\, \omega_i^2 x_i^2$. Les valeurs moyennes sont prises sur la densité à l'équilibre (par exemple $\langle V_{oh}\rangle = \int d\mathbf{r} n_0(\mathbf{r}) V_{oh}(\mathbf{r})$). Nos résultat montre pour les exemples considérés que les deux méthodes coïncident à quelques pour milles, ce qui les confortent l'une l'autre !

Par ailleurs, nous nous sommes intéressés, motivés par les expériences du groupe de R. Grimm à Innsbruck, au mode de compression d'un gaz de fermions dans le crossover entre la limite unitaire et BEC. La géométrie est unidimensionnelle (le long de l'axe z) et nous avons supposé ici encore que la température était suffisamment basse pour être considérée comme nulle. Nous avons calculé la fréquence du mode pour deux théorie concurrentes : d'une part la théorie BCS la plus simple (dénotée MF-BCS pour "mean-field BCS") et d'autre part nous avons utilisé les données de calcul numériques effectués par G. Astrakharchik et S. Giorgini [11] (dénoté MC pour Monte-Carlo). Les résultats sont montrés Fig.3.2. On remarque qu'on peut distinguer les deux théorie via le calcul des modes. Par ailleurs, les points expérimentaux du groupe de R. Grimm[12], indiqués avec leurs barres d'erreur, étaient plutôt à l'époque en faveur de la théorie MF-BCS, qui est la moins correcte ! Ce résultat inattendu a motivé le groupe de R. Grimm à revoir ces données (déjà très précises !). Les résultats expérimentaux sont maintenant en faveur des calculs numériques Monte-Carlo (courbe MC) [13].
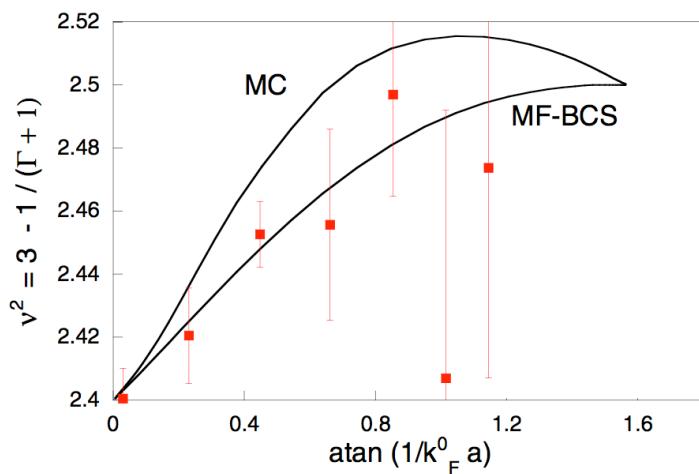

FIG. 3.2 – $\nu^2 = \omega^2/\omega_z^2$ le long du crossover limite unitaire (à gauche)-limite BEC (à droite). Les points exprérimentaux et leurs barres d'erreur étaient à l'époque en faveur de la théorie MF-BCS. Le paramètre Γ est défini dans l'équation 3.6.

Chapitre 4

Transition BEC-BCS

Considérons deux atomes (par exemple de ^6Li) dans deux états internes (par exemple deux sous-niveaux Zeeman) distincts que nous noterons par la suite ↑ et ↓ (ou "up" et "down"). Ils interagissent via un potentiel à deux corps V, comme représenté Fig.4.1. Si le potentiel est suffisament profond, il peut y avoir un état lié à deux corps, c'est-à-dire une *molécule* (ou *dimère*). La longueur de diffusion a est alors positive. En diminuant la profondeur du puits de potentiel, l'état lié disparaît, la longueur de diffusion a diverge et change de signe : il y a une *résonance*. En 1980, Leggett [14] considéra une assemblée
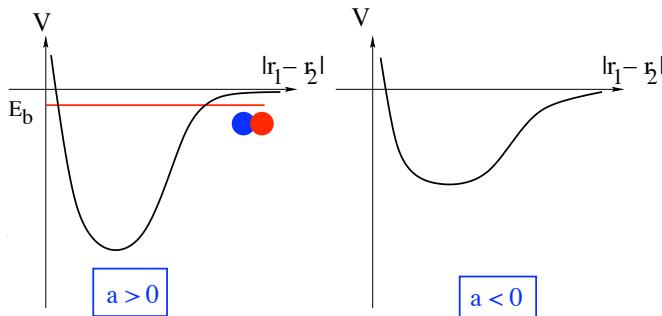
FIG. 4.1 – Le potentiel à deux corps avec (gauche) et sans (droite) état lié moléculaire.

de tels fermions identiques, à température nulle et de densité par spin n. En prenant la fonction d'onde BCS comme ansatz variationnelle à tout a, il retrouve tout d'abord les deux limites diluées. Si $k_F\, a \to 0_-$ (avec $n \equiv \frac{k_F^3}{6\pi^2}$), on se retrouve dans la situation où les atomes s'apparient sous la forme de paires de Cooper, dont la taille est très grande devant la distance interparticule (droite de la Fig.4.2). On retrouve ici la limite BCS des supraconducteurs (pour Bardeen-Cooper-Schrieffer). Dans l'autre limite diluée, $k_F\, a \to 0_+$, les atomes de spins opposés s'assemblent dans des molécules, dont la taille a est petite devant la distance interatomique (gauche de la Fig.4.2). On a donc un condensat de Bose de molécules diatomiques, c'est la limite BEC (pour Bose Einstein Condensate). Le résultat très surprenant de l'analyse de Leggett, est qu'on passe *continument* d'une limite à l'autre (d'où l'anglicisme "crossover"). En particulier, la situation résonnante $a \to \pm\infty$ (que l'on qualifierait d'interaction "infinie") est traversée sans aucun signe de singularités.
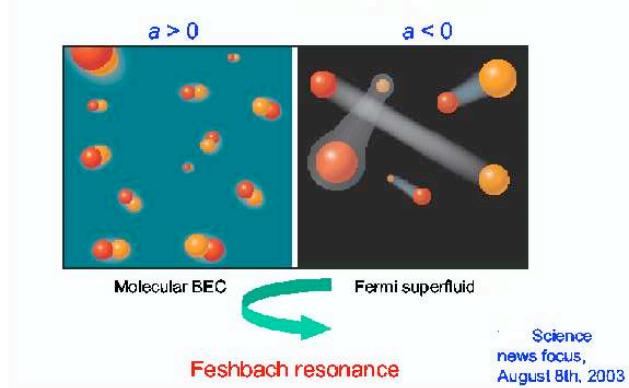
FIG. 4.2 – Dessin illustrant le crossover BEC-BCS.

Dans le cadre des gaz ultrafroids [1], cette situation physique a été réalisée jusqu'à présent pour deux atomes : ^6Li et ^{40}K. Dans les deux cas, la longueur de diffusion a diverge lorsqu'on varie le champ magnétique extérieur **B**. On a alors affaire à une résonance de Feschbach, comme il est illustré Fig.4.3.
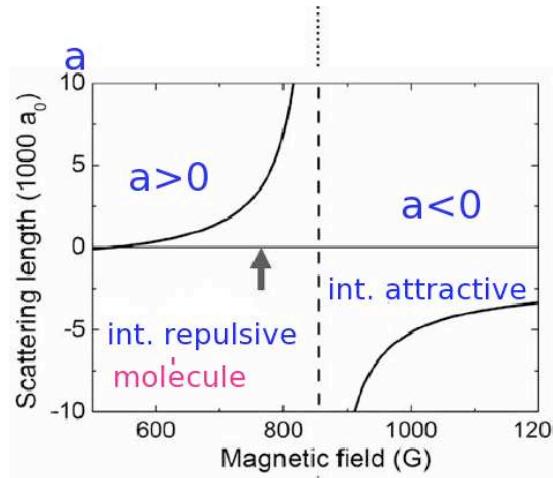
FIG. 4.3 – Résonance de Feschbach pour le ^6Li : longueur de diffusion a en fonction du champ magnétique B [10]. La résonance se situe à $834\,G$.

---

[1] Le crossover BEC-BCS a aussi été envisagé pour la matière nucléaire [15, 16, 17].

4.1 Crossover BEC-BCS dans l'approximation des "échelles"

J'ai étudié, en collaboration avec R. Combescot et Maxim Y. Kagan (Kapitza Institute, Moscou, Russie) le problème du "crossover BEC-BCS" (publication $n°17$). En particulier, nous avons déterminé le diagramme de phase température en fonction de l'inverse de la longueur de diffusion $(T/E_F, 1/k_F a)$. L'énergie de Fermi E_F est donnée par $E_F = k_F^2/(2m)$. Le cadre théorique est exposé Fig.4.4, où les diagrammes de Feynman retenus pour la fonction de Green sont dessinés. L'intérêt de cette approximation, dans
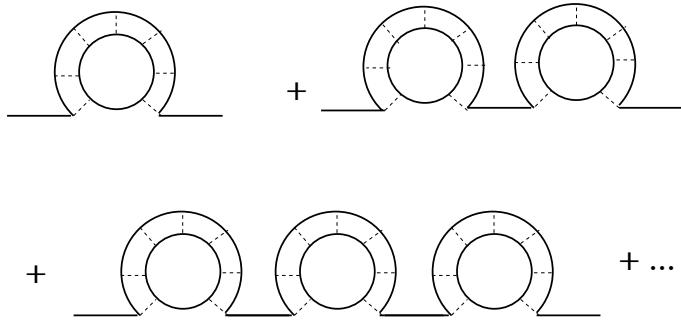
Fig. 4.4 –

la phase normale, est qu'elle permet de tenir compte d'un état lié moléculaire d'une part et surtout de décrire correctement la température critique dans la limite BEC. L'approximation originale de Nozières et Schmitt-Rink [18] correspond à ne retenir que les diagrammes avec une seule roue dans la Fig.4.4; par conséquent, notre approximation apparaît comme une amélioration de leur approche. Nous avons déterminer numériquement la ligne de transition fluide normal-superfluide (voir Fig.4.5). Celle-ci est en accord avec les travaux de Pieri et Strinati, [19] dont l'approche coïncide avec la nôtre sur la ligne de transition.

Nous avons également déterminé la ligne de formation moléculaire. Dans le vide, c'est la ligne $1/k_F a = 0$, correspondant à la résonance. A cause du principe de Pauli, qui gêne la formation de molécule de petit vecteur d'onde, celle-ci est déplacée du côté BEC. A droite de cette ligne, il y a formation de molécules de toutes impulsions. Cette ligne est déterminée en cherchant l'apparition de molécules d'impulsion totale nulle.

Nous avons étudié analytiquement différents cas limites dilués (limites BEC, BCS, liquide de Fermi dilué, développement du viriel dans la limite classique) et nous retrouvons les résultats connus. Notre approche a mélangé des calculs numériques ainsi que des développements analytiques qui ont, je crois, amélioré notre compréhension du sujet. Je pense que cette théorie est un bon départ pour développer des approches plus sophistiquées.

Un des points faibles de la théorie, visible sur les diagrammes de la Fig.4.4, est qu'elle ne tient pas compte de possibles interactions entre molécules. Cependant, on sait que celles-ci sont déterminantes dans la phase superfluide moléculaire (en bas à droite du diagramme de phase Fig.4.5. Or, on sait que pour un superfluide constitué de bosons ponctuels, l'interaction est entièrement déterminée, du fait de la faiblesse des énergies
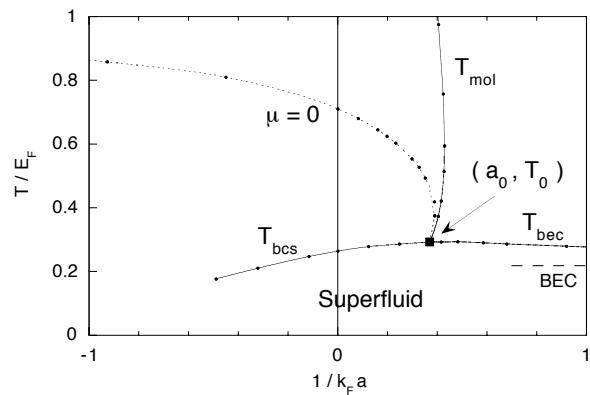
FIG. 4.5 – Diagramme de phase pour le crossover BEC-BCS (ligne $T_{bcs} - T_{bec}$). Sont également indiquées la ligne de potentiel chimique nulle $\mu = 0$, ainsi que la ligne de formation moléculaire T_{mol}.

mises en jeu, par la *longueur de diffusion a*. Il est donc naturel de déterminer la longueur de diffusion molécule-molécule - c'est l'objet de la section qui suit.

4.2 Problème de mécanique quantique à 3 ou 4 corps

La longueur de diffusion molécule-molécule apparaît alors comme une quantité cruciale. Elle repose sur un calcul de mécanique quantique à 4 corps. C'est la raison pour laquelle nous avons étudié, dans l'optique des gaz froids, les problèmes à 3 et 4 corps. L'originalité de l'approche vient de la technique employée : les diagrammes de Feynman. Nous avons ainsi déterminé la longueur de diffusion molécule-molécule, ainsi que les énergies d'états liés à 3 ou 4 corps, en dimension 2 (publications $n°16$, 18).

On peut être surpris de prime abord que l'on puisse résoudre un problème de mécanique quantique à trois corps (sans parler de quatre corps !). Cela vient bien sûr de l'hypothèse ô combien simplificatrice-mais justifiée- de potentiel d'interaction à deux corps *à courte portée*.

L'idée est simple. Considérons à titre d'exemple trois particules $1, 2$ et 3, avec 1 et 3 dans l'état interne $\uparrow$ et 2 dans $\downarrow$. Sans entrer dans les détails, il est aisé de comprendre intuitivement que l'interaction à courte portée se manifeste uniquement par des conditions aux limites pour la fonction d'onde lorsque deux particules de spin opposés se trouvent à la même position (voir Fig.4.6 a). Il est alors évident que seul le vecteur $\mathbf{R}$ reliant $\mathbf{1} - \mathbf{2}$ à $\mathbf{3}$ est pertinent. Par symétrie sphérique, seule la norme R est la variable importante. Le problème ne dépend donc que d'une seule variable scalaire R. Cette énorme simplification est bien sûr confirmée par les calculs. On peut appliquer ce raisonnement au cas de quatre particules, en rajoutant une particule 4 de spin $\downarrow$ (Fig.4.6 b). Dans ce cas, l'invariance par rotation fait que le problème ne dépend que des normes des vecteurs $\mathbf{x}$ et $\mathbf{y}$ ainsi que de l'angle α entre ces deux vecteurs. On se rend compte ici qu'on aboutit à trois variables indépendantes, ce qui est vraiment remarquablement simple pour un problème avec quatre particules ! C'est ce qui permet de le résoudre en pratique.
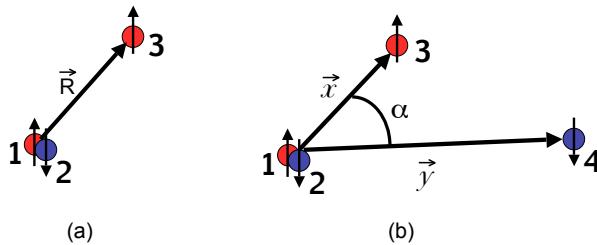
Fig. 4.6 – (a) Le problème à trois corps dans le cas d'interaction à courte portée ne fait intervenir que la norme du vecteur $\mathbf{R}$. (b) Le problème à quatre corps ne fait intervenir que les normes des vecteurs $\mathbf{x}$ et $\mathbf{y}$, ainsi que l'angle α.

4.2.1 Problème à 3 corps

Je montre ici, en suivant la Réf.[21], comment on peut facilement résoudre le problème à trois corps avec des diagrammes de Feynman. Pour fixer les idées, il y a deux fermions de spin $\uparrow$ et un de spin $\downarrow$. Il faut pour cela considérer le vertex $T_3(p_1, p_2; P)$ (appelé aussi matrice T à trois corps) avec un fermion de spin $\uparrow$ entrant (respectivement sortant) de

moment p_1 (respectivement p_2) et un dimère entrant (respectivement sortant) de moment $P - p_1$ (respectivement $P - p_2$). Le dimère est représenté par une double ligne en traits épais et est noté T_2. Il est la somme de tous les diagrammes "échelles" correspondant à l'interaction répétée de deux fermions de spins opposés. Le diagramme le plus simple que l'on peut dessiner correspond à l'interaction du fermion de spin up entrant avec le fermion de spin down du dimère entrant. Mais nous pouvons resommer toutes les interactions répétées entre ces deux fermions, ce qui correspond à T_2. Nous voyons ainsi que cela correspond à un échange de spin up comme montré Fig.4.7. De manière générale,
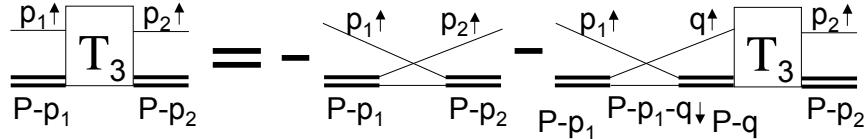
FIG. 4.7 – Resommation des diagrammes dans le problème à trois corps.

après le premier échange des fermions de spin up, il y a un fermion de spin up et un dimer entrant. Par conséquent, tous les diagrammes suivants sont exactement ceux du vertex fermion-dimer T_3. On obtient donc une relation fermée pour T_3 (Fig.4.7), qui est une équation intégrale.

En résolvant numériquement cette équation, nous pouvons ainsi retrouver aisément la longueur de diffusion fermion-dimère $a_3 = 1.18\,a$, déjà obtenu dans les Réf.[20] (à l'aide de l'équation de Schrödinger) et [21] (à l'aide de diagrammes de Feynman).

Nous avons aussi déterminé des états liés à 3 corps et 2 dimensions d'espace ($2D$), dans le cas de trois bosons identiques (2 états liés) et de deux bosons identiques et un fermion (1 état lié), ce qui n'avait pas été fait auparavant.

4.2.2 Problème à 4 corps

Le cas du problème à 4 corps s'avère beaucoup plus difficile. Nous définissons de la même manière une matrice T à 4 corps T_4, avec deux dimères entrants et deux sortants (Fig.4.8 a). Cependant il n'est pas possible de trouver une équation fermée pout T_4 comme nous l'avions fait pour T_3. Il s'est avéré essentiel d'introduire un nouveau vertex Φ. Celui-ci ressemble à T_4, à la différence qu'un des deux dimères incidents est remplacé par une paire de fermions up et down *qui n'interagissent pas l'un avec l'autre* (Fig.4.8 b). Il est alors possible de resommer les diagrammes pour T_4 (et Φ) en fonction de ceux de T_4 et Φ [2]. On aboutit à des équations fermées, que l'on peut résoudre numériquement. Nous avons pu ainsi calculer la longueur de diffusion molécule-molécule $a_M = 0.60\,a$, en accord avec la référence [22]. Nous avons aussi déterminé à $2D$ les énergies des états liés dans les cas où il y a 4 bosons identiques (2 états liés), ou bien un fermion interagissant avec 3 bosons identiques (1 état lié), ou encore deux fermions discernables interagissant avec deux bosons identiques (2 états liés).

---

[2]L'explication détaillée de la resommation est donnée dans la publication n°19.
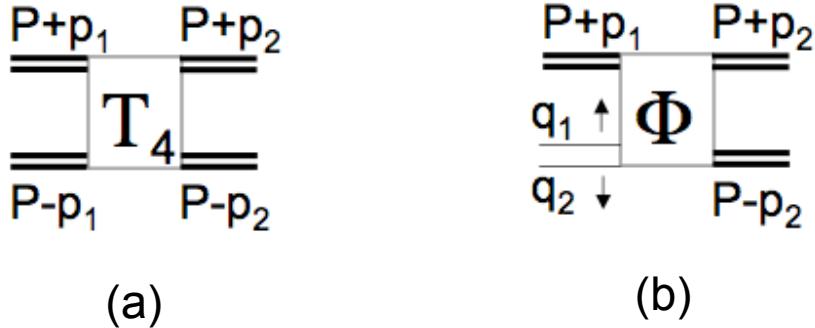
FIG. 4.8 – (a) Matrice T du problème à 4 corps, et (b) le nouveau vertex Φ.

4.2.3 Conclusion

Ces calculs de problèmes "à quelques corps" à l'aide de technique diagrammatique de la théorie des champs peuvent paraître un peu artificiel, puisqu'après tout, il suffit de résoudre l'équation de Schrödinger ! Ils présentent cependant des avantages. Tout d'abord, une fois que l'on a déterminé comment resommer les diagrammes, on peut généraliser aisément, comme nous l'avons fait, à n'importe quel type de particules (bosons, fermions, masses différentes) et dimension d'espace ($2D$ ou $3D$).

Mais la motivation la plus profonde et originale à notre travail est que ce type d'approche diagrammatique s'inscrit parfaitement dans le problème à N-corps : dans les deux cas on utilise des diagrammes de Feynman. C'est l'objet de la prochaine section de montrer comment utiliser ces résultats des problèmes à 3 et 4 corps dans le problème à N corps qu'est l'équation d'état de Lee-Huang-Yang.

4.3 Equation d'état de Lee-Huang-Yang

4.3.1 Position du problème

La limite BEC du crossover BEC-BCS correspond physiquement à une situation où tous les fermions de spins opposés forment des molécules, qui sont en première approximation des bosons, et condensent donc à température nulle. Cependant, lorsqu'on diminue $1/(k_F a)$ (en augmentant la densité), on se rapproche de la limite BCS, où les paires de Cooper s'entrelacent et ne correspondent donc plus du tout à des bosons ponctuels. La question qu'on se pose est alors la suivante : dans quelle mesure le caractère composite des bosons apparaît-il lorsque la densité augmente ? Cette question est très générale. On va donc se restreindre au calcul plus modeste du développement basse densité du potentiel chimique (équation d'état) et se demander si le caractère composite des bosons apparaît dans l'éqation d'état. Nous donnons tout de suite le résultat : le potentiel chimique μ de nos fermions de densité n par spin, dans le régime BEC est donné par

$$\mu \;=\; -\frac{E_b}{2} + \frac{\hbar^2 \pi a_M}{m}\, n\, \left[1 + \frac{32}{3\sqrt{\pi}}(na_M^3)^{1/2} \right] + \cdots \tag{4.1}$$

où l'énergie de liaison d'un dimère vaut $E_b = \hbar^2/ma^2$. Mis à part le premier terme évident, c'est très précisément le résultat trouvé par Lee, Huang et Yang (LHY) [23] pour $\mu_{Bose} = 2\mu$ et des bosons de densité n, masse $m_B = 2m$ et de longueur de diffusion $a_B = a_M$. Le premier terme linéaire en densité ("champ moyen") était assez prévisible. Cependant, la correction LHY est totalement identique, ce qui n'était pas du tout évident. Il apparaît d'ores et déjà la difficulté du problème dans l'expression. En effet, celle-ci contient la longueur de diffusion dimère-dimère a_M, qui, comme on l'a vu précédemment, fait intervenir un calcul de mécanique quantique à 4 corps. "Mettre du 4 corps dans le N corps", c'est en quelque sorte ce qu'il faut faire afin de résoudre le problème. Par la suite, j'explique qualitativement comment intervient le problème à 4 corps. J'expose ensuite la démarche générale du calcul menant à l'Eq.4.1. Le terme correctif en $n^{3/2}$ vient de la prise en compte des modes collectifs. Les explications fournies sont nullement suffisantes, mais permettront je l'espère au lecteur de comprendre la démarche. En particulier, le non-spécialiste pourra suivre je l'espère l'argumentation visuelle des diagrammes, sans entrer dans les détails de calcul. Pour plus de détail, le lecteur pourra se référer à l'article original [24] et à la version longue [25].

4.3.2 Le fond du problème : du 4 corps dans le N corps

Dans la technique diagrammatique, l'existence d'un superfluide se traduit par l'apparition de fonctions de Green "anormales" F et $F^\dagger$ [26](à température nulle)

$$F(\mathbf{k}, t) \;=\; i\, \langle T\left[c_{\mathbf{k}\uparrow}(t) c_{-\mathbf{k}\downarrow} \right] \rangle \tag{4.2}$$

ainsi que sa transformée de Fourier $F(k)$ ($k \equiv \{\mathbf{k}, \omega\}$). On définit de même des self-energies anormales $\Delta(k)$. En terme de diagrammes de Feynman, $\Delta(k)$ correspond à la destruction d'une paire d'atomes ($k\uparrow, -k\downarrow$) qui vont dans le condensat. Réciproquement $\Delta^*(k)$ correspond à la création d'une paire hors du condensat. On est alors amené à écrire $\Delta(k)$ comme la somme de deux contributions $\Delta(k) = \delta_1(k) + \delta_2(k)$. Le premier terme, qui

est le seul retenu dans la théorie BCS, regroupe *tous* les diagrammes où les deux atomes interagissent *en premier* l'un avec l'autre via le potentiel à deux corps de transformée de Fourier $V(\mathbf{q})$. On a donc (Fig.4.9)

$$\delta_1(\mathbf{k}) \;\; = \;\; \sum_{k_1} V(\mathbf{k} - \mathbf{k_1}) F(k_1) \tag{4.3}$$

où il apparaît la fonction de Green anormale F *exacte* (elle est symbolisée par un trait épais) et on utilise par la suite la notation compacte $\sum_k \equiv i \int \frac{d^3 \mathbf{k}}{(2\pi)^3} \int_{-\infty}^{+\infty} \frac{d\omega}{2\pi}$.
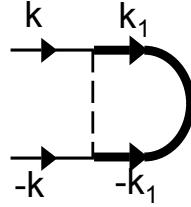
FIG. 4.9 – Contribution "à la BCS" à Δ

Pour la deuxième classe de diagramme, on procède à un développement basse densité, ce qui correspond dans cette limite BEC, à un développement en puissance de Δ. Puisque Δ détruit 2 particules et Δ^* en crée 2, il doit y avoir un Δ de plus que de Δ^* dans l'expression de $\delta_2(k)$. Le terme avec un seul Δ est inclus dans δ_1, donc il faut tenir compte des termes qui contiennent $\Delta\Delta^*\Delta$, les autres diagrammes étant constitués de propagateurs normaux. De plus, ces diagrammes normaux ne peuvent contenir de boucles de propagateurs normaux, puisque cela correspondrait à la création de paires particules-trous. De tels processus sont impossibles dans l'état normal à $T = 0$ et pour $\mu < 0$, puisque tous les propagateurs libres sont retardés [24, 25]. L'ensemble des diagrammes que l'on obtient peut être symbolisé par le dessin de gauche de la Fig.4.10, dans lequel on voit que 4 fermions entrent à gauche du bloc (deux fermions ($k \uparrow, -k \downarrow$) et une paire du condensat "sortant" de Δ^*) et 4 fermions en sortent à droite (deux paires "retournent" dans le condensat, d'où deux Δ). Si l'on tient compte du fait que les deux fermions ($k \uparrow, -k \downarrow$) n'interagissent pas en premier, alors on retrouve exactement la fonction $\Phi(k, -k; 0, 0)$ rencontrée précédemment dans l'étude du problème à 4 corps. A la différence près que les diagrammes retenus doivent être une-particule irréductible, c'est-à-dire ne pas contenir de propagateur $G_0(k)$ ou $G_0(-k)$. Ceci est expliqué en détail dans [24, 25]. On tient compte de cette difference en notant Φ' la contribution. A l'ordre Δ^3, on a donc [3]

$$\delta_2(k) = \frac{1}{2}\, |\Delta|^2 \Delta\, \Phi'(k, -k; 0, 0) \tag{4.4}$$

Notre objectif est donc rempli : on a réussi à mettre en évidence le problème à 4 corps, au travers de la fonction-hautement non triviale !-Φ, dans le problème à N corps.

---

[3]Le facteur 1/2 vient du fait qu'il y a deux Δ en sortie du bloc, et qu'on ne veut pas compter deux fois les mêmes diagrammes, comme par exemple on peut aisément le voir dans la contribution "de Born" (pas de "double comptage").
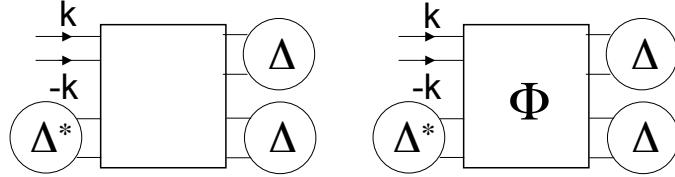
FIG. 4.10 – Ces diagrammes montrent comment le problème à 4 corps émerge dans le problème à N corps.

Avant de poursuivre, nous pouvons développer de la même manière la self-energie normale $\Sigma(k)$. A l'ordre 0 en Δ, c'est la self-energie de l'état normal, qui pour $\mu < 0$ et $T = 0$ est le vide ! Par conséquent (et on le justifie par le calcul), la self-energie, qui décrit physiquement l'interaction entre l'atome introduit et le milieu (ici le vide), vaut 0. A l'ordre Δ^2, on trouve, comme pour $\Delta(k)$, que $\Sigma(k)$ est donné par les diagrammes de la Fig.4.11, où il apparaît cette fois la matrice T du problème à trois corps !

$$\Sigma(k) \quad = \quad \Delta \Delta^* T_3'(k, k; k) \tag{4.5}$$

Ici encore, il faut retenir les diagrammes une-particule irréductible, ce qui est pris en
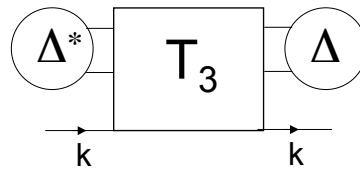
FIG. 4.11 – Self-energie normale à l'ordre le plus bas.

compte par la notation T_3'. On trouve facilement que seule "l'approximation de Born" de T_3, $-G_0(-k)$, donne une contribution réductible, d'où $T_3'(k, k; k) = T_3(k, k; k) - (-G_0(-k))$. En conclusion de cette section, remarquons que le que le diagramme Fig.4.11 a une interprétation physique simple : un atome k et une paire d'atome du condensat (Δ) sont créés , puis ils interagissent (ce qui est totalement décrit par T_3), puis l'atome k est détruit et la paire d'atomes retourne dans le condensat (Δ^*).

4.3.3   Principe du calcul

Le principe du calcul ressemble au calcul classique "à la BCS" [14] : on écrit une équation pour la densité et une pour le gap. Puis on élimine le gap Δ des deux équations pour exprimer μ en fonction de n.

De manière générale, la densité est reliée à la fonction de Green normale $G(k)$ via

$$n \quad = \quad -\sum_k e^{i\omega 0_+} G(k) \tag{4.6}$$

On développe par la suite $G(k)$ en puissance de Δ. De plus, le potentiel chimique apparaît aussi dans les expressions (par exemple dans $G_0(k)$) et on a donc pour n

$$n = f(\Delta, \mu) \tag{4.7}$$

L'équation du gap est un peu plus subtile. On écrit tout d'abord

$$F'(k) \equiv +F(k) - G_0(k)\delta_1(\mathbf{k})G_0(-k)$$

On peut éliminer δ_1 (qui contient le potentiel à deux corps V) au profit de la longueur de diffusion a et le potentiel chimique μ. On obtient alors [24, 25]

$$a^{-1} - \sqrt{2m|\mu|} = \frac{4\pi}{m}\sum_k F'/\Delta \tag{4.8}$$

$$a^{-1} - \sqrt{2m|\mu|} = g(\Delta, \mu) \tag{4.9}$$

A l'ordre le plus bas déterminé en section 4.3.2, on trouve [4]

$$n = \frac{m^2}{8\pi\left[2m|\mu|\right]^{1/2}}|\Delta|^2 + o(|\Delta|^2) \tag{4.10}$$

$$a^{-1} - \sqrt{2m|\mu|} = \frac{m^2 a^2}{8}\,a_M\,|\Delta|^2 + o(|\Delta|^2) \tag{4.11}$$

Si l'on élimine Δ des Eq.4.10 and 4.11, on retrouve les deux premiers termes du développement de LHY Eq.4.1.

4.3.4 Contribution des modes collectifs

On pourrait être tenté de développer G à l'ordre Δ^4, puis F' à l'ordre Δ^5. Cependant, on se rend compte alors que ces termes apportent des corrections d'ordre n^2 à μ, qui est négligeable devant le terme en $n^{3/2}$ de LHY. Ce comportement singulier en $n^{3/2}$ vient en fait de l'existence de modes collectifs (à grande longueur d'ondes des ondes sonores). En effet, dans ce superfluide neutre, il y a une branche du spectre d'excitation dont l'énergie tend vers zéro lorsque l'impulsion tend vers zéro. Nous avons donc étudié les modes, en tirant partie de la faible densité atomique. A grande longueur d'onde, nous retrouvons un mode collectif de type Bogolubov. L'expression mathématique de celui-ci contient la longueur de diffusion moléculaire-donc le problème à 4 corps. Les diagrammes correspondants sont indiqués Fig.4.12. Ils sont obtenus en remplaçant le produit $\Delta\Delta^*$ ou $\Delta\Delta$ par des propagateurs de modes, représentés par des lignes en traits épais [5]. Une fois ceci fait, le développement des Eqs.4.10 et 4.11 est complété aux ordres $\Delta^3 = O(n^{3/2})$ et $\Delta^4 = O(n^2)$ respectivement. Eliminant Δ des équations, on retrouve l'Eq.4.1.

---

[4]Il est remarquable -mais assez simple à comprendre [24, 25]- que le problème à trois corps n'apparaît pas dans le résultat.

[5]Les propagateurs de modes "barrés" sont obtenus en soustrayant les termes d'ordre Δ^0 et Δ^2 afin d'éviter le "double comptage".
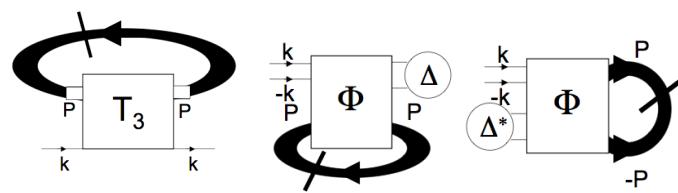
Fig. 4.12 – Self-energies normale et anormale dues aux modes collectifs.

Chapitre 5

Autres travaux

J'ai collaboré de manière ponctuelle avec Monique Combescot du groupe de Physique des Solides (Jussieu, actuel INSP) sur deux articles. Plus récemment, je collabore avec C. Mora et N. Regnault du Laboratoire Pierre Aigrain de l'ENS sur des calculs de bruits de courants dans des boîtes quantiques ou des nanotubes de carbone.

5.1 Caractère bosonique des excitons-calcul de la norme d'un état à N excitons

Nous avons travaillé, avec M. Combescot, sur le problème du caractère bosonique des excitons dans les semi-conducteurs. En effet, lorsque la distance inter-particule devient de l'ordre de la taille de l'exciton, celui-ci ne peut plus être considéré comme un boson ponctuel. Il s'agissait plus précisément de calculer la norme d'un état avec N excitons. Ceci n'est pas trivial dû à la nature composite d'un exciton (état lié particule-trou). J'ai pu apporter ma connaissance de la théorie BCS de la supraconductivité afin de faire ce calcul. Cet article (publication $n°10$) s'inscrit dans le cadre du travail mené par Monique Combescot sur la nature non parfaitement bosonique des excitons. Notons que cette question intéressante se pose aussi pour les grandes molécules produites dans les gaz ultra froids.

5.2 Puits quantique et Excitons

Un autre article, en collaboration avec M. Combescot, a porté sur le calcul des niveaux d'énergie E d'une particule de masse m dans un puits quantique de profondeur V et de largeur $2\,R$, à une, deux et trois dimensions. Une formule analytique reproduisant très précisément les résultats numériques a été établie. La figure 5.1 montre les résultats numériques et analytiques, pour $\alpha = \sqrt{2mR^2\,E/\hbar^2}$ en fonction du paramètre de profondeur de puits $\nu = \sqrt{2mR^2\,V/\hbar^2}$. On voit qu'ils sont quasi-indiscernables. Outre son intérêt théorique évident, ce résultat pourra aussi être utile aux expérimentateurs des nanostructures (publication $n°8$).
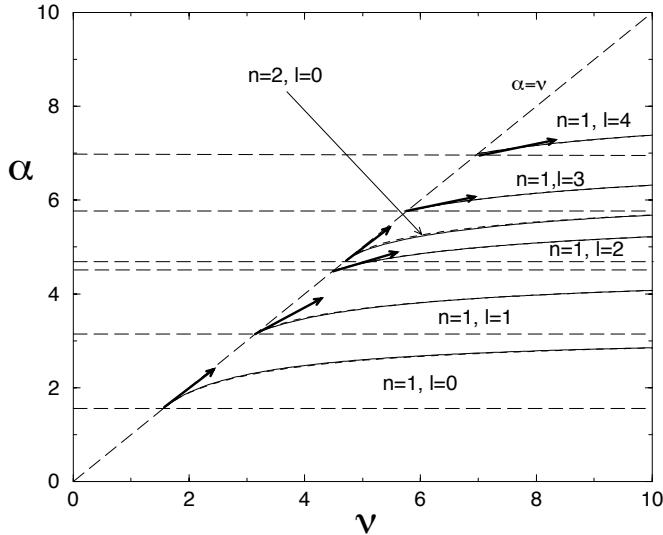
FIG. 5.1 – Le paramètre d'énergie $\alpha = \sqrt{2mR^2\,E/\hbar^2}$, pour le n^{me} niveau de l'état (l, m) d'un puits sphérique (*i.e.* 3D), en fonction du paramètre $\nu = \sqrt{2mR^2\,V/\hbar^2}$. Le calcul numérique est en trait plein, le calcul de la formule analytique approchée est en tiret.

5.3   Bruit de courant à travers un point quantique

Récemment, j'ai collaboré avec Christophe Mora et Nicolas Regnault du Laboratoire Pierre Aigrain de l'ENS. Nous avons travaillé sur un problème de physique mésoscopique. Nous avons calculé le bruit de courant pour un modèle qui pourrait s'appliquer aux nanotubes de carbone (publication $n°20$) . Une des motivations de ce travail vient du fait que Takis Kontos, du Laboratoire Pierre Aigrain de l'ENS, mène actuellement des expériences de mesure de bruit dans les nanotubes de carbone. Plus spécifiquement, considèrons un dispositif nanométrique (par exemple une boîte quantique ou un nanotube de carbone) couplé à deux fils (électrodes) soumis à une différence de potentiel. Dans certaine situation, le dispositif peut être assimilé à une impureté magnétique [27]. Celle-ci interagit avec les électrons des fils via un couplage antiferromagnétique dans le cas le plus simple. A basse température, d'après les travaux de Nozières [28], l'impureté se comporte comme un obstacle statique à l'ordre le plus bas (toute la dynamique de l'impureté-dispositif est contenue dans un simple déphasage). En augmentant la température, selon l'idée des liquides de Fermi, des quasiparticules sont créées et modifient les propriétés de transport. Techniquement, cela revient à traiter perturbativement une interaction effective entre électrons des fils induite par l'impureté. Le calcul du bruit de courant est un peu compliqué, en particulier car il faut tenir compte de plusieurs contributions (six) diagrammatiques et qu'il faut utiliser un formalisme qui permet de traiter des situations hors équilibre (formalisme de Keldysh)[1].

Notre calcul a été effectué à température et tension aux bornes des électrodes non nulles. Il montre entre autres que les corrections en température sont importantes et que la limite de température nulle est assez difficilement atteinte.

---

[1] En effet, les électrodes sont à des potentiels chimiques différents.

Chapitre 6

Projets de recherche

Je décris ci-dessous mes projets de recherche. Ils portent sur les gaz fermioniques ultra-froids. La première partie concerne des travaux sur le crossover BEC-BCS. Dans la deuxième partie, je présente des directions de recherche sur les mélanges de fermions d'espèces différentes, un sujet qui devrait voir des développements expérimentaux durant les prochaines années. La troisième partie explique brièvement les travaux possibles, dans le prolongement de ma collaboration avec C. Mora et N. Regnault du LPA.

6.1 Cross-over BEC-BCS

Ce sujet est extrèmement riche et je détaille ci-dessous les questions auxquelles je souhaite répondre, dans le prolongement de la publication $n°17$.

6.1.1 Compressibilité dans la phase normale

Dans le modèle de champ moyen le plus naïf, la compressibilité diverge lorsque $k_F a = -\pi/2$, ce qui correspond à une instabilité (effondrement ou "collapse") qui n'a jamais été observé expérimentalement. Un calcul intéressant est donc, dans le cadre du modèle expliqué Chapitre 4, celui de la compressibilité. On verra alors si cette dernière diverge ou non. F. Alzetto, actuellement en thèse avec R. Combescot et moi-même, travaillons sur ce sujet.

6.1.2 Limite unitaire

Récemment, plusieurs équipes ont effectué des mesures d'entropie et d'énergie dans la limite unitaire du crossover BEC-BCS [29, 30, 31]. Il apparaît donc très intéressant de calculer dans le cadre de notre théorie l'entropie et l'énergie, lorsque la température diminue. Pour cela, il nous faut étendre la théorie à la phase superfluide. Une théorie qui est en continuité avec la nôtre est celle proposée par le groupe de Pieri et Strinati [19]. F. Alzetto travaille actuellement sur ce projet, qui est, lui aussi en direct continuité des travaux du Chapitre 4 .

6.1.3   Densité spectrale et gap dans la limite BEC

Nos travaux sur l'équation d'état de Lee-Huang-Yang contiennent en fait plus que le résultat du développement du potentiel chimique à basse densité. En effet, nous avons déterminé également des développements pour les quantités dynamiques que sont les self-energies normales et anormales. Ceci doit nous permettre de calculer, dans cette limite diluée, la densité spectrale, et donc en particulier le gap à une particule (énergie minimum à fournir pour rajouter une particule).

6.1.4   Amélioration de la théorie du cross-over BEC-BCS

Le calcul de l'approximation "des échelles" du chapitre 4 ne tient pas compte de l'interaction entre molécules. Nous avons réussi à tenir compte de cette interaction dans la limite BEC. Il serait donc très intéressant d'étendre cette approche à l'ensemble du crossover. Techniquement, il faut inclure les collisions à 3 et 4 corps, ce qui n'a jamais été fait jusqu'à présent.

6.2   Superfluides dans des mélanges fermioniques ul-trafroids

6.2.1   Limite BEC d'un mélange de fermions

Considèrons un mélange de fermions de "spin 1/2" avec une interaction résonante menant au cross-over BEC-BCS, mais avec un déséquilibre de population ($n_\uparrow \neq n_\downarrow$). Je pense qu'il est possible, dans la limite BEC, de déterminer par exemple un développement en puissance de la densité de l'équation d'état. On aurait alors une généralisation de l'équation d'état de Lee-Huang-Yang, mais pour un rapport $n_\downarrow/n_\uparrow$ quelconque. Dans ce résultat figurerait certainement le problème à trois corps résultant de la collision entre les dimères condensés et les fermions "célibataires" de l'espèce en excès.

6.2.2   Mélange de fermions d'espèces différentes

Différents groupe expérimentaux (par exemple au LKB ENS, ou dans l'équipe de R. Grimm à Innsbruck) montent actuellement des expériences avec deux voire trois espèces d'atomes différents. Ces expériences donneront certainement des résultats très intéressants dans le futur. Un des points à noter est qu'elle n'ont pas d'équivalent en matière condensée : tous les électrons ont la même masse ! Du point de vue théorique, la limite diluée fera certainement intervenir les problèmes à quelques corps. L'étude du problème à trois corps, dans la lignée du Chapitre 4 section 4.2.1, mais avec des masses différentes peut réserver des surprises. En effet, même dans le cas de trois fermions, il peut y avoir des états liés à trois corps très particuliers : les états d'Efimov [32]. Je pense avoir tous les outils pour inclure ces effets dans le problème à N corps, dans la lignée de nos travaux sur l'équation d'état de Lee-Huang-Yang.

Un autre exemple : les auteurs de la Réf.[33] ont récemment considéré un mélange de fermions de masses différentes. Ces fermions peuvent former des molécules hétéro-nucléaires diatomiques. La prédiction de [33] est qu'à température nulle, si le rapport

des masses entre les deux espèces est suffisamment grande, il peut y avoir une phase *cristalline.*

En conclusion, je voudrais encore souligner que ces systèmes ont été peu étudiés et il y a certainement des phénomènes nouveaux à découvrir, à l'image de la cristallisation prédite en [33].

6.3   Bruit de courant et effet Kondo

Tout d'abord, nous travaillons, en collaboration avec C. Mora du LPA, à une version plus détaillée de notre travail sur le bruit de courant dans l'effet Kondo (publication numéro 20). Nous voulons ainsi généraliser le calcul au cas où le couplage de l'"impureté" avec les électrodes droite et gauche n'est pas symétrique, comme c'est fatalement le cas expérimentalement. Enfin, dans un avenir plus lontain, nous souhaiterions étudier ce qu'il se passe lorsque les électrodes sont supraconductrices.

Bibliographie

[1] W. N. Hardy *et al.*, Phys. Rev. Lett., **70**, 3999 (1993).

[2] U. Sivan *et al.*, Europhys. Lett. **25**, 605 (1994).

[3] B. L. Altshuler *et al.*, Phys. Rev. Lett., **78**, 2803 (1997) .

[4] M. Ueda and A. J. Leggett, Phys. Rev. Lett. **80**, 1576 (1998).

[5] F. Dalfovo *et al.*, Rev. Mod. Phys., **71**, 463 (1999).

[6] M. Olshanii, Phys. Rev. Lett. **81**, 938 (1998).

[7] C. Menotti and S. Stringari, Phys. Rev. A **66**, 043610 (2002).

[8] E. H. Lieb and W. Liniger, Phys. Rev. **130**, 1605 (1963).

[9] M. Greiner *et al.*, Nature (London) **426**, 537 (2003) ; S. Jochim *et al.*, Science **302**, 2101 (2003) ; M. Zwierlein *et al.*, Phys. Rev. Lett. **91**, 250401 (2003) ; T. Bourdel *et al.*, *ibid*, **93**, 050401 (2004).

[10] M. Bartenstein *et al.*, Phys. Rev. Lett. **92**, 120401 (2004).

[11] G. Astrakharchik *et al.*, Phys. Rev. Lett. **93**, 200404 (2004).

[12] M. Bartenstein *et al.*, Phys. Rev. Lett. **92**, 203201 (2004).

[13] A. Altmeyer *et al.*, Phys. Rev. Lett. **98**, 040401 (2007).

[14] A. J. Leggett, J. Phys. (Paris), Colloq. **41**, C7-19 (1980).

[15] M. Baldo, U. Lpmbardo and P. Schuck, Phys. Rev. C **52**, 975 (1995)

[16] H. Stein, A. Scnell, T. Alm and G. Röpke, Z. Phys. A **351**, 295 (1995)

[17] M. Schmidt, G. Röpke and H. Schulz, Ann. Phys. (N. Y.) **202**, 57 (1985)

[18] P. Nozières and S. Schmitt-Rink, J. Low Temp. Phys., **59**, 195 (1985).

[19] A. Perali *et al.*, Phys. Rev. Lett. **92**, 220404 (2004).

[20] G. V. Skorniakov and K. A. Ter-Martirosian, Zh. Eksp. Teor. Fiz. **31**, 775 (1956) [Sov. Phys. JETP **4**, 648 (1957)].

[21] P. F. Bedaque and U. van Kolck, Phys.Lett. B **428**, 221 (1998).

[22] D. S. Petrov *et al.*, Phys. Rev. Lett. **93**, 090404 (2004).

[23] T. D. Lee and C. N. Yang, Phys. Rev. **105**, 1119 (1957) ; T. D. Lee, K. Huang and C. N. Yang, Phys. Rev. **106**, 1135 (1957).

[24] X. Leyronas and R. Combescot, Phys. Rev. Lett. **99**, 170402 (2007).

[25] R. Combescot and X. Leyronas, en préparation.

[26] A. A. Abrikosov, L. P. Gorkov and I. E. Dzyaloshinski, *Methods of quantum field theory in statistical physics* (Dover, 1975).

[27] L. Kouwenhoven and L. I. Glazman, Phys. World **14**, 33 (2001).

[28] P. Nozières, J. Low Temp. Phys. **17**, 31 (1974).

[29] G. B. Partridge *et al.* Science **311**, 503-505 (2006).

[30] J. T. Stewart *et al.* Phys. Rev. Lett. **97**, 220406 (2006).

[31] L. Luo *et al.* Phys. Rev. Lett. **98**, 080402 (2007).

[32] E. Braaten and H.-W. Hammer Phys. Rept. **428** (2006) 259-390.

[33] D. S. Petrov *et al.*, Phys. Rev. Lett. **99**, 130407 (2007).

Sélection d'articles :

Dans ces quatre articles, il est question de physique des gaz ultrafroids.
– le premier article porte sur les modes hydrodynamiques.
  R. Combescot and X. Leyronas *Hydronamic modes in dense trapped ultracold gases*
  Phys. Rev. Lett. **89** 190405 (2002)
– le deuxième article examine la théorie microscopique présentée section 4.1.
  R. Combescot, X. Leyronas, M.Yu. Kagan *Self-consistent theory for molecular instabilities in a normal degenerate Fermi gas in the BEC-BCS crossover*
  Phys. Rev. A. **73**, 023618 (2006) [cond-mat/0507636]
– dans ce troisième article, il est question de problèmes à trois et quatre corps.
  I.V. Brodsky, A. V. Klaptsov, M. Yu Kagan, R. Combescot
  and X. Leyronas
  Exact diagrammatic approach for dimer-dimer scattering and bound states of three and four resonantly interacting particles Phys. Rev. A **73**, 032724 (2006)
– le dernier article déduit l'équation d'état de Lee-Huang-Yang pour des bosons composites.
  X. Leyronas and R. Combescot *Superfluid equation of state of dilute composite bosons* Phys. Rev. Lett. **99**, 170402 (2007)

Ce mémoire présente un résumé de mon travail de chercheur en théorie de la matière condensée.

Je présente tout d'abord mon travail de doctorat sur un modèle du supraconducteur à haute température critique $YBa_2Cu_3O_7$. Je décris aussi les calculs de la profondeur de pénétration du champ magnétique, motivés par des expériences, dans le cadre de la théorie de couplage fort électron-phonon d'Eliashberg. La deuxième partie est consacrée aux travaux effectués lors de mon séjour postdoctoral sur la durée de vie d'une quasiparticule dans une boîte quantique. Puis j'aborde le sujet des atomes ultra-froids : modes collectifs et transition BEC-BCS. A cette occasion sont entre autres présentés mes travaux sur les problèmes à trois et quatre corps en mécanique quantique, ainsi que l'équation d'état d'un condensat de bosons composites. Je passe ensuite à mes travaux sur les excitons et le calcul de bruit de courant à travers un point quantique. Enfin, je présente mes projets de recherche.

Mots clés : supraconducteurs à haute température critique, théorie d'Eliashberg, superfluides fermioniques, transition BEC-BCS, problèmes à trois et quatre corps, excitons, effet Kondo, bruit de grenaille.

This document presents my research work, as a condensed-matter theorist.

First, I explain my thesis work about a model for the High Temperature Superconductor $YBa_2Cu_3O_7$. I also describe magnetic field penetration depth calculations within the strong coupling Eliashberg theory. These were motivated by experiments. The second part of this dissertation deals with my work as a postdoctorate on the lifetime of a quasiparticle in a quantum dot. Then, I tackle the subject of ultra-cold atoms : collective modes and BEC-BCS crossover. Within this last item, I descibe my work on the three and four body problem in quantum mechanics, as well as the equation of state of a condensate made of composite bosons. Then, I proceed with my works on excitons and shot noise through a quantum dot. Finally, I describe my research projects.

Key words : High Temperature Superconductors, Eliashberg strong coupling theory, fermionic superfluids, BEC-BCS crossover, three and four body problemsproblèmes, excitons, Kondo effect, shot noise.

Hydrodynamic Modes in Dense Trapped Ultracold Gases

R. Combescot and X. Leyronas

Laboratoire de Physique Statistique, Ecole Normale Supérieure, * *24 rue Lhomond, 75231 Paris Cedex 05, France*
(Received 30 January 2002; published 21 October 2002)

We consider the hydrodynamic modes for dense trapped ultracold gases, where the interparticle distance is comparable to the scattering length. We show that the experimental determination of the hydrodynamic mode frequencies allows one to obtain quite directly the equation of state of a dense gas. As an example, we investigate the case of two equal fermionic populations in different hyperfine states with attractive interaction.

Most of the fascinating recent work on ultracold gases [1] has been dealing with dilute situations. Naturally, even in this regime interactions play an important role, as in the case of Bose-Einstein condensation (BEC) where they strongly increase the size of the condensate compared to the free boson case. In this dilute regime the scattering length is small compared to the interparticle distance and the mean field approximation is valid. However, it is of great interest to explore the dense gas regime where scattering length and interparticle distance are comparable and mean field is no longer valid. This would lead to physical systems which are very simple examples of strongly interacting systems. These have much more complicated counterparts in condensed matter physics, such as liquid ^{4}He or ^{3}He, or the electron gas in metals. This regime is also of major experimental interest in the search for a BCS superfluid in fermion gases [2], since this is the range where the higher critical temperatures [3,4] will be found, which should make the transition more accessible. This dense regime corresponds to large scattering lengths, which can be reached in the vicinity of Feshbach resonances, as it has already been seen in optical traps [5]. Naturally, we assume that inelastic collisions, such as three-body recombination, will be small enough to be negligible.

In this paper we show that the experimental determination of the mode frequencies in the hydrodynamic regime allows one to obtain quite efficiently and directly the equation of state of a dense gas. Hydrodynamic equations are valid in the limit of low frequency (compared to elastic scattering time) and long wavelength, and have already been used to study the dilute Bose gas [1,6] (with very good experimental agreement) and the free Fermi gas [7]. In these cases the equation of state is known. We show that, rather surprisingly, the analysis of the equation giving the mode frequencies is not much more complicated when the equation of state is unknown and that one can conveniently invert the problem and get the equation of state from the mode spectrum. As an example, we apply our treatment to the case of two equal fermionic populations in different hyperfine states with attractive interaction; in particular, we investigate

the vicinity of the collapse, a very interesting physical situation analogous to ^{7}Li BEC collapse.

Although one might consider the extension to higher temperature, we work in the low temperature range where thermal effects are small and we neglect dissipation, so we deal with a perfect fluid. This should be valid for a strongly degenerate Fermi gas in its normal state (residual collisions would lead to a damping of the modes). Naturally, our results apply also to a superfluid when normal liquid effects (which would, in particular, produce damping) are negligible, such as low temperature Bose condensates or low temperature simple scalar BCS superfluids. We consider, for simplicity, an isotropic trapping potential $V(r)$ (mostly the harmonic case) but, somewhat surprisingly, most of our procedures can be generalized to the case of anisotropic harmonic traps. Also, we treat the 3D case, but lower dimensions can be handled in the same way.

With our hypotheses hydrodynamics reduces to the Euler equation $mn\,d\mathbf{v}/dt = -\nabla P - n\nabla V(r)$ supplemented by particle conservation $\partial n/\partial t + \nabla(n\mathbf{v}) = 0$ for density $n(\mathbf{r}, t)$ and thermodynamics. Since $\partial P/\partial n_0 = n_0 \partial \mu/\partial n_0$, the equilibrium particle density $n_0(r)$ satisfies $\mu(n_0(r)) + V(r) = \tilde{\mu}$, where $\tilde{\mu}$ is the overall chemical potential. Below, we refer for short to $\mu(n)$ as the equation of state. Linearizing these equations around equilibrium, one finds that the density fluctuation $n_1(\mathbf{r}, t) = n(\mathbf{r}, t) - n_0(r)$ oscillating at frequency ω satisfies $\nabla^2(n_1 \partial P/\partial n_0) + \nabla(n_1 \nabla V) + m\omega^2 n_1 = 0$. Of particular interest is the "neutral mode" solution $n_1^0(r)$, corresponding to the density fluctuation produced by a small shift $\delta\tilde{\mu}$ of the overall chemical potential, that is $n_1^0(r) = (\partial \mu/\partial n_0)^{-1}\delta\tilde{\mu}$. Since the result is still an equilibrium situation, this mode corresponds to $\omega = 0$ but is not physical since it does not conserve particle number.

We make the change $n_1(\mathbf{r}) = n_1^0(r)w(r)Y_{lm}$ (i.e., the local fluctuation of the chemical potential is a convenient variable) and obtain

$$rw'' + [2 + rL'(r)]w' - \left[\frac{l(l+1)}{r} + \frac{m\omega^2 r}{V'(r)}L'(r)\right]w = 0, \quad (1)$$

where we have set $L(r) = \ln(n_0(r))$ with $L'(r) = dL/dr$,

and $V'(r) = dV(r)/dr$. This equation for the mode frequencies has a quite simple form. In particular, as soon as $V(r)$ is known, the properties of the fluid appear only through $L(r)$, which is itself simply related to the equation of state. Therefore it appears much more convenient to model $L(r)$, rather than $\mu(n)$. Indeed Eq. (1) lends itself to a very large number of specific models with analytical solutions or quasianalytical solutions, as we will see below in the case of the harmonic trap. Before proceeding to this case, it is also interesting to note that Eq. (1) may be written with the form of a one-dimensional Schrödinger equation (with energy equal to zero) by making the further change $w(r) = \psi(r)/(r\sqrt{n_0(r)})$. The corresponding potential is found to be $(1/r + m\omega^2/V')L' + (1/4)L'^2 + (1/2)L'' + l(l+1)/r^2$ and is simply related to $L(r)$. This form is of particular interest when one has an explicit analytical solution for an approximate model, as we find below. One can then easily correct the results by a first order perturbation calculation.

Let us now specialize to the case of the harmonic trap $V(r) = \frac{1}{2}m\Omega^2 r^2$. It is then convenient to make the further change $w(r) = r^l v(r)$ which leads to

$$r v'' + [2(l+1) + r L'(r)] v' - (\nu^2 - l) L'(r) v = 0, \quad (2)$$

where $\nu^2 = \omega^2/\Omega^2$. We check on this equation that, whatever the equation of state $\mu(n)$ of the fluid, we have as expected the dipole mode ($l = 1$) corresponding to the gas oscillating in the trap as a whole, at frequency $\omega = \Omega$. It corresponds [6] to $\nu = 1$ with $\nu^2 = 1$. Furthermore $\nu = 1$ gives also $\omega = \Omega\sqrt{l}$ whatever $L(r)$, i.e., independent of the equation of state of the fluid (and, in particular, whether it is a Bose or Fermi gas) [8]. This generalizes for an interacting fluid, at low temperature, results obtained by Griffin et al. and Stringari [6,9] for a Bose gas and by Bruun and Clark [7] for a free Fermi gas.

Note that Eq. (2) is invariant under the change of scale $r \to Kr$, provided we make the same change of scale for $L(r)$. So we take in the following the gas radius R as unity (consistently with hydrodynamics we use the Thomas-Fermi approximation). Next notice that Eq. (2) is only slightly modified by the change $y = r^\alpha$ provided again that the same change is made for $L(r)$. This gives

$$y \frac{d^2 v}{dy^2} + \left(1 + \frac{2l+1}{\alpha} + y \frac{dL}{dy}\right)\frac{dv}{dy} - \frac{\nu^2 - l}{\alpha}\frac{dL}{dy} v = 0. \quad (3)$$

A convenient feature of Eq. (3) is also that the absolute scale in density disappears in L' and only $\bar{n}(r) \equiv n(r)/n(0)$ enters. We introduce similarly a normalized local chemical potential $\bar{\mu}(r) \equiv \mu(n(r))/\mu(n(0))$, where $\mu(n(0))$ is simply obtained from the gas radius R by $\mu(n(0)) = \frac{1}{2}m\Omega^2 R^2$, leading to $\bar{\mu} = 1 - r^2$.

Looking now for simple situations where we can solve Eq. (3), we consider first the case of the noninteracting Fermi gas [7]. This gives $\bar{\mu} = \bar{n}^{1/p}$ with $p = 3/2$. Similarly, we can consider an interacting dilute Bose gas [6] where $\mu = gn$ (g being the coupling constant) leading again to $\bar{\mu} = \bar{n}^{1/p}$ with now $p = 1$. These two

cases imply $L(r) = p\ln(1 - r^\alpha)$ with $\alpha = 2$ in Eq. (3). Hence, we are led to consider for any α and p the model $dL/dy = -p/(1-y)$ for which Eq. (3) becomes

$$y(1 - y)\frac{d^2 v}{dy^2} + [c - y(p + c)]\frac{dv}{dy} + p\frac{\nu^2 - l}{\alpha} v = 0, \quad (4)$$

with $c = 1 + \frac{2l+1}{\alpha}$. The general solution [10] of this equation, giving a nondivergent density fluctuation for $r = 0$, is the hypergeometric function $F(a, b; c; y)$, with $a + b = p + c - 1$ and $ab = -p[(\nu^2 - l)/\alpha]$. We have furthermore to require that the solutions satisfy the boundary condition that the outgoing particle current is zero everywhere on the sphere $r = 1$. This is not verified by the general solution, except if $a = -n$ where n is a nonnegative integer, in which case the solution is a polynomial [6]. This leads to the normal mode frequencies:

$$\frac{\omega^2}{\Omega^2} = l + \frac{\alpha}{p} n\left(n + p + \frac{2l+1}{\alpha}\right), \quad (5)$$

which agrees with Stringari [6] for $\alpha = 2$ and $p = 1$, and with Bruun and Clark [7] for $\alpha = 2$ and $p = 3/2$.

One may naturally wonder about the interest of these results for other values of our parameters α and p. These cases correspond to the density $\bar{n}(r) = (1 - r^\alpha)^p$ and the equation of state $\bar{\mu} = 1 - (1 - \bar{n}^{1/p})^{2/\alpha}$. Our point is that these corresponding models can be used to represent closely the equation of state $\mu(n)$ for a general fluid [with a given maximum density $n(0)$]. We show explicitly below that the flexibility offered by the two parameters α and p makes it a very convenient and efficient procedure. However, these general models do not seem very physical since, although their density properly vanishes at the gas radius, they give near this border $\bar{\mu} \approx \bar{n}^{1/p}$, whereas one should get the dilute gas behavior $p = 1$ (bosons) or $p = 3/2$ (fermions). However, just because the gas is dilute near $r = 1$, we do not expect this part of the gas to play a significant role. Similarly, these models give $\bar{n} \approx 1 - pr^\alpha$ for small r, whereas one expects only the case $\alpha = 2$ to occur for a regular equation of state. Nevertheless if $\bar{n}_0(r)$ is closely approximated over the whole range, one may expect this modeling to be already quite good, as we see explicitly below. Before going into this, let us consider the possibility of more refined models.

Indeed, it is clearly of interest to consider more complicated models which could display proper behavior near the center and the border of the cloud. Although we have not obtained such models with completely analytical solutions, we have found a large class of models with quasianalytical solutions which are in practice not different from fully analytical solutions. These are the models $dL/dy = -\sum_{k=0}^{K} p_k y^k/(1-y)$ (where we could take $\alpha = 2$ and $p \equiv \sum_{k=0}^{K} p_k = 1$ or $3/2$ in order to have the proper center and border behavior). To be simple and specific, let us take the case $K = 1$, giving $-dL/dy = (p_0 + p_1 y)/(1 - y)$. This corresponds to the equation of state $\bar{n} = \bar{\mu}^p \exp[p_1(1 - \bar{\mu})]$ when $\alpha = 2$. In this case Eq. (3) becomes

$$y(1-y)\frac{d^2v}{dy^2} + (q_2 y^2 + q_1 y + q_0)\frac{dv}{dy} + (r_1 y + r_0)v = 0,$$

$$(6)$$

with $q_2 = -p_1$, $q_1 = -(c + p_0)$, $q_0 = c$, $r_1 = p_1 \frac{v^2-l}{\alpha}$, and $r_0 = p_0[(v^2 - l)/\alpha]$. When we look for a series expansion of the solution $v = \sum_{n=0}^{\infty} a_n y^n$, we find the following recursion relation (with $a_{-1} = 0$): $[(n + 1)(n + q_0)]a_{n+1} + [-n(n - 1) + nq_1 + r_0]a_n + [(n - 1)q_2 + r_1]a_{n-1} = 0$ which does not allow in general for a polynomial solution. For large n, this relation becomes asymptotically $a_{n+1} - a_n = -(q_2/n)a_{n-1}$. This leads to the standard behavior $a_{n+1} \approx a_n$ giving a convergence radius equal to 1. This is the same situation as for the hypergeometric function in Eq. (4) and leads in the same way to a singular behavior for $y = 1$ which disagrees with boundary conditions. But the above asymptotic relation may also have solutions $a_{n+1} \ll a_n$ implying $a_n \approx (q_2/n)a_{n-1}$ which gives $a_n \sim 1/n!$. This very rapidly convergent series has an infinite convergence radius and no singularity for $y = 1$. It corresponds to the physically acceptable solutions. Since we have only $y \in [0, 1]$, this solution is a quasipolynomial since the higher order terms in the series are very rapidly negligible. This is quite analogous to the polynomial solution of the hypergeometric differential equation. Naturally, these solutions arise only for special values of our parameters, which gives finally the mode frequencies. In practice, these parameters are found very easily in the following way. We solve iteratively the recursion relation for a_n with $0 \leq n \leq N$, and we require $a_{N+1} = 0$ (as if we had a polynomial solution). Since r_0 and r_1 are linear in $v^2 - l$, this is equivalent to find the roots of an equation of order N for $v^2 - l$. We then increase the value of $N = 1, 2, \ldots$ until the roots have converged. For the lowest root, this is usually a very fast convergence, so one could obtain approximate analytical expressions. But the numerics is so easy that this seems unnecessary. All this analysis and procedure can be extended to the case of $K > 1$.

As an example, we turn now to the specific case of two equal populations of fermions in different hyperfine states. This may be the case of ^{6}Li or ^{40}K near a Feshbach resonance [11]. We assume an attractive interaction between unlike atoms with an interaction g, related to the (negative) diffusion length by $g = 4\pi\hbar^2 a/m$, and we take the Hartree approximation to describe this system. For total atomic density n, $\mu(n) = \hbar^2 k_F^2/2m - |g|n/2$ with $3\pi^2 n = k_F^3$. To solve directly this case, it is more convenient to rewrite Eq. (2) (taking $\alpha = 2$) with the variable $u \equiv k_F/k_F(0)$, where $k_F(0)$ is the equilibrium Fermi wave vector at $r = 0$. This leads to

$$PP'v'' + \left[\left(l+\frac{3}{2}\right)P'^2 + \frac{3}{u}PP' - PP''\right]v' -$$

$$\frac{3(v^2 - l)}{2}\frac{P'^2}{u}v = 0, \quad (7)$$

with $P' = dP/du$ and $P'' = d^2P/du^2$. We have set $P(u) = 1 - u^2 - \frac{2}{3}\lambda(1 - u^3)$ with the coupling constant $\lambda = 2k_F(0)|a|/\pi$. This coupling constant goes from 0, for the very dilute regime corresponding to free fermions, to 1 when we reach at the center the instability where the gas is going to collapse.

We have solved Eq. (7) numerically, as a function of λ, for the first three monopole mode frequencies ($l = 0$). Results are given in Fig. 1. As expected, the frequencies decrease for increasing attractive interaction, since the gas gets more compressible when near the instability. However, we do not find the lowest mode frequency going to zero at the instability. This can be understood because the instability density is reached only at the center, and the rest of the gas still provides a restoring force accounting for the nonzero frequency (actually this instability limit cannot be reached experimentally since the modes correspond to infinitesimal density oscillations; finite oscillations will induce nonlinear effects and produce a collapse of the gas). This result for a Fermi gas is in sharp contrast with the one found for a Bose gas with attractive interaction [1]. In this last case, the gas cloud size is always of order of the extension l_{ho} of the harmonic potential ground state wave function. For hydrodynamics, this is a microscopic scale, so hydrodynamics is never valid and a full quantum calculation is required. On the other hand, the Fermi pressure makes the gas much larger than l_{ho}, which justifies the use of hydrodynamic. Indeed, at the collapse the typical Fermi wavelength λ_F is comparable to the scattering length $|a|$ while the radius of the cloud R_c is comparable to the size of a free fermion gas. This gives $R_c/l_{ho} \sim l_{ho}/|a| \gg 1$ in typical experiments.
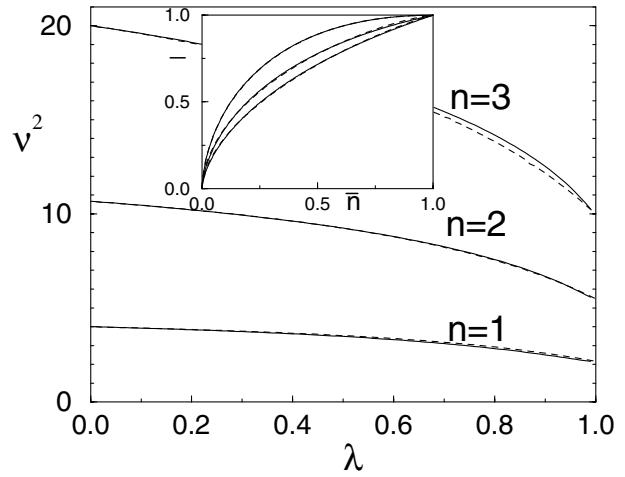
FIG. 1.   Reduced mode frequency $v^2 = (\omega/\Omega)^2$ for a Fermi gas within the Hartree approximation as a function of the coupling constant λ. Solid line: exact result from the numerical solution of Eq. (7). Dashed line: approximate analytical solution. Inset: normalized Hartree chemical potential $\bar{\mu}$ as a function of the normalized density $\bar{n}$ (solid lines) for $\lambda = 0.6, 0.8, 1$ ($\bar{\mu}$ increases with λ) and the corresponding modeling (dashed lines) by $\bar{\mu} = 1 - (1 - \bar{n}^{1/p})^{2/\alpha}$.

Actually, we believe that improving the hydrodynamic description by including quantum effects (hydrodynamic is not correct at the scale of the Fermi wavelength) will lead to modifications very near the instability and to a zero frequency mode at the instability $\lambda = 1$ (preliminary calculations support this view).

It is now of interest to consider an approximate solution of this same problem with the modeling we have discussed above. With the Hartree approximation, the relation between the reduced chemical potential $\bar{\mu}$ and the reduced density $\bar{n}$ is $\bar{\mu} = (3\bar{n}^{2/3} - 2\lambda\bar{n})/(3 - 2\lambda)$. For each value of λ, we approximate $\bar{\mu}(\bar{n})$ by $\bar{\mu} = 1 - (1 - \bar{n}^{1/p})^{2/\alpha}$, where we obtain the parameters p and α by a least square fit. Then the mode frequencies are given by $\nu^2 = \frac{\alpha}{p} n(n + p + \frac{1}{\alpha})$ for $n = 1, 2, 3$. As seen in the inset of Fig. 1, the model is very close to the Hartree equation of state. The mean difference is maximum for $\lambda \approx 0.84$ where it reaches $6 \ 10^{-3}$. The results for the mode frequencies are given in Fig. 1 and they are surprisingly close to our exact results from numerical integration.

A major interest of this approximate treatment is that it is easily inverted and allows to analyze readily experimental data. Let us consider, for example, the case where we have from experiment only the lowest monopole frequency as a function of particle number N in a trap of frequency Ω. It is clear that the information on the equation of state $\mu(n)$ is contained in such data. We show now how to obtain it explicitly. We will obtain $\mu(n)$ recursively: Knowing $\mu(n)$ for n between 0 and n_m, we find the increase $d\mu_m$ corresponding to an increase of n from n_m to $n_m + dn_m$. Hence, we will find a kind of first order differential equation which can be easily integrated numerically. The boundary condition for low n corresponds to recover the dilute gas results which are exactly known.

When $\mu(n)$ is known, the density n_m at the trap center is related to the particle number by $N = 4\pi \int_0^R dr r^2 n(r)$, where the cloud radius R is linked to n_m and to chemical potential μ_m at the trap center by $\frac{1}{2}m\Omega^2 R^2 = \mu_m = \mu(n_m)$: $n(r)$ is obtained by inverting $\frac{1}{2}m\Omega^2 r^2 = \mu(n_m) - \mu(n(r))$. So, for simplicity, in the argument we assume that n_m is known experimentally (but the procedure is basically unchanged if we work with N).

Also, for simplicity of the presentation, let us assume that our model depends only on a single parameter p instead of two (p and α) or more. Then our least square fit to the model $\bar{\mu} = \bar{n}^{1/p} \equiv m(\bar{n}, p)$ corresponds to make $\int_0^1 d\bar{n}[M(\bar{n}, n_m) - m(\bar{n}, p)]^2$ minimal, where $M(\bar{n}, n_m) \equiv \mu(\bar{n}n_m)/\mu(n_m)$ is the normalized chemical potential. This is equivalent to solve the equation $F(p, n_m) \equiv \int_0^1 d\bar{n}[M(\bar{n}, n_m) - m(\bar{n}, p)](\partial m/\partial p) = 0$ which gives the dependence of p on n_m. Now, if we have an increase dn_m, this produces a change dp of our parameter p. They are linked by $(\partial F/\partial p)dp + (\partial F/\partial n_m)dn_m = 0$. On the other hand, dp and dn_m are also linked because our analytical result Eq. (5) for the mode frequency (which depends on p) must be equal to the experimental result (which depends on n_m). This experimental data provides us with an explicit relation between $\partial F/\partial p$ and $\partial F/\partial n_m$. Then $\partial F/\partial p$ is just an integral which contains $M(\bar{n}, n_m)$ and can be calculated numerically. On the other hand, $\partial F/\partial n_m$ contains $\partial M(\bar{n}, n_m)/\partial n_m = \bar{n}\mu'(\bar{n}n_m)/\mu(n_m) - \mu(\bar{n}n_m)\mu'(n_m)/\mu^2(n_m)$, where $\mu'(n) \equiv d\mu/dn$. The second term introduces precisely the quantity $\mu'(n_m) = d\mu_m/dn_m$ we are looking for while all the other ingredients in $\partial F/\partial n_m$ can be calculated numerically from $M(\bar{n}, n_m)$. In this way, we obtain for $d\mu_m/dn_m$ an expression which can be explicitly calculated numerically when we know $\mu(n)$ for n varying between 0 and n_m. This leads by integration to a determination of $\mu(n)$ from the experimental mode frequency $\omega(n_m)$ as a function of the density n_m at the center of the trap or, equivalently, as a function of the particle number N in the trap. The generalization to more than a single parameter does not make any problem.

This inversion method is quite convenient since it gives a univocal answer for $\mu(n)$ from a given set of experimental data. Moreover, if more than a single mode is measured, the comparison between the results from the various modes will provide checks on the resulting $\mu(n)$. Finally, we can improve our modeling by making use of the richer models with quasipolynomial solutions we have already discussed.

---

*Laboratoire associé au Centre National de la Recherche Scientifique et aux Universités Paris 6 et Paris 7.

[1] F. Dalfovo, S. Giorgini, L. P. Pitaevskii, and S. Stringari, Rev. Mod. Phys. **71**, 463 (1999), and references therein; C. Cohen-Tannoudji, cours du collège de France, http://www. ens.fr/cct; M. H. Anderson *et al.*, Science **269**, 198 (1995); K. B. Davis *et al.*, Phys. Rev. Lett. **75**, 3969 (1995).

[2] H. T. C. Stoof *et al.*, Phys. Rev. Lett. **76**, 10 (1996).

[3] R. Combescot, Phys. Rev. Lett. **83**, 3766 (1999).

[4] M. Holland *et al.*, Phys. Rev. Lett. **87**, 120406 (2001).

[5] S. Inouye *et al.*, Nature (London) **392**, 151 (1998); J. L. Roberts *et al.*, Phys. Rev. Lett. **81**, 5109 (1998).

[6] S. Stringari, Phys. Rev. Lett. **77**, 2360 (1996).

[7] G. M. Bruun and C. W. Clark, Phys. Rev. Lett. **83**, 5415 (1999); M. Amuroso *et al.*, Eur. Phys. J. D **7**, 441 (1999).

[8] This has also been pointed out very recently by A. Minguzzi and M. P. Tosi, Phys. Rev. A **63**, 023609 (2001).

[9] A. Griffin, W. C. Wu, and S. Stringari, Phys. Rev. Lett. **78**, 1838 (1997).

[10] *Handbook of Mathematical Functions*, edited by M. Abramowitz and I. A. Stegun (U.S. Government Printing Office, Washington, DC, 1964).

[11] J. L. Bohn, Phys. Rev. A **61**, 053409 (2000).

Self-consistent theory for molecular instabilities in a normal degenerate Fermi gas in the BEC-BCS crossover

R. Combescot,[1] X. Leyronas,[1] and M. Yu. Kagan[2]

[1]*Laboratoire de Physique Statistique, Ecole Normale Supérieure, 24 rue Lhomond, 75231 Paris Cedex 05, France*
[2]*P.L. Kapitza Institute for Physical Problems, Kosygin street 2, Moscow, Russia, 119334*

We investigate within a self-consistent theory the molecular instabilities arising in the normal state of a homogeneous degenerate Fermi gas, covering the whole Bose-Einstein condensate (BEC) to BCS crossover. These are the standard instability for molecular formation, the BCS instability which corresponds to the formation of Cooper pairs, and the related Bose-Einstein instability. These instabilities manifest themselves in the properties of the particle-particle vertex, which we calculate in a ladder approximation. To find the critical temperatures corresponding to these various instabilities, we handle the properties of the interacting Fermi gas on the same footing as the instabilities by making use of the same vertex. This approximate treatment is shown to be quite satisfactory in a number of limiting situations where it agrees with known exact results. The results for the BCS critical temperature and for the BE condensation are found to be in fair agreement with earlier results. The threshold for formation of molecules at rest undergoes a sizable shift toward the BEC side, due to quantum effects arising from the presence of the degenerate Fermi gas. This should make its experimental observation fairly easy. This shift remains important at least up to temperatures comparable to the Fermi energy of the gas.

PACS number(s): 03.75.Ss, 05.30.Fk, 71.10.Ca, 74.72.−h

I. INTRODUCTION

Experimental progress in the field of the Bose-Einstein condensate (BEC) to BCS crossover in ultracold fermionic gases has been going on recently at a very fast pace [1]. In particular after the observation of the Bose-Einstein condensation of diatomic molecules [2] both in ^{6}Li and in ^{40}K, evidence for superfluidity on the BCS side of the crossover has been provided by the study of collective modes by Bartenstein *et al.* [3], which shows a strong attenuation peak, whose likely interpretation is pair breaking in the vicinity of the BCS transition. Further evidence has come from "projection" technique experiments [4] where a fast sweep from the BCS to BEC side allows one to infer the existence of superfluidity on the BCS side. Very recently the observation of vortices in these Fermi gases on the BCS side [5] has given much clearer evidence for superfluidity.

One major interest of the study of the BEC-BCS crossover is to obtain a clear and precise picture of the way in which Cooper pairs go progressively into diatomic molecules when the strength of the attractive interaction between fermionic atoms is progressively increased, and in particular to explore if the BCS formalism gives a proper description of this evolution. The occurrence of this crossover within the BCS formalism and its interest has been put forward by the works of Leggett [6], and Nozières and Schmitt-Rink [7] (NSR), and further investigated by Sa de Melo, Randeria, and Engelbrecht [8]. A review of the situation for the BEC-BCS crossover has been made by Randeria [9], just before the experimental realization of Bose-Einstein condensation in atomic gases. Actually the fact that the BCS formalism also gives a correct description of the condensation of molecules in the strong-coupling limit of dilute molecules was known much earlier [10,11].

Apart from its fundamental physical interest this question is also highly relevant for high-T_c superconductors since in this case Cooper pairs are known to be quite small and much closer to molecules than in standard superconductors. The situation in high-T_c superconductors would accordingly be close to a Bose condensation of molecules. The natural simple theoretical framework for this solid state problem is the attractive Hubbard model, and the self-consistent T-matrix approximation [12,13] used to obtain a qualitative analytical understanding of the Hubbard model corresponds exactly to the framework we will use in the present paper to handle the case of fermionic atomic gases.

In practice the BEC-BCS crossover is realized experimentally by going through a Feshbach resonance, by varying a static and homogeneous magnetic field applied to the atomic gas. Due to the very low temperature only s-wave scattering occurs in the gas and one needs atoms belonging to two different hyperfine states in order to obtain a nonzero scattering, which is forbidden by the Pauli principle between atoms belonging to the same hyperfine state. The scattering length a varies accross the Feshbach resonance, starting with fairly small negative values at high field, which corresponds to a weakly attractive effective interaction between atoms belonging to two different hyperfine states. When the field is lowered a goes to highly negative values and diverges right at the resonance, where it jumps to an infinite positive value. When the field is further lowered the positive scattering length a decreases down to fairly small values. On the low-field side where $a > 0$, molecules exist made of two fermionic atoms belonging to two different hyperfine states, while such a bound state does not exist on the $a < 0$ side.

An interesting experimental result has come from the fact that this singular behavior, which occurs for two atoms in vacuum or for dilute Fermi gases, disappears when one goes

to dense gases. For example the energy of the gas, measured in expansion experiments [14], does not display any singularity and is perfectly smooth when one goes through the resonance, while the scattering length a displays a singularity at the same location. This has been explained [15] by the effect of the dense Fermi gas, which introduces another length scale, namely, the Fermi wavelength, related to the Fermi wave vector k_F, defined from the density n of atoms belonging to a given hyperfine state (we assume that the densities of the two hyperfine states are equal) $n = k_F^3/(6\pi^2)$. The associated energy scale is the Fermi energy $E_F = k_F^2/(2m)$. The presence of the dense gas washes out the Feshbach resonance.

This effect is quite reasonable when one recalls that the very existence of the Cooper pairs, in the case of a very weak interaction, is due to the existence of the Fermi sea without which a bound state could not form. In other words the existence of the dense fermionic gas, or equivalently the Fermi sea, affects the formation of bound states, that is, of molecules. In particular it has been shown explicitly[16], that in the normal state, the threshold for the formation of molecules is affected by the presence of the dense gas. Instead of having, as in vacuum, all the molecular bound states appearing (with zero binding energy) at the same magnetic field corresponding to the Feshbach resonance, characterized by $a^{-1} = 0$, the threshold for the appearance of these bound states depends now on the total momentum of the molecule. Qualitatively this effect is easily understood. Indeed, seen from a **k**-space point of view, the formation of the molecular bound state requires the partial occupation of plane-wave states (the amplitude for the occupation probability is the Fourier transform of the molecular wave function). However, in the presence of a dense gas, some of these states are already occupied and Pauli exclusion makes them unavailable for building up the molecular wave function. As a result, with fewer plane-wave states available, the formation of the molecular bound state becomes more difficult and the threshold is naturally pushed toward stronger interactions, that is, toward positive scattering lengths a.

It is also clear that this effect depends on the total momentum **K** of the molecule. If this momentum is very high, the molecular formation is unaffected since the plane waves required to make up the wave function are near **K**, and they are all essentially empty. In this case the threshold is at the same location as in vacuum, that is, $a^{-1} = 0$, independent of temperature. On the other hand for a molecule with **K** = **0** the required plane waves have small wave vectors and these states are partially occupied. This is the case where the presence of the dense gas is the most strongly felt and the shift of the threshold is strongest, and this is the case we will more specifically consider. Naturally in all cases the effect depends on temperature since, when temperature is raised, the occupation of plane-wave states gets smaller and accordingly the effect on molecular formation is reduced. Ultimately at quite high temperature, the effect disappears because all the plane-wave states have very low occupation probability and we go back to the classical gas situation where the threshold is at $a^{-1} = 0$ for any molecular state.

Naturally the experimental observation of this effect would be quite interesting, not the least because it goes

against the simple intuition one gets from classical gas physics. This implies having reasonable evaluations of the domain of physical parameters where it occurs. Unfortunately the evaluation made in Ref. [16] was very rough since the parameters of the Fermi sea were taken as those of a noninteracting Fermi gas. This is naturally quite inconsistent since the appearance of molecules is due to interaction, which are in particular expected to have strong effects in the vicinity of the Feshbach resonance. This is even more so when one goes toward the BEC side, since one ends up with a system that is physically described as a dilute gas of molecular bosons, which has naturally little to do with a free Fermi sea. The initial purpose of the present paper is to proceed to a coherent calculation and describe the Fermi sea, taking into account self-consistently the interaction responsible for molecular formation.

More specifically the location of the molecular threshold has been obtained in Ref. [16] by writing that the full vertex for atomic scattering has a pole at zero energy $\omega = 0$. This vertex has been obtained by a ladder approximation, which is a natural extension of the exact treatment for two atoms in vacuum. Here the existence of the dense gas has been taken into account by making use of the free fermion propagator for a given chemical potential μ, instead of the fermionic propagator in vacuum. Now if we want to have consistently the properties of the fermionic gas, we should make use of this same vertex within the ladder approximation as a starting point. This is what is done in the present paper. From the vertex, we will obtain the fermionic self-energy, and then the fermionic density n as a function of chemical potential μ and temperature T. In this way we will have in a consistent manner what is essentially the equation of state of the fermionic gas in the presence of interactions.

The appearance of the molecular bound state is not the only feature which is signaled by a pole in the vertex, the BCS transition appears also as a pole for an energy per particle equal to the chemical potential, so $\omega = 2\mu$. This corresponds physically to the appearance of Cooper pairs, which are quite analogous to molecules. Hence it is natural to consider also the location of the BCS transition within our approximation, and to go toward the BEC side of the crossover to determine the critical temperature for the Bose condensation of molecules, once we are beyond the threshold for their formation. This makes the link with previous work devoted to the BEC-BCS transition [7,8].

As it happens the above approximation that we have been led naturally to consider has been already considered quite often in the literature in other contexts, dealing with interacting Fermi systems. It is often named the self-consistent T-matrix approximation and, as we mentionned above, it has been in particular used to handle the Hubbard model (see [12,13] and references therein). In the context of ultracold fermionic gases, it has been already studied and used, in particular in the superfluid phases (see Refs. [17,18,20] and references therein). More specifically Pieri and Strinati [17] obtain their equations as the result of a specific regularization for the well-known ultraviolet divergence which appears in the theory for a contact interaction. In their way the omission of diagrams other than ladder diagrams appears as an exact result. In our case we do not restrict ourselves to a contact

interaction and keeping only ladder diagrams is just an approximation (physically quite reasonable), considered as to be possibly improved. Nevertheless we end up with the same equations, as can be more clearly seen by taking the normal-state limit of the equations of Perali *et al.* [18].

On the other hand we will be concerned only by the normal-state properties in the present paper, with more specifically in mind the study of the threshold for the molecular bound state, which might be relevant for quite recent experimental work [5] as we will see. These normal-state properties have been also investigated by Perali *et al.* [19], but their work is focused on the physics of high-T_c superconductors and considers the real-frequency-axis properties, mostly the spectral function, motivated by the comparison with angle-resolved photoemission spectroscopy experiments. Here we will not consider the spectral function, except quite briefly in Sec. VIII. On the other hand their work on cold gases [18,20] concentrates on the superfluid phase. Also they have focused on trapped gases, while we will deal only with the homogeneous gas. Actually the only overlap is at the level of the critical temperature of the superfluid phase, which they have also calculated for the homogeneous system [18]. However, our specific handling of the equations are different from theirs, each one having its own interest. More details and comparisons will be given in the course of our paper. Another specificity of our paper is that, in order to check the quality of our approximation, we will compare it in various nontrivial limiting cases with exact results already known in the literature. In all cases we will find a perfect agreement which establishes the self-consistent T-matrix approach as a physically very reasonable approximation. In some cases that we will indicate, this agreement is already known. In some others this specific comparison has not yet been done to our knowledge. Yet it is very important to assert precisely the quality of our description of the normal state. This is obviously quite necessary if we want to have a proper description of the superfluid state. This point has already been stressed quite a number of times in the context of high-T_c superconductivity, where it is often asserted that the normal-state properties are even less well understood than the superconducting ones. We stress that our handling of the equations will be made without any approximations, with either analytical or numerical treatment. In summary the present paper is complementary to the work of Pieri, Strinati, and co-workers. In particular it shares the same spirit of trying to describe the physics of these ultracold gases starting from a single coherent fermionic picture for the whole crossover, in contrast to more phenomenologically oriented approaches where a bosonic field describing the molecular states is introduced immediately at the level of the Hamiltonian.

The organization of our paper is as follows. In the next section we introduce our basic equations to calculate the particle number in terms of the chemical potential and the temperature and we give explicitly the expressions for the self-energy and the vertex we will use throughout the paper. Then in the following section we consider the high-temperature range and show explicitly that in this regime our approximation reduces to the exact virial expansion of Beth and Uhlenbeck [21,22] for the quantum gas. This agreement has already been pointed out by Randeria [9]. The interest of this

limiting case has been emphasized recently by Pitaevskii and Stringari who showed that it does not have any singular behavior at the unitarity limit when the Feshbach resonance $a^{-1} = 0$ is crossed, despite the appearance of molecular bound states. Then we show that, in the large-momentum regime, at zero temperature, our approximation reduces to the known exact asymptotic result of Belyakov [23]. It is of particular experimental interest to emphasize this limiting case since very often the high-momentum tail of the particle distribution is analyzed experimentally in order to extract the temperature, by comparison with the ideal case distribution, thereby ignoring the effects of interactions on this tail. We analyze also the dilute regime on the BCS side and we show how our approximation can be corrected to obtain perfect agreement with Galitskii's result [24]. Finally we show explicitly how the molecular bound state arises from the vertex and give the corresponding contribution to the self-energy. We analyze then the dilute limit on the BEC side of the crossover and show that one ends up, in the normal state, with the expected physical situation with the proper Bose distribution for molecules and the expected wave function for this nearly resonating situation. Finally we discuss in this regime another temperature, which is quite important in the context of high-T_c superconductivity, namely, the pseudogap temperature T_*, which corresponds to a smooth crossover between the low-temperature domain, where molecules (i.e., preformed pairs) dominate and the high-temperature range where one has only free fermions. Then, gathering the different contributions to the self-energy, we calculate the momentum distribution for the atoms and total particle number. We emphasize in particular that a separation between particles corresponding to free atoms and particles belonging to a molecule has a quite restricted range of validity, although this analysis is quite often found in the literature in phenomenological analyses. Finally we end up by displaying and discussing our phase diagram for the molecular, the BCS, and the Bose-Einstein instabilities.

II. SELF-ENERGY AND PARTICLE NUMBER

The particle number n in a single hyperfine state is obtained from the temperature Green's function $G(\mathbf{k}, i\omega_n)$, where $\omega_n = (2n+1)\pi T$ (with n an integer) is the Matsubara frequency, by (we take $\hbar = 1$ and $k_B = 1$)

$$n = T \sum_n \int \frac{d\mathbf{k}}{(2\pi)^3} G(\mathbf{k}, i\omega_n) e^{i\omega_n \tau} \qquad (1)$$

where $\tau \rightarrow 0_+$. It is convenient, for actual calculations, to separate out in this equation the free-particle contribution $G_0(\mathbf{k}, i\omega_n) = [i\omega_n - (\epsilon_\mathbf{k} - \mu)]^{-1}$, where $\epsilon_\mathbf{k} = k^2/2m$ is the free-particle kinetic energy, for which the result n_0 for the particle number is known to be

$$n_0 = 4\pi \int_0^\infty \frac{dk}{(2\pi)^3} \frac{k^2}{\exp\left(\dfrac{\xi_\mathbf{k}}{T}\right) + 1} \qquad (2)$$

where we have set $\xi_\mathbf{k} = \epsilon_k - \mu$. The remaining contribution is given by

$$n - n_0 = T\sum_n \int \frac{d\mathbf{k}}{(2\pi)^3} \frac{\Sigma(k,i\omega_n)}{[i\omega_n - \xi_\mathbf{k} - \Sigma(k,i\omega_n)][i\omega_n - \xi_\mathbf{k})]} \tag{3}$$

since the Green's function is related to the self-energy $\Sigma(k,i\omega_n)$ by $G(\mathbf{k},i\omega_n) = [i\omega_n - \xi_\mathbf{k} - \Sigma(k,i\omega_n)]^{-1}$.

In our ladder approximation the self-energy can be written as

$$\Sigma(k,i\omega_n) = T\sum_\nu \int \frac{d\mathbf{K}}{(2\pi)^3} \Gamma(\mathbf{K},i\omega_\nu)G_0(\mathbf{K}-\mathbf{k},i\omega_\nu - i\omega_n). \tag{4}$$

In contrast with the more general situation [25], we have here a single term because only atoms belonging to different hyperfine states do interact, which forbids an exchange term. Here $\Gamma(\mathbf{K},i\omega_\nu)$ is the standard vertex [25] in the ladder approximation. Note that in this vertex, $\omega_\nu = 2\pi\nu T$ (with ν being an integer) is a bosonic Matsubara frequency. Since the wave-vector dependence of $\Gamma(\mathbf{K},i\omega_\nu)$ is actually only on K, the angular integration of G_0 on $\mathbf{K}$ can be performed in Eq. (4) and gives

$$\int d\Omega_\mathbf{K} G_0(\mathbf{K}-\mathbf{k},i\omega_m) = \frac{2\pi m}{kK} \ln \frac{i\omega_m + \mu - K_-^2/2m}{i\omega_m + \mu - K_+^2/2m} \tag{5}$$

with $K_\pm \equiv K \pm k$.

In the following we find it more convenient to work with reduced variables. We take as unit of energy the absolute value of the chemical potential $|\mu|$. This is the natural choice at low temperature in the degenerate regime, but not at high temperature in the classical regime where T is a more convenient scale. Anyhow it is easy to switch in our formulas from one scale to another. Another inconvenience with our choice is that we have to keep track of the sign s of μ, defined by $s = \mu/|\mu| = \pm 1$, since it changes when one goes from the degenerate to the classical regime. We similarly define a wave-vector scale k_0 by $k_0^2/2m = |\mu|$. Hence we set $\omega = |\mu|\bar{\omega}$ and so on for all the frequencies, together with $k = k_0\bar{k}$ and $K = k_0\bar{K}$. We also introduce the reduced temperature $t = T/|\mu|$.

The explicit expression for $\Gamma(\mathbf{K},i\omega_\nu)$ is obtained, for example, as in Ref. [15], but keeping a nonzero wave vector:

$$\Gamma^{-1}(\mathbf{K},i\omega_\nu) = -\frac{mk_0}{2\pi^2\lambda} + \int \frac{d\mathbf{k}'}{(2\pi)^3} \left(T\sum_m G_0(\mathbf{k}',i\omega_m) \right.$$

$$\left. \times G_0(\mathbf{K}-\mathbf{k}',i\omega_\nu - i\omega_m) - \frac{1}{2\epsilon_{k'}} \right) \tag{6}$$

where we have introduced the standard coupling constant $\lambda = -2k_0 a/\pi$. The angular integration and the Matsubara summation can be performed and give, with the change of variable $k' = k_0 x$,

$$\bar{\Gamma}^{-1}(\bar{K},\bar{\omega}) = \lambda^{-1} + \int_0^\infty dx \left(1 - \frac{xt/\bar{K}}{x^2 + (\bar{K}/2)^2 - s - \bar{\omega}/2} \right.$$

$$\left. \times \ln \frac{\cosh[((x+\bar{K}/2)^2 - s)/2t]}{\cosh[((x-\bar{K}/2)^2 - s)/2t]} \right) \tag{7}$$

where we have introduced a "reduced" vertex defined by $\bar{\Gamma} = -mk_0\Gamma/(2\pi^2)$ and used reduced variables.

In principle one could keep working with Matsubara frequencies and perform numerically the discrete frequency summation coming in the expression of the self-energy Eq. (4). This is the procedure chosen for example by Perali *et al.* [18]. However, the corresponding series turn out to be rather slowly converging, which is numerically unpleasant. Hence we will rather transform here this summation into integrals over frequency in a standard way [26] by introducing the Fermi distribution $f(\omega/T) = 1/[\exp(\omega/T)+1]$ which has its poles at $i\omega_n$, writing the summation as an integral over contours encircling these poles and deforming the contours. The contribution coming from the part of the contour at infinity is checked to be zero, and in general we are left with two contributions. We leave out for the moment a third possible contribution from a pole of Γ on the real negative-frequency axis, corresponding physically to a molecular state. This will be taken up in Sec. VI. Both of our contributions turn out to be rapidly convergent for large frequencies because of the Fermi distribution. One of them, which we call Σ_Γ, arises from the cut of $\Gamma(\mathbf{K},i\omega_n+\omega)$ which extends from the branch point $\bar{\omega}_b = 2[(\bar{K}/2)^2 - s] - i\bar{\omega}_n$ to ∞. The other one Σ_L comes from the logarithm in Eq. (5) and encircles the cut going from $\bar{\omega}_- = \bar{K}_-^2 - s$ to $\bar{\omega}_+ = \bar{K}_+^2 - s$, where $\bar{K}_\pm = \bar{K} \pm \bar{k}$. For both contours we can rewrite their contributions as an integral along the corresponding cut by introducing the jump across the cut of the function to be integrated. We obtain in this way $\bar{\Sigma}(k,i\omega_n) \equiv \Sigma(k,i\omega_n)/|\mu| = \bar{\Sigma}_\Gamma(\bar{k},i\bar{\omega}_n) + \bar{\Sigma}_L(\bar{k},i\bar{\omega}_n)$ where

$$\bar{\Sigma}_L(\bar{k},i\bar{\omega}_n) = -\frac{1}{2\bar{k}} \int_0^\infty d\bar{K}\,\bar{K} \int_{\bar{\omega}_-}^{\bar{\omega}_+} dy\, f\left(\frac{y}{t}\right) \bar{\Gamma}(\bar{K},y+i\bar{\omega}_n), \tag{8}$$

$$\bar{\Sigma}_\Gamma(\bar{k},i\bar{\omega}_n) = -\frac{1}{2\pi\bar{k}} \int_0^\infty d\bar{K}\,\bar{K} \int_{\bar{K}^2/2-2s}^\infty dy\, b\left(\frac{y}{t}\right)$$

$$\times \ln\left(\frac{y - \bar{K}_-^2 + s - i\bar{\omega}_n}{y - \bar{K}_+^2 + s - i\bar{\omega}_n}\right) \text{Im}\,\bar{\Gamma}(\bar{K},y) \tag{9}$$

where $\text{Im}\,\bar{\Gamma}(\bar{K},y)$ is for $\text{Im}\,\bar{\Gamma}(\bar{K},y+i\epsilon)$ with $\epsilon \to 0_+$. We have introduced in the expression for $\bar{\Sigma}_\Gamma$ the Bose distribution $b(y) = 1/[\exp(y)-1]$. Equations (7)–(9), completed by Eqs. (30) and (31) when there is a molecular state, are our basic equations from which all our results are derived.

III. HIGH-TEMPERATURE RANGE

It is of interest to consider the high-temperature limit of our approximation. We will see that it reduces to the virial

expansion of Beth and Uhlenbeck [21,22] which means that it becomes exact in this limit. This is naturally quite a satisfactory feature of this approximation. Actually this has already been pointed out by Randeria [9] who emphasized that, in this regime, the NSR approximation would hold, and that, by making use of the phase shift introduced by NSR, one would obtain the Beth-Uhlenbeck result. Here we want to show that this results directly and explicitly from the above equations. For simplicity we restrict ourselves to the $a < 0$ range where there is no molecular bound state. We have also proceeded to this comparison in the $a > 0$ case, where the presence of bound states modifies the Beth and Uhlenbeck result, and we have found that our approximation reduces also to their result in this case.

In this limit we go to the classical regime where $\mu \to -\infty$ with $1/t = |\mu|/T \to \infty$ and in the above formulas we have $s = -1$. In this case the cosh's in Eq. (7) may be replaced by exponentials and the integral on the right-hand side reduces to $(\pi/2)\sqrt{(\bar{K}/2)^2 + 1} - \bar{\omega}/2$. This is just what one would get from the scattering amplitude of two particles in vacuum. This is naturally expected since, in this classical regime, one goes in a dilute limit. One can then see that the cut contribution $\bar{\Sigma}_\Gamma$ to the self-energy goes to zero as $e^{-2|\mu|/T}$ because of the presence of the Bose distribution $b(y/t)$ and of the lower bound on the y integration. It is therefore negligible compared to the pole contribution $\bar{\Sigma}_L$ which goes as $e^{-|\mu|/T}$ as we will now see. Indeed in Eq. (8) we may replace the Fermi distribution $f(y/t) = 1/[\exp(y/t) + 1]$ by its classical limit $\exp(-y/t)$. Moreover, since $t \to 0$, y is restricted in Eq. (8) to a vanishingly small range above the lower bound $\bar{\omega}_- = (\bar{K} - \bar{k})^2 + 1$, so in $\bar{\Gamma}$ we can replace y by this lower bound. The y integration is then easily performed. Similarly we want to have this lower bound as small as possible, in order to pick the dominant contribution from the Fermi distribution. This restricts $\bar{K}$ to a vanishingly small range around $\bar{k}$. Hence we can replace $\bar{K}$ by $\bar{k}$, except in the exponential, and the remaining integral is again easily performed. Finally it is more convenient to go back from our reduced variables to the physical ones, since in this limit the actual energy scale is $(2mT)^{1/2}$. This leads to

$$\Sigma(k, i\omega_n) = -\sqrt{\frac{2}{\pi}} T^{3/2} e^{-|\mu|/T} \frac{1}{-m^{-1/2}a^{-1} + \sqrt{|\mu| - i\omega_n}}$$

$$= \frac{4\pi n_0/m}{a^{-1} - \sqrt{m(|\mu| - i\omega_n)}}. \quad (10)$$

Actually we have omitted a term $(1/2)\epsilon_k$ in the square root, which turns out to be negligible since we will naturally find that only $\epsilon_k \sim T$ is relevant in our calculation, while $|\mu| \to \infty$. Hence the self-energy depends only on the frequency.

Let us first consider the case of small coupling $|\lambda| \ll 1$, where the square root in the denominator is negligible compared to $m^{-1/2}a^{-1}$. In this case the self-energy is just a frequency-independent constant $\Sigma = a(2m/\pi)^{1/2}T^{3/2} \exp(-|\mu|/T)$. Actually this result coincides, as it should, with the mean-field expression $\Sigma = gn_0$ with the coupling constant

$g = 4\pi a/m$. Hence this is just as if we had free particles, and had shifted the chemical potential from μ to $\mu - \Sigma$. The resulting change δn_k in the single-hyperfine-state particle distribution n_k is, in this classical regime,

$$\delta n_k = -\frac{\Sigma}{T} e^{-(\epsilon_k - \mu)/T}. \quad (11)$$

After integration over **k**, this leads to a change of particle density

$$\delta n = -\frac{\Sigma}{T} \Lambda_T^{-3} e^{-|\mu|/T}, \quad (12)$$

where we have introduced the thermal de Broglie wavelength $\Lambda_T = [2\pi/(mT)]^{1/2}$. After substitution of the expression for Σ, this is $\delta n = -2a\Lambda_T^{-4} \exp(-2|\mu|/T)$, which is just the result of the virial expansion for our case.

Let us now come back to the general case where we have to take into account the frequency dependence of the self-energy. For simplicity we keep assuming that $a < 0$, so we have no bound state. Since the self-energy is small in this regime, the integrand in Eq. (3) reduces to $\Sigma(k, i\omega_n)/(i\omega_n - \xi_{\mathbf{k}})^2$. The integration over k is done first and gives $2i\pi(m/2)^{3/2}/(i\omega_n - |\mu|)^{1/2}$ where the determination of the complex square root is with a positive imaginary part. On the other hand the square root $(|\mu| - i\omega_n)^{1/2}$ coming in Eq. (10) for the self-energy has the sign of its imaginary part opposite to the sign of ω_n, as can be seen from the starting expression Eq. (7). Hence this square root has a cut on the real positive axis, starting from $\omega = |\mu|$.

The remaining summation over Matsubara frequencies is transformed in the standard way [26] into an integral over frequency on a contour encircling the poles of the Fermi distribution $f(\omega/T) = 1/[\exp(\omega/T) + 1]$. This contour is then deformed into a contour C which goes in a clockwise way around the cut $[|\mu|, \infty[$ of the square root [27], which gives

$$\delta n = -\frac{1}{2\pi^2}\left(\frac{m}{2}\right)^{3/2} \int_C d\omega \frac{\Sigma(\omega)}{e^{\omega/T} + 1} \frac{1}{(\omega - |\mu|)^{1/2}}. \quad (13)$$

Taking into account that the determination of $(\omega - |\mu|)^{1/2}$ in the denominator changes sign when one crosses the cut $[|\mu|, \infty[$, this integral is twice the integral of its real part on the cut. Making the change of variable $\omega = |\mu| + p^2/m$ and using Eq. (10) for $\Sigma(\omega)$, we obtain finally in this classical limit $|\mu|/T \to \infty$

$$\delta n = -\frac{1}{\pi} a \left(\frac{mT}{\pi}\right)^{3/2} e^{-2|\mu|/T} \int_0^\infty dp \frac{e^{-p^2/mT}}{1 + p^2 a^2}, \quad (14)$$

which is just the Beth-Uhlenbeck result for our case. In the unitarity limit where $mTa^2 \to \infty$ the integral reduces to $\pi/(2|a|)$ which gives $\delta n = (1/2)(mT/\pi)^{3/2}e^{-2|\mu|/T}$. Naturally we have just written here the contribution coming from the interaction. The statistical correction [21,22] in the virial expansion will come out if we expand the Fermi distribution in Eq. (2).

IV. LARGE-MOMENTUM BEHAVIOR

Another limiting situation which is of interest to consider is the large-momentum regime. A perturbative calculation in this limit has been done a long time ago by Belyakov [23]. Since his calculation was performed at $T=0$, we will also restrict ourselves to this case. Just as in the above section it is convenient to transform the summation over Matsubara frequencies in

$$n_k = T \sum_n G(\mathbf{k}, i\omega_n) e^{i\omega_n \tau} \qquad (15)$$

into an integral over frequency on a contour encircling the poles of the Fermi distribution and to deform this contour into the contour $C = C_1 + C_2$ with $C_1 =]i\infty - \epsilon, -i\infty - \epsilon[$ and $C_2 =]-i\infty + \epsilon, i\infty + \epsilon[$ with $\epsilon \to 0_+$. At $T=0$ the second part C_2 of this contour does not contribute, and we close the first part C_1 on the singularities of $G(\mathbf{k}, \omega)$ in the half plane $\omega < 0$.

For large $\bar{k}$, we see from Eq. (8) that the bounds $\bar{\omega}_\pm = (\bar{K} \pm \bar{k})^2 - 1$ are large, and the contribution to $\bar{\Sigma}_L$ negligible, except for the lower bound if $\bar{K}$ is very near $\bar{k}$. This makes $\bar{K}$ also large and, from Eq. (7), one can use the limiting form $\bar{\Gamma}^{-1}(\bar{K}, y + \bar{\omega}) \approx \lambda^{-1} + (\pi/2)\sqrt{(\bar{K}/2)^2 - \bar{\omega}}/2$, since y is bounded due to the Fermi distribution. The remaining integral is easily performed at $T=0$ to give

$$\bar{\Sigma}_L(\bar{k}, \bar{\omega}) = -\frac{2}{3} \frac{1}{\lambda^{-1} + (\pi/2)\sqrt{(\bar{k}/2)^2 - \bar{\omega}}}. \qquad (16)$$

For $\bar{\omega} < 0$ this term in the self-energy has no singularity and does not generate any singularity in $G(\mathbf{k}, \omega)$. Hence we would merely have $n_k = 0$ without the contribution of $\bar{\Sigma}_\Gamma$.

When $T \to 0$ the Bose distribution in Eq. (9) restricts y to negative value, which implies also from the lower bound of the integral that $\bar{K} \leq 2$. Hence for large $\bar{k}$ the logarithm in this equation can be replaced by $-4\bar{k}\bar{K}/(\bar{k}^2 + i\bar{\omega}_n)$. This gives for this case the following expression:

$$\bar{\Sigma}_\Gamma(\bar{k}, \bar{\omega}) = \frac{C}{\bar{\omega} + \bar{k}^2}, \qquad (17)$$

where the constant C is given by

$$C = -\frac{2}{\pi} \int_0^2 d\bar{K} \, \bar{K}^2 \int_{\bar{K}^2/2-2}^0 dy \, \text{Im} \, \bar{\Gamma}(\bar{K}, y). \qquad (18)$$

This constant is easily evaluated since the imaginary part of $\bar{\Gamma}^{-1}(\bar{K}, y)$ becomes simple from Eq. (7) at $T=0$ and, if we restrict ourselves to the perturbative situation of small λ investigated by Belyakov, its real part is merely λ^{-1}. This leads to $C = 4\lambda^2/9$.

Since $\bar{\Sigma}_\Gamma$ has a pole for $\bar{\omega} = -\bar{k}^2$, it is easy to see that $G(\mathbf{k}, \omega)$ itself has a pole in the vicinity. In this vicinity $\bar{\Sigma}_L$ is small and can be neglected. This leaves us with

$$G^{-1}(\mathbf{k}, \omega) = |\mu| \left(\bar{\omega} - \bar{k}^2 - \frac{C}{\bar{k}^2 + \bar{\omega}} \right)$$

$$\simeq \frac{-2|\mu|\bar{k}^2}{\bar{k}^2 + \bar{\omega}} \left(\bar{\omega} + \bar{k}^2 + \frac{C}{2\bar{k}^2} \right). \qquad (19)$$

The pole of $G(\mathbf{k}, \omega)$ at $\bar{\omega} = -(\bar{k}^2 + C/2\bar{k}^2)$ has a residue $C/(4|\mu|\bar{k}^4)$ which leads to

$$n_k = \frac{C}{4\bar{k}^4} = \left(\frac{2}{3\pi} k_0 a \right)^2 \frac{k_0^4}{k^4} \qquad (20)$$

in agreement with Belyakov [23]. One would also obtain this result by performing straight away an expansion in the small parameter C, but this is not so obvious to justify since the denominator $\bar{k}^2 + \bar{\omega}$ in Eq. (19) can vanish.

V. DILUTE LIMIT FOR NEGATIVE SCATTERING LENGTH

The result of Belyakov was obtained by second-order perturbation theory, and the agreement we find with his result would let us believe that our approximation is completely valid up to second order in perturbation. This is actually not completely correct, as can be seen by comparing our results with Galitskii's dilute-limit theory [24,25]. We just sketch here the calculation, at $T=0$, which is basically an expansion in powers of the scattering length a of the expression of the particle density n in terms of the chemical potential μ.

If we insert in Eq. (1) the first-order expression $\Sigma^{(1)} = gn_0$ where $g = 4\pi a/m$, we have for the particle density

$$n^{(1)} = \int \frac{d\mathbf{k}}{(2\pi)^3} \int \frac{d\omega}{2\pi} \frac{e^{i\omega 0_+}}{(i\omega - \xi_\mathbf{k} - gn_0)}. \qquad (21)$$

As is well known, this is just the zeroth-order result $n_0(\mu')$, with a shifted chemical potential $\mu' = \mu - gn_0$. To proceed, we consider the difference $n - n^{(1)}$ and we evaluate the self-energy up to second order $\Sigma(k, i\omega) - gn_0 \simeq \Sigma^{(2)}(k, i\omega)$. Similarly to Eq. (3) this gives

$$n - n^{(1)} = \int \frac{d\mathbf{k}}{(2\pi)^3} \int \frac{d\omega}{2\pi} \frac{\Sigma^{(2)}(k, i\omega)}{(i\omega - \xi_\mathbf{k}')[i\omega - \xi_\mathbf{k}' - \Sigma^{(2)}(k, i\omega)]} \qquad (22)$$

where we have set $\xi_\mathbf{k}' = \epsilon_k - \mu'$. If one sets directly $\Sigma^{(2)} = 0$ in the denominator, one finds $n - n^{(1)} = 0$. In order to get the proper expansion, we subtract from Eq. (22) the corresponding expression without $\Sigma^{(2)}$ in the denominator, which leads to

$$n - n^{(1)} = \int \frac{d\mathbf{k}}{(2\pi)^3} \int \frac{d\omega}{2\pi} \frac{\Sigma^{(2)}(k, i\omega)}{i\omega - \xi_\mathbf{k}'}$$

$$\times \left(\frac{1}{i\omega - \xi_\mathbf{k}' - \Sigma^{(2)}(k, i\omega)} - \frac{1}{i\omega - \xi_\mathbf{k}'} \right). \qquad (23)$$

We see that the integrand is important only when $i\omega - \xi_\mathbf{k}'$ is small, i.e., when the variables are close to $\omega = 0$ and $k = k_0'$,

where $\xi'_{\mathbf{k}'_0}=0$. Therefore, one may replace in the integral $\Sigma^{(2)}(k,i\omega)$ by $\Sigma^{(2)}(k'_0,0)=C'(k'_0 a)^2\mu$, where C' is a positive constant to be evaluated, and consider a small domain of integration around $\omega=0$ and $k=k'_0$. Performing the integrations gives $n-n^{(1)}=-(k_0^3/4\pi^2)(k_0 a)^2 C'$, where we have made in this second-order term $k'_0\approx k_0$. We have therefore, for $n \equiv k_F^3/6\pi^2$, the second-order expansion we were looking for:

$$\frac{k_F^3}{6\pi^2}=\frac{1}{6\pi^2}[2m(\mu-gn_0)]^{3/2}-\frac{C'}{4\pi^2}k_0^3(k_0 a)^2+\cdots, \quad (24)$$

where $k_0=\sqrt{2m\mu}$ and $n_0=k_0^3/(6\pi^2)$.

The constant C' is determined by considering the second-order values of the self-energy contributions $\Sigma_L^{(2)}$ and $\Sigma_\Gamma^{(2)}$. Performing analytically the integrals for $\Sigma_\Gamma^{(2)}$, one finds $\Sigma_\Gamma^{(2)}(k_0,0)=(2+\ln 2)(8/15\pi^2)(k_0^2/2m)(k_0 a)^2$. The integrals entering $\Sigma_L^{(2)}$ are more easily calculated numerically and we get $\Sigma_L^{(2)}(k_0,0)=0.2818(4/\pi^2)(k_0^2/2m)(k_0 a)^2$. From this we obtain the numerical value $C'=0.2597$. Inverting the expansion in Eq. (24) in order to express the chemical potential in powers of $k_F a$, we have

$$\mu=\frac{k_F^2}{2m}(1+\alpha k_F a+\beta(k_F a)^2+\cdots). \quad (25)$$

We get $\alpha=4/3\pi$ and $\beta=8/3\pi^2+C'$. This is in apparent disagreement with Galitskii's result where $\beta=(4/15\pi^2)(11-2\ln 2)\simeq 0.2597$.

This is due to the fact that our self-consistent calculation does not include all the second-order contributions. Indeed when we consider the Hartree term gn, we see that we have taken it into account only to zeroth order, in $\Sigma^{(1)}=gn_0$. However if we want to have a result that is valid up to second order, we want to have the relation $n(\mu)$ in gn correct up to first order while we have it only to zeroth order. Technically this is because we do not have any self-energy contribution in the propagator G which comes in the familiar diagram that corresponds to the Hartree term, that is, we take $G=G_0$ in this diagram, instead of taking into account a first-order correction to G. We note that this defect of our scheme is easily corrected by hand: since we know that the exact result for the Hartree term (to any order) is anyway gn, proportional to the actual density, we can make this correction directly in our formalism. Indeed if we replace in Eq. (24) gn_0 by gn, we obtain $\beta=C'$, in full agreement with Galitskii. It is worth remarking that, in the $T=0$ formalism [25], which works at fixed k_F instead of fixed chemical potential μ, there is no need to correct the Hartree term since, in contrast with μ, k_F is not changed by interactions due to the Luttinger theorem [26]. Finally we note that this point, about the need to add a correction to the self-energy in order to recover Galitskii's result, has also been made quite recently by Pieri, Pisani, and Strinati [28] in the course of their comparison with Monte Carlo results.

VI. MOLECULAR BOUND STATE

As mentioned in Sec. III, we have not yet considered the possibility that $\Gamma(\mathbf{K},\omega)$ has a pole on the real frequency axis,

corresponding physically to the existence of a bound state formed by two fermions belonging to two different hyperfine states, in other words a molecular state. Naturally this will occur only for $a>0$. This is what we will study in the present section.

This pole will appear below the branch point for the cut, which is at $\bar{K}^2/2-2s$. Let us denote by $y_0(\bar{K})$ the corresponding zero occurring in Eq. (7). The equation for $Y_0(\bar{K})=y_0(\bar{K})-\bar{K}^2/2+2s$, which is negative, is given explicitly by

$$\lambda^{-1}+\int_0^\infty dx\left(1-\frac{xt/\bar{K}}{x^2-Y_0/2}\ln\frac{\cosh\{[(x+\bar{K}/2)^2-s]/2t\}}{\cosh\{[(x-\bar{K}/2)^2-s]/2t\}}\right)=0. \quad (26)$$

For increasing coupling strength this zero will first appear when it is right at the branch point, that is, $Y_0=0$. This gives for the corresponding coupling strength threshold $\lambda_{th}(\bar{K})$

$$-\lambda_{th}^{-1}(\bar{K})=\int_0^\infty dx\left(1-\frac{t}{x\bar{K}}\ln\frac{\cosh\{[(x+\bar{K}/2)^2-s]/2t\}}{\cosh\{[(x-\bar{K}/2)^2-s]/2t\}}\right). \quad (27)$$

As expected this coupling strength is always negative, since one can check that the quantity to be integrated in Eq. (27) is positive. This result gives the threshold for formation of a molecule with total momentum $K=k_0\bar{K}$. In particular, for zero momentum $\bar{K}=0$, one obtains

$$-\lambda_{th}(0)^{-1}=\int_0^\infty dx\left(1-\tanh\frac{x^2+1}{2t}\right) \quad (28)$$

which has already been studied in Ref. [16]. In this case we have taken $s=-1$ since otherwise one is already in the phase diagram domain where the BCS instability occurs [16]. On the other hand for $\bar{K}\neq 0$ both $s=\pm 1$ are possible. Finally one checks that, for large $\bar{K}$, Eq. (26) gives merely $y_0=\bar{K}^2/2-2s-8/(\pi\lambda)^2$. In particular the threshold is given by $\lambda_{th}^{-1}(\bar{K})=0$. This is expected since in this case atoms become insensitive to the presence of the other fermions, and one should recover the result for atoms in vacuum.

The existence of a bound state implies that we have to consider in Eq. (4) the additional contribution $\bar{\Sigma}_m$ coming from the corresponding pole occurring at y_0. It is given by

$$\bar{\Sigma}_m(\bar{k},i\bar{\omega}_n)=-\frac{1}{2\bar{k}}\int_0^\infty d\bar{K}\,\bar{K}b\left(\frac{y_0}{t}\right)$$

$$\times\ln\left(\frac{y_0-i\bar{\omega}_n-\bar{K}_-^2+s}{y_0-i\bar{\omega}_n-\bar{K}_+^2+s}\right)\left(\frac{\partial\bar{\Gamma}^{-1}}{\partial\bar{\omega}}\right)_{y_0}^{-1}. \quad (29)$$

Introducing

$$J(\bar{K}) = \int_0^\infty dx \frac{xt/\bar{K}}{[x^2 + |Y_0/2|]^2} \ln \frac{\cosh\{[(x + \bar{K}/2)^2 - s]/2t\}}{\cosh\{[(x - \bar{K}/2)^2 - s]/2t\}} \tag{30}$$

we can rewrite the above contribution as

$$\bar{\Sigma}_m(\bar{k}, i\bar{\omega}_n) = -\frac{1}{\bar{k}} \int_0^\infty d\bar{K} \, \bar{K} b\left(\frac{y_0}{t}\right) \frac{1}{J(\bar{K})}$$
$$\times \ln\left(\frac{y_0 - \bar{K}_-^2 + s - i\bar{\omega}_n}{y_0 - \bar{K}_+^2 + s - i\bar{\omega}_n}\right). \tag{31}$$

VII. DILUTE LIMIT FOR POSITIVE SCATTERING LENGTH

We consider now the behavior of our approximation on the BEC side of the phase diagram, going to the dilute limit. Naturally we expect to find the limiting situation of a dilute gas of molecules. This is coherent with the results of Refs. [6–11], except that we are in the normal state instead of the superfluid. But it is important to check the validity of this expectation in order to obtain confidence in our later result on the molecular instability, which results from the same equations. This dilute regime corresponds to taking $a > 0$ small enough. In this case we will have the presence of molecular bound states, corresponding to the pole of the vertex considered in the preceding section. The binding energy becomes large when a is small. Since physically the chemical potential will be at most half the bound-state energy, it will be large and negative in this range. This implies that $t = T/|\mu| \ll 1$ and $s = -1$. More specifically in this case, the arguments of the cosh's in Eq. (26) are always large and we find $|Y_0| = 2(2/\pi\lambda)^2$. For a molecule at rest (i.e., $\bar{K} = 0$) this means that the molecular binding energy is $|\mu||Y_0| = \epsilon_b = 1/(ma^2)$ as expected. Similarly, from Eq. (30), the expression of $J(\bar{K})$ simplifies into $J(\bar{K}) = \pi/(4\sqrt{|Y_0/2|}) = \pi^2|\lambda|/8$.

Turning now to the self-energy we see from Eqs. (8) and (9) that, because of the Fermi and Bose distributions, these contributions $\bar{\Sigma}_L$ and $\bar{\Sigma}_\Gamma$ to the self-energy will contain exponentially small factors, respectively, $\exp(-1/t)$ and $\exp(-2/t)$, since the lower bound for the y integral is larger than (or equal to) 1 or 2, respectively. Hence we can neglect these two contributions in this small-t limit, and retain only the contribution $\bar{\Sigma}_m$ considered in the preceding section, which can be checked at the end of our calculation to be indeed exponentially larger than the two other ones.

The expression Eq. (31) for $\bar{\Sigma}_m$ simplifies since the Bose distribution factor forces $\bar{K}$ to be very small, and the argument of the logarithm is very near unity. This leads to

$$\bar{\Sigma}_m(\bar{k}, \bar{\omega}) = \frac{C}{\bar{\omega} + |Y_0| + \bar{k}^2 - 1} \tag{32}$$

where the constant

$$C = \frac{16}{\pi} \sqrt{\frac{|Y_0|}{2}} \int_0^\infty d\bar{K} \, \bar{K}^2 b\left(\frac{y_0}{t}\right) \tag{33}$$

is small in the dilute regime we are interested in.

The expression for the self-energy is made clearer by going back to physical variables and making use of Eq. (36) below, which gives

$$\Sigma_m(k, i\omega_n) = \frac{16\pi a |\mu| n/m(k_0 a)^2}{i\omega_n + \xi_k + \mu_B} \tag{34}$$

where we have set $\mu_B = 2\mu + \epsilon_b$, which we will justify physically just below. Note that $\Sigma_m(k, i\omega_n)$ has a "holelike" dispersion in the denominator $i\omega_n + \xi_k + \mu_B$ in contrast to the "particlelike" dispersion $i\omega_n - \xi_k$ in the bare Green's function G_0.

The situation is now similar to the one we had in Sec. IV for the large-momentum behavior. Since we have $t \ll 1$ (which does not imply that T itself goes to zero), once again only the singularities of $G(\mathbf{k}, \omega)$ in the half plane $\omega < 0$ will contribute in the calculation of n_k given by Eq. (20). The self-energy Eq. (32) has a pole for $\bar{\omega} = 1 - |Y_0| - \bar{k}^2$ and we find that $G(\mathbf{k}, \omega)$ itself has a pole in its vicinity at $\bar{\omega} = 1 - |Y_0| - \bar{k}^2 - C/(|Y_0| + 2\bar{k}^2)$. The corresponding residue is $C/(|Y_0| + 2\bar{k}^2)^2$. This leads to

$$n_k = \frac{C}{(|Y_0| + 2\bar{k}^2)^2} \tag{35}$$

and after integration over $\bar{k}$ we have finally for the total density for a single hyperfine state

$$\frac{n}{k_0^3} = \frac{C}{2\pi^2} \int_0^\infty d\bar{k} \frac{\bar{k}^2}{(|Y_0| + 2\bar{k}^2)^2} = \frac{C}{32\pi} \sqrt{\frac{2}{|Y_0|}} = \frac{C}{32\pi} k_0 a. \tag{36}$$

These results Eqs. (35) and (36) are just what one expects in this regime. Indeed taking Eq. (33) into account and going back from reduced to physical variables we can rewrite Eq. (36) as

$$n = \frac{4\pi}{(2\pi)^3} \int_0^\infty dk \frac{k^2}{\exp[(k^2/4m - \epsilon_b - 2\mu)/T] - 1} \tag{37}$$

which is just what is expected for the density of noninteracting bosonic molecules with binding energy ϵ_b, mass $2m$, and chemical potential $\mu_B = 2\mu + \epsilon_b$. Similarly we know that the wave function for the relative motion of atoms in these large nearly resonating molecules is $\psi(r) = (A/r)e^{-r/a}$, where A is a normalization constant. The momentum distribution is proportional to the square of the Fourier transform of this wave function, that is, $(k^2 + 1/a^2)^{-2}$, which is just what we find in Eq. (35) in reduced variables, since $|Y_0| = \epsilon_b/|\mu| = 2/(k_0 a)^2$. It is worthwhile to note that we are in the normal state, in contrast with the similar result obtained from the approximate BCS wave function in the strong-coupling limit, which holds in the superfluid state.

We may wonder if our calculation could also produce interactions between our molecular states. Although this is

not so obvious, this does not seem to be the case. Indeed in our expression Eq. (31) for the self-energy, we have only a single Bose distribution which is appearing, which merely leads to the expression Eq. (36) for the density where this Bose factor appears again. Hence if we had interactions we would expect the appearance of products of Bose distributions, which we do not have. In a related way we notice that this Bose factor is linked to the existence of ladders in the diagrammatic writing of our formulation. This corresponds physically to the propagation of a single molecule. However, in our formulation there are no diagrams where two ladders interact. Physically this means that we have no interactions between molecules. In order to find them one has to consider more complicated diagrams, describing such an interaction, as has been done, for example, by Pieri and Strinati [17] and very recently by Brodsky et al. [29], giving an exact agreement with the four-fermion calculation of Petrov et al. [30].

VIII. TEMPERATURE EVOLUTION OF THE SYSTEM IN THE MOLECULAR LIMIT

In this dilute molecular limit $\epsilon_b = 1/(ma^2) \gg E_F$ it is interesting to consider in more details the temperature evolution of the system. At high temperatures $T \gg E_F$ the situation is governed here by the dynamical equilibrium between molecules and unbound fermions. This situation is described by the well-known Saha (or law of mass action) formula (see [22]). In three dimensions it reads

$$\frac{n_F^2}{n_B} = \frac{1}{2\pi^{3/2}}(mT)^{3/2}\exp(-\epsilon_b/T),$$ (38)

where the total particle density $\tilde{n} = 2n = n_F + 2n_B$, with n_F the sum of the free-fermion density and n_B the bosonic molecular density. The crossover temperature T_* for which $n_F = 2n_B = \tilde{n}/2$ is given by

$$T_* \approx \frac{\epsilon_b}{(3/2)\ln(\epsilon_b/E_F)},$$ (39)

where the logarithm in the denominator of Eq. (39) has an entropic character. For $T \gg T_*$ one has $n_F \gg 2n_B$; hence $\tilde{n} \approx n_F$ and the fermionic chemical potential $\mu \approx -\frac{3}{2}T\ln(T/T_c^{BEC})$ has the standard Boltzmann form ($T_c^{BEC} \sim E_F$ is a typical temperature for Bose-Einstein condensation).

At much lower temperatures $E_F \ll T \ll T_*$ the situation drastically changes. The number of unpaired fermions $n_F \sim \exp(-\epsilon_b/2T)$ becomes exponentially small and hence $\tilde{n} \approx 2n_B$. The fermionic chemical potential acquires a kink:

$$\mu \approx -\frac{\epsilon_b}{2} - \frac{3}{4}T\ln\frac{T}{T_c^{BEC}}.$$ (40)

In this low-temperature regime we have essentially $2\mu = -\epsilon_b$, that is, $k_0 a = 1$. This simplifies the expression Eq. (34) into

$$\Sigma_m(k, i\omega_n) = \frac{16\pi a|\mu|n/m}{i\omega_n + \xi_k + \mu_B}.$$ (41)

It is important to emphasize that for $T \ll T_*$ our two-particle vertex has the simple pole structure:

$$\Gamma(\mathbf{K}, i\omega_\nu) = \frac{4|\mu|4\pi a/m}{i\omega_\nu - K^2/4m + \mu_B},$$ (42)

where, as we have seen in the preceding section, $\mu_B = 2\mu + \epsilon_b$ is the molecular chemical potential. Correspondingly we have $\mu_B \approx -\frac{3}{2}T\ln(T/T_c^{BEC})$.

The dressed one-particle Green's function $G^{-1}(\mathbf{k}, i\omega_n) = G_0^{-1}(\mathbf{k}, i\omega_n) - \Sigma(\mathbf{k}, i\omega_n)$ has a two-pole structure for $T \ll \epsilon_b$:

$$G = \frac{1}{i\omega_n - \xi_k - 16\pi a|\mu|n/m/(i\omega_n + \xi_k + \mu_B)},$$ (43)

where, as before, $\xi_k = k^2/2m - \mu$.

The spectral function $A(\mathbf{k}, \omega) = -(1/\pi)\mathrm{Im}\, G(\mathbf{k}, \omega + i0_+)$ reads

$$A(\mathbf{k}, \omega) \approx \left(1 - \frac{4\pi a|\mu|n/m}{\xi_k^2}\right)\delta(\omega - \xi_k)$$

$$+ \frac{4\pi a|\mu|n/m}{\xi_k^2}\delta(\omega + \xi_k + \mu_B).$$ (44)

It reflects for $T \ll T_*$ the existence of two bands: the filled bosonic band and, separated by the correlation gap ϵ_b, the almost empty band of unbound fermions. Integrating the spectral weight it is easy to check that in this regime

$$\frac{4\pi a|\mu|n}{m}\frac{1}{2\pi^2}\int_0^\infty \frac{k^2 dk}{\xi_k^2} = n \approx n_B.$$ (45)

The specific heat of the system,

$$C_v = \frac{\partial E}{\partial T} = \frac{\partial}{\partial T}\left[\int \frac{k^2}{4m}\frac{k^2 dk}{2\pi^2}\exp\left(-\frac{k^2}{4mT}\right)\exp\frac{\mu_B}{T}\right]$$

$$\sim n = \mathrm{const},$$ (46)

is temperature independent in agreement with general thermodynamic requirements.

IX. GENERAL MOMENTUM DISTRIBUTION

An intermediate step in our calculation is naturally the particle momentum distribution $n_k = n_{0k} + \delta n_k$, where $n_{0k} = [\exp(\xi_k/T) + 1]^{-1}$ is the Fermi distribution and the correction due to interactions is, with our reduced units, given by

$$\delta n_k = 2t\,\mathrm{Re}\sum_{n=0}^\infty \frac{\bar{\Sigma}(\bar{k}, i\bar{\omega}_n)}{[i\bar{\omega}_n - \bar{k}^2 + s - \bar{\Sigma}(\bar{k}, i\bar{\omega}_n)](i\bar{\omega}_n - \bar{k}^2 + s)}$$ (47)

with $k = k_0\bar{k}$ and we have used $\Sigma(k, -i\omega_n) = \Sigma^*(k, i\omega_n)$, and we have explicitly in terms of the contributions considered above $\bar{\Sigma}(\bar{k}, i\bar{\omega}_n) = \bar{\Sigma}_\Gamma(\bar{k}, i\bar{\omega}_n) + \bar{\Sigma}_L(\bar{k}, i\bar{\omega}_n) + \bar{\Sigma}_m(\bar{k}, i\bar{\omega}_n)$. Then the particle number is obtained by $n = (1/2\pi^2)\int_0^\infty dk\, k^2 n_k$. The calculations of δn_k and of n are both handled numerically.

The above Matsubara summation is numerically quite convenient since it converges fairly rapidly [for large $\bar{\omega}_n$ the

terms in the series Eq. (47) behave typically as $1/\bar{\omega}_n^3$]. Nevertheless it is of interest to consider another possible calculation where this summation would be transformed in a contour integration over frequency as we have done for example in Secs. IV and VII. The contour would be deformed to enclose the singularities of the Green's function occurring on the real-frequency axis, and the result could be expressed in terms of the spectral density. This would allow us to ascribe a physical meaning to the various contributions, as we have done in Sec. IV where we had to deal with a fermion pole, whereas in Sec. VII we had a molecular pole. This is of interest since the total particle number n is very often split in the literature into a free-fermion term plus a molecular term as $n = n_{\text{ferm}} + n_{\text{mol}}$.

It is easy to see that this split is not possible in general because the Green's function has a cut on the real axis extending from $-\infty$ to $+\infty$. There is no way to split the Green's function itself in a sum of a free-fermion term and a molecular term since this is rather at the level of the self-energy that such a separation occurs. We have indeed found for the self-energy a molecular contribution Σ_m, linked to the molecular pole of $\Gamma(\mathbf{k}, \omega)$. The contribution Σ_Γ can also be understood as linked to molecules [as is clear from the Bose factor it contains in Eq. (9)], but this is rather the continuous spectrum of molecules broken into two fermions, rather than the discrete spectrum linked to Σ_m. Finally the contribution Σ_L is linked to single fermions since it arises in Eq. (4) from the pole of the Green's function G_0 which is clearly signaled by the Fermi factor in Eq. (8). We could still think of separating a molecular contribution from a fermionic contribution if we had in the spectral density of the Green's function an energetically well separated part, similar to what we had in Sec. VII. However, this is likely to occur only when the molecular binding energy is large compared to temperature, in which case we will have dominantly molecules, and the separation of the density into a molecular part and a fermionic part is rather uninteresting. Anyhow it is clear from the above discussion that such a separation is in general unwarranted and, if it is used, it must be taken cautiously.

X. COMPARISON WITH OTHER WORKS

As we have already indicated our approach is in complete agreement with the equations written by Perali *et al.* [18] when we restrict them to the normal state. It is also of interest to compare our framework with the one used by Nozières and Schmitt-Rink [7], but since a comparison between the T-matrix formulation and the NSR approach has already been done by [35], we summarize here only the conclusions. The NSR scheme corresponds to take $G - G_0 = G_0 \Sigma G_0$, that is, the first-order term in the expansion of $G = (G_0^{-1} - \Sigma)^{-1}$. By contrast our expression contains all orders in this expansion for G, while naturally keeping the same approximate expression for the self-energy. Diagrammatically we have any number of wheels interconnected as can be seen in Fig. 1, while only a single wheel appears in the NSR scheme.

XI. CRITICAL TEMPERATURES AND MOLECULAR INSTABILITY

In this section, before turning to the molecular instability line, we first recall the results for the BCS and the BEC
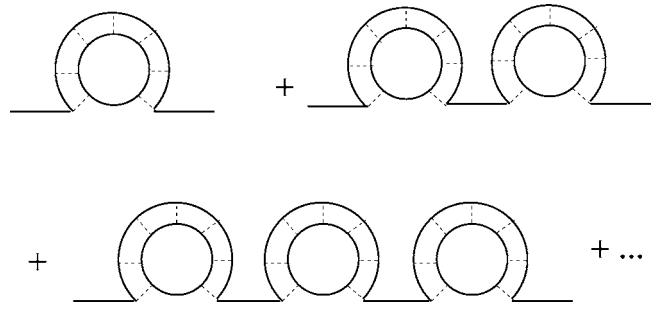

FIG. 1. Diagrams for the full propagator included in our approximation, in addition to the free-particle propagator.

transition lines. Indeed, as we mentioned already in the introduction, all these lines are intimately related, both qualitatively since they represent molecular instabilities of the normal state, and quantitatively since they meet at the same end point as we will see. In the case of the BCS transition temperature, for which $\mu > 0$, the relation between the critical temperature T_c and the chemical potential is given by the standard equation:

$$-\frac{1}{\lambda} = \int_0^\infty dx \left(1 - \frac{x^2}{x^2 - 1} \tanh \frac{x^2 - 1}{2t_c}\right) \quad (48)$$

where $t_c = T_c/\mu$. With the standard physical variables this equation reads:

$$1 = \frac{2a}{\pi} \int_0^\infty dk \left(1 - \frac{\epsilon_k}{\epsilon_k - \mu} \tanh \frac{\epsilon_k - \mu}{2T_c}\right) \quad (49)$$

where the chemical potential μ is positive. This equation is obtained by writing that $\Gamma(\mathbf{K}, \omega)$ has a pole at the chemical potential for zero total momentum $\mathbf{K} = \mathbf{0}$, that is, by setting $Y_0 = 2$, $s = 1$, and $\bar{K} \to 0$ in Eq. (26). This BCS transition line terminates when $\mu = 0$ (this implies $t_c \to \infty$) which gives the relation between the limiting critical temperature T_0 and the corresponding scattering length a_0. This is more directly obtained from the equation with physical variables Eq. (49) and is given by $\pi/\sqrt{8ma_0^2 T_0} = \int_0^\infty dz[1 - \tanh(z^2/2)]$, i.e., explicitly $ma_0^2 T_0 = 1.07 = T_0/\epsilon_{b0}$ in terms of the molecular binding energy $\epsilon_{b0} = 1/ma_0^2$ at this point. Obtaining T_0/E_F and $1/k_F a_0$ requires the numerical calculation of the gas density at that point (knowing that it satisfies $\mu = 0$), along the procedure described in the preceding Sec. IX.

In the weak-coupling limit $|a|k_F \ll 1$ this gives for the dominant order $T_c \sim E_F \exp(-1/\lambda)$. When the calculation is carried out to the next-order term, one finds the numerical coefficient in front of the exponential as

$$T_c^{BCS} \simeq 0.61 E_F \exp\left(-\frac{\pi}{2k_F|a|}\right). \quad (50)$$

However, already at the level of this coefficient, the simple weak-coupling limit is not correct and one needs to take into account polarization contributions to the effective interaction, arising from second-order diagrams in the gas parameter λ, as has been shown by Gor'kov and Melik-Barkhudarov [32]. This leads to their well-known formula

$$T_c^{BCS} \simeq 0.28 E_F \exp\left(-\frac{\pi}{2k_F|a|}\right). \tag{51}$$

Hence, at this level already, our approximation does not yield the exact result. In order to improve it on this side we should take into account polarization diagrams at the level considered by Gor'kov and Melik-Barkhudarov, and beyond as it has been done for example in Refs. [33,34,36].

On the other hand we meet also naturally in our calculations the Bose-Einstein transition for the molecular states we have discussed in Secs. VI and VII. Indeed it is reached when the Bose factor $b(y_0/t)$ entering the self-energy in Eq. (31) diverges, since this factor corresponds physically to the statistical occupation of the molecular states. This divergence occurs for $y_0(\bar{K})=0$. Naturally this is for a zero total molecular momentum $\bar{K}=0$ that it occurs first. This implies that $Y_0(\bar{K})=y_0(\bar{K})-\bar{K}^2/2+2s=-2$, since we need $s=-1$ in order to have $\bar{K}=0$ molecules, as noted above. From Eq. (26) we find for the critical temperature $T_c=|\mu|t_c$

$$\frac{1}{|\lambda|} = \int_0^\infty dx\left(1 - \frac{x^2}{x^2+1}\tanh\frac{x^2+1}{2t_c}\right) \tag{52}$$

where we use the fact that this transition occurs only for $\lambda < 0$ to write $-\lambda=|\lambda|$. We see from this equation that, by letting $\mu \to 0$ (which implies again $t_c \to \infty$), the Bose-Einstein transition line terminates at the same point $\mu=0$ and $T=T_0$ as the BCS transition line. This Eq. (52) is actually in agreement with the finding of Ref. [8] (as more easily seen when we go back to unreduced units). However, in contrast to the approach of these authors which treat the superfluid state, our reasoning involves only the normal state and its instabilities.

Going back to physical variables the above equation reads

$$1 = \frac{2a}{\pi}\int_0^\infty dk\left(1 - \frac{\epsilon_k}{\epsilon_k+|\mu|}\tanh\frac{\epsilon_k+|\mu|}{2T_c}\right). \tag{53}$$

In the dilute molecular limit $k_F a \ll 1$ (or equivalently $na^3 \ll 1$), we have $\epsilon_b \gg E_F$ and we have seen in Sec. VII that $\mu_B=2\mu+\epsilon_b$, implying $|\mu| > \epsilon_b/2$. This gives in Eq. (53) $|\mu| \gg T_c \sim E_F$ and hence $\tanh[(\epsilon_k+|\mu|)/2T_c] \approx 1$. Accordingly,

$$1 = \frac{2a}{\pi}\int_0^\infty dk\frac{|\mu|}{\epsilon_k+|\mu|} = \sqrt{2m|\mu|a^2} = \sqrt{2|\mu|/\epsilon_b}. \tag{54}$$

Hence in this limit our equation reduces to $\mu_B(T_c)=0$ as expected for the Bose-Einstein condensation of dilute gas. Using the standard formula for bosons [22] with density $n_B=n$ and mass $2m$, one finds [31]

$$T_c^{BEC} = 3.31\frac{n^{2/3}}{2m} \simeq 0.218 E_F. \tag{55}$$

It is also worthwhile to note that actually, in the general case, we do not need the above physical interpretation of the Bose factor to find the Bose-Einstein transition. Indeed if we were to calculate as discussed above the particle number as a function of temperature and chemical potential, and were to enter the condensate domain of the phase diagram without

realizing it, we would find that we could not accommodate all the particles we have in our system, even by further lowering the temperature, because the particle number would decrease with temperature. This would signal the appearance of a condensate in order to accommodate the remaining particles. In other words we cannot miss the transition, which appears automatically in our approach.

Finally our major interest is the line in the phase diagram where molecules begin to form. As stressed in Ref. [16] this threshold line is shifted from its standard location for molecules in vacuum, which is at unitarity. This is due to the presence of all the other fermions, which influence the formation of a molecule in much the same way as they do for the formation of Cooper pairs. Moreover, in contrast with the situation in vacuum and in similarity with Cooper pairs, the location of the threshold line where molecules begin to form depends on the total momentum of the molecule under consideration. For a very large momentum the molecule is insensitive to the presence of the other fermions, and the threshold line is at unitarity $a^{-1}=0$, just as in vacuum. On the other hand the molecules with zero momentum are the most sensitive to the presence of the other fermions. The question of molecular formation has already been considered in Sec. VI and the location of this threshold line is given by Eq. (27). Again this line terminates at $\mu=0$, at the same point as the BCS line and the BEC line. Hence the three physical lines of interest in this section terminate at the same point.

The last step in order to draw a physical phase diagram is to express the critical temperature in terms of the particle density n, rather than in terms of the chemical potential μ. This is done by calculating numerically n as a function of μ, as indicated in Sec. IX. As indicated in the Introduction, we use, as usual wave-vector and energy scales directly related to the atomic density n for a single hyperfine state, namely, the Fermi wave vector k_F defined by $n=k_F^3/(6\pi^2)$, and the Fermi energy $E_F=k_F^2/(2m)$. The results are displayed in Fig. 2.

Let us first discuss the BCS and the BEC lines. Qualitatively the general shape is similar to the NSR result. The maximum of T_c/E_F is very close to the terminal point a_0,T_0 and (at the scale of our figure) it is very smooth. This shape is also found in later work [8,18], including phenomenological approaches [31]. Quantitatively our results are slightly higher than those of Perali *et al.* [18] for the homogeneous case, as can be seen from the T_c^h in their Fig. 1. Although this discrepancy is rather small, it is somewhat puzzling since both numerical calculations have been performed in a careful way, although the specific starting equations for the numerics are different as we have seen in Sec. II. Anyway the difference can be taken as a typical uncertainty arising in this kind of numerical calculation.

We consider finally the molecular threshold line. The quite interesting feature is that, for all the temperatures satisfying $T < E_F$ (and clearly even somewhat above), $1/k_F a$ stays typically around 0.4, that is, roughly its value at the terminal point. This is in contrast with what one would expect from the fact that, at high temperature, this line goes toward the unitarity line $1/k_F a=0$ since this quantum shift of the molecular threshold clearly disappears in the classical regime. Hence the region between the molecular line and
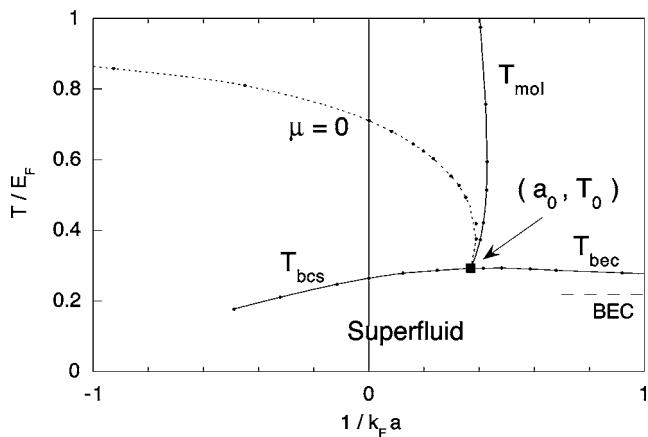
FIG. 2. Threshold line T_{mol} for the formation of molecules with zero total momentum $\mathbf{K}=0$, critical temperature for the BCS instability T_{BCS}, and critical temperature for the Bose-Einstein condensation of molecules T_{BEC}, as a function of the scattering length a. Dots are the actual numerical results. Curves are smooth interpolations through these results. The wave vector k_F is related to the gas density n by $n=k_F^3/(6\pi^2)$, and the Fermi energy is defined by $E_F=\hbar^2 k_F^2/(2m)$. The line $\mu=0$ is drawn to show roughly the region (below this line) where the physics is qualitatively that of a degenerate Fermi gas with $\mu>0$. The terminal point a_0,T_0 common to the molecular line, the BCS line, and the BEC line is located at $1/(k_F a_0)=0.37$ and $T_0/E_F=0.29$. The BEC limit for the dilute molecular gas is at $T_c=0.218 E_F$.

unitarity could have been pretty small, in contrast with what we find in Fig. 2. This makes naturally easier the experimental observation of the shift. It may even be that it has already been seen in the very recent vortex experiment [5]. Indeed in order to observe vortices, experimentalists have to let the Fermi gas expand while at the same time forming molecules, in order to see the depression in molecular density associated with the vortex in the same way as is done for standard Bose condensates. In the experimental process, it has been observed that, when forming vortices on the BCS side $a<0$, it is necessary to switch the magnetic field to somewhere below the Feshbach resonance in order to be able to see the vortices (the corresponding $1/k_F a$ is of order 0.35, in nice agreement with the location of the molecular line). A possible explanation might be that, because (low-momentum) molecules cannot form beyond the molecular line, the formation of molecules necessary to see the vortices cannot occur when the magnetic field is not brought to low enough values. However, the answer lies in the trajectory of the Fermi gas in Fig. 2 during expansion, which is not at all obvious to determine since the expansion is clearly a complicated dynamical process. Hence we can certainly not exclude that the explanation for this experimental observation lies somewhere else.

The fact that molecules form only progressively instead of forming right at unitarity is naturally expected to affect basically any physical property when the system is in the region between unitarity and the molecular line. However, the most direct way to observe experimentally this effect should be via some spectroscopic experiment, looking directly at the existence and the binding energy of molecules. This could even be performed in the molecular domain beyond the mo-

lecular line (but not too far from it) since the binding energy of the molecules will not be the same as for molecules in vacuum. We can think of, at least, three kinds of spectroscopic experiments. A first one would make use of the fact that, in a number of experimental setups [37], the frequency of the optical transition used to detect atoms is slightly modified when the relevant atoms belong to molecules. As a result these atoms are not seen, and this appears as an experimental deficit in the number of atoms. According to our result such an experiment should see more atoms in the region between unitarity and the molecular line, compared to what one would expect if all the molecules were formed at unitarity.

Another kind of spectroscopic experiment could be in the radio-frequency domain, analogous to the work of Chin *et al.* [38], where the molecular binding energy as well as the BCS pairing gap have been observed as a shift in a rf resonance. In our case we have actually a distribution of molecular binding energies in the region between unitarity and the molecular line (and, again, even beyond) since molecules are more or less (or not at all) bound depending on their total momentum. Accordingly one should see a smooth onset of the molecular line, somewhat analogous to their data at low temperature at 822 G (see their Fig. 1), when one works slightly above the critical temperature. The line shape itself could be compared to theory, making use of a local density approximation.

Finally another kind of spectroscopic experiment could be performed along the line followed by Partridge *et al.* [39]. Their experiment used an optical transition between the molecular state and an electronically excited molecular singlet level. Accordingly they detected only the singlet part of the molecular wave function, linked to the closed channel, which has a very small weight Z and they were insensitive to free atoms. This type of experiment, which accordingly sees only molecules, could be used to see that molecules form progressively between unitarity and the molecular line.

XII. CONCLUSION

In this paper we have treated in a self-consistent way the various molecular instabilities arising in the normal state of a degenerate Fermi gas. We have stressed that these instabilities have to be contrasted with the smooth crossover in the nondegenerate regime, corresponding to the temperature T_* where the formation of the predominant molecules occurs as the temperature is lowered. We have covered all the range of scattering lengths, so as to cover the whole BEC-BCS crossover. The molecular instabilities manifest themselves mostly as poles of the vertex corresponding to particle-particle scattering. This vertex has been calculated in a ladder approximation. The threshold for the appearance of standard molecules corresponds to the existence of a pole at zero energy in the vertex. The BCS instability corresponds also to the appearance of molecularlike objects, namely, Cooper pairs, but the pole in the vertex appears at the chemical potential. Finally the equation giving the Bose-Einstein condensation instability is a simple, but elegant, continuation of the equation giving the BCS instability. In order to find the critical temperatures corresponding to these various instabilities, we

have taken into account the interactions between fermions in this normal gas, by making use of the same vertex as the one used to obtain the instabilities themselves. This leads to the self-consistent T-matrix approximation. We have shown that this approximation is quite satisfactory since it leads in a number of limiting cases to results which are in agreement with known exact results. These are specifically the high-temperature regime, the large-momentum limit at $T=0$, and the dilute limit on both the BCS and the BEC sides of the crossover, which we have investigated successively. The calculated phase diagram shows that, in particular, the threshold for formation of molecules at rest undergoes a sizable shift toward the BEC side, due to the hindering effect of the quantum gas on the molecular wave function. This shift remains important up to temperatures comparable to the Fermi energy of the gas. Finally, our approximation is somewhat defective on the BEC side since it does not allow us to describe inter-action between molecules. Improvement is clearly needed in this direction and will be the subject of future work.

[1] Proceedings of Workshop on Ultracold Fermi Gases, Levico, 2004, http://bec.science.unitn.it/fermi04/

[2] M. Greiner, C. A. Regal, and D. S. Jin, Nature (London) **426**, 537 (2003); S. Jochim, M. Bartenstein, A. Altmeyer, G. Hendl, S. Riedl, C. Chin, J. Hecker Denschlag, and R. Grimm, Science **302**, 2101 (2003); M. W. Zwierlein, C. A. Stan, C. H. Schunck, S. M. F. Raupach, S. Gupta, Z. Hadzibabic, and W. Ketterle, Phys. Rev. Lett. **91**, 250401 (2003); T. Bourdel, L. Khaykovich, J. Cubizolles, J. Zhang, F. Chevy, M. Teichmann, L. Tarruell, S. J. J. M. F. Kokkelmans, and C. Salomon, *ibid.* **93**, 050401 (2004).

[3] M. Bartenstein, A. Altmeyer, S. Riedl, S. Jochim, C. Chin, J. H. Denschlag, and R. Grimm, Phys. Rev. Lett. **92**, 203201 (2004).

[4] C. A. Regal, M. Greiner, and D. S. Jin, Phys. Rev. Lett. **92**, 040403 (2004); M. W. Zwierlein, C. A. Stan, C. H. Schunck, S. M. F. Raupach, A. J. Kerman, and W. Ketterle, *ibid.* **92**, 120403 (2004).

[5] M. W. Zwierlein, J. R. Abo-Shaeer, A. Schirotzek, C. H. Schunk, and W. Ketterle, Nature (London) **435**, 1047 (2005).

[6] A. J. Leggett, J. Phys. (Paris), Colloq. **41**, C7-19 (1980).

[7] P. Nozières and S. Schmitt-Rink, J. Low Temp. Phys. **59**, 195 (1985).

[8] C. A. R. Sa de Melo, M. Randeria, and J. R. Engelbrecht, Phys. Rev. Lett. **71**, 3202 (1993).

[9] M. Randeria, in *Bose-Einstein Condensation*, edited by A. Griffin, D. W. Snoke, and S. Stringari (Cambridge University Press, Cambridge, U.K., 1995), p. 355.

[10] L. V. Keldysh and A. N. Kozlov, Zh. Eksp. Teor. Fiz. **54**, 978 (1968) [Sov. Phys. JETP **27**, 521 (1968)].

[11] D. M. Eagles, Phys. Rev. **186**, 456 (1969).

[12] M. Yu. Kagan, R. Frésard, M. Capezzali, and H. Beck, Phys. Rev. B **57**, 5995 (1998).

[13] M. Yu. Kagan, R. Frésard, M. Capezzali, and H. Beck, Physica B **284–288**, 447 (2000).

[14] T. Bourdel, J. Cubizolles, L. Khaykovich, K. M. F. Magalhães, S. J. J. M. F. Kokkelmans, G. V. Shlyapnikov, and C. Salomon, Phys. Rev. Lett. **91**, 020402 (2003).

[15] R. Combescot, Phys. Rev. Lett. **91**, 120401 (2003).

[16] R. Combescot, New J. Phys. **5**, 86 (2003); Eur. Phys. J. D **32**, 69 (2005).

[17] P. Pieri and G. C. Strinati, Phys. Rev. B **61**, 15370 (2000).

[18] A. Perali, P. Pieri, L. Pisani, and G. C. Strinati, Phys. Rev. Lett. **92**, 220404 (2004).

[19] A. Perali, P. Pieri, G. C. Strinati, and C. Castellani, Phys. Rev. B **66**, 024510 (2002).

[20] A. Perali, P. Pieri, and G. C. Strinati, Phys. Rev. Lett. **93**, 100404 (2004).

[21] E. Beth and G. E. Uhlenbeck, Physica (Amsterdam) **4**, 915 (1937).

[22] L. D. Landau and E. M. Lifshitz, *Statistical Physics*, Course of Theoretical Physics Vol. 5 (Butterworth-Heinemann, Oxford, 1999).

[23] V. A. Belyakov, Sov. Phys. JETP **13**, 850 (1961).

[24] V. M. Galitskii, Sov. Phys. JETP **7**, 104 (1958).

[25] A. L. Fetter and J. D. Walecka, *Quantum Theory of Many-Particle Systems* (McGraw-Hill, New York, 1971).

[26] A. A. Abrikosov, L. P. Gorkov, and I. E. Dzialoshinski, *Methods of Quantum Field Theory in Statistical Physics* (Dover, New York, 1975).

[27] In the case $a>0$ we would have in addition a pole for $\Sigma(\omega)$, corresponding to the presence of a bound state (see Sec. VI). This would give rise to an additional term when the contour is deformed, leading to the bound-state contribution in the Beth-Uhlenbeck result [21].

[28] P. Pieri, L. Pisani, and G. C. Strinati, Phys. Rev. B **72**, 012506 (2005).

[29] I. V. Brodsky, A. V. Klaptsov, M. Yu. Kagan, R. Combescot, and X. Leyronas, e-print cond-mat/0507240.

[30] D. S. Petrov, C. Salomon, and G. V. Shlyapnikov, Phys. Rev. Lett. **93**, 090404 (2004).

[31] J. N. Milstein, S. J. J. M. F. Kokkelmans, and M. J. Holland, Phys. Rev. A **66**, 043604 (2002).

[32] L. P. Gor'kov and T. K. Melik-Barhudarov, Zh. Eksp. Teor. Fiz. **40**, 1452 (1961) [Sov. Phys. JETP **13**, 1018 (1961)].

[33] M. Yu. Kagan, and A. Chubukov, JETP Lett. **47**, 525 (1988);

M. A. Baranov, A. V. Chubukov, and M. Yu. Kagan, Int. J. Mod. Phys. B **6**, 2471 (1992).

[34] M. A. Baranov, D. V. Efremov, M. S. Marenko, and M. Yu. Kagan, JETP **90**, 861 (2000).

[35] V. M. Loktev, R. M. Quick, and S. G. Sharapov, Phys. Rep. **349**, 1 (2001).

[36] R. Combescot, Phys. Rev. Lett. **83**, 3766 (1999).

[37] See, for example, J. Cubizolles, T. Bourdel, S. J. J. M. F. Kokkelmans, G. V. Shlyapnikov, and C. Salomon, Phys. Rev. Lett. **91**, 240401 (2003).

[38] C. Chin, M. Bartenstein, A. Altmeyer, S. Riedl, S. Jochim, J. Hecker Denschlag, and R. Grimm, Science **305**, 1128 (2004).

[39] G. B. Partridge, K. E. Strecker, R. I. Kamar, M. W. Jack, and R. G. Hulet, Phys. Rev. Lett. **95**, 020404 (2005).

Exact diagrammatic approach for dimer-dimer scattering and bound states of three and four resonantly interacting particles

I. V. Brodsky and M. Yu. Kagan*

P.L. Kapitza Institute for Physical Problems, Kosygin street 2, Moscow, Russia, 119334

A. V. Klaptsov

Russian Research Centre "Kurchatov Institute," Kurchatov square 1, Moscow, Russia, 123182

R. Combescot and X. Leyronas

Laboratoire de Physique Statistique, Ecole Normale Supérieure, 24 rue Lhomond, 75231 Paris Cedex 05, France

We present a diagrammatic approach for the dimer-dimer scattering problem in two or three spatial dimensions, within the resonance approximation where these dimers are in a weakly bound resonant state. This approach is first applied to the calculation of the dimer-dimer scattering length a_B in three spatial dimensions, for dimers made of two fermions in a spin-singlet state, with corresponding scattering length a_F, and the already known result $a_B = 0.60 \, a_F$ is recovered exactly. Then we make use of our approach to obtain results in two spatial dimensions for fermions as well as for bosons. Specifically, we calculate bound-state energies for three bbb and four $bbbb$ resonantly interacting bosons in two dimensions. We consider also the case of a resonant interaction between fermions and bosons, and we obtain the exact bound-state energies of two bosons plus one fermion bbf, two bosons plus two fermions $bf_\uparrow bf_\downarrow$, and three bosons plus one fermion $bbbf$.

I. INTRODUCTION

Following the experimental realization of the Bose-Einstein condensation in ultracold bosonic gases, together with its intensive study, the physics of ultracold Fermi gases has taken off recently with a strong development of experimental and theoretical investigations within the last few years [1]. In particular, much advantage has been taken of various Feshbach resonances which offer the possibility observing experimentally the so-called Bose-Einstein-condensate–(BEC) BCS crossover. This has been done in particular in ^{6}Li and ^{40}K. In the weak-coupling limit of small negative scattering length, which is realized far away on one side of the resonance, the corresponding weak attractive interaction between fermions leads to a BCS-type condensate of Cooper pairs. On the other side of the resonance, where the scattering length is positive, weakly bound dimers, or molecules, consisting of two different fermions are formed. When one goes far enough from the resonance on this positive side, one obtains a weakly interacting gas of these dimers, which may in particular form a Bose-Einstein condensate, as it has been recently observed experimentally [2–5].

In the present paper, motivated by the problem raised by the physics of this dilute gas of composite bosons, we will deal with the dimer-dimer elastic scattering and present an exact diagrammatic approach to its solution. This will be done by staying in the so-called resonance approximation which is quite suited to the physical situation found with a Feshbach resonance. In this case the (positive) scattering

length greatly exceeds the characteristic radius r_0 for the attractive interaction between fermionic atoms. A problem of this kind was first investigated by Skorniakov and Ter-Martirosian [6] in the case of the three-body fermionic problem. They showed that the scattering length of a fermion on a weakly bound dimer is determined by a single parameter—namely, the two-body scattering length a_F between fermions—and it is equal to $1.18a_F$ in the zero-range limit for the interatomic potential. A similar situation is found in the case of four fermions, where the dimer-dimer scattering length is fully determined by this same scattering length a_F. More generally the fact that the properties of few-body systems with large scattering length can be expressed in terms of the scattering length (and, depending on the system, possibly a three-body parameter) is known as "universality." For more details we refer to a recent review article [7] that discusses the phenomenon of universality in few-body systems with large scattering length in great depth.

In a study of the crossover problem Haussmann [8] calculated this scattering length of composite bosons a_B at the level of the Born approximation and found it equal to $2a_F$. This result was later on much improved by Pieri and Strinati [9], who took into account the repeated scattering of these composite bosons in the ladder approximation. This diagrammatic approach led them to a scattering length approximately equal to $a_B \simeq 0.75a_F$. However, this ladder approximation is not exact, because it misses an infinite number of other diagrams which in principle lead to a contribution of the same order of magnitude as those taken into account. Very recently this problem has been solved exactly by Petrov, Salomon, and Shlyapnikov [10,11] who found for the scattering length of these composite bosons $a_B = 0.6a_F$. This has been achieved by solving directly the Schrödinger equation for four fermi-

*Corresponding author. Electronic address: kagan@kapitza.ras.ru

$$T_2(P) \quad = \quad$$

FIG. 1. The graphic representation of the two-particle vertex $T_2(P)$ [the four external propagators do not belong to $T_2(P)$].

ons, using the well-known method of pseudopotentials. Here we will give an exact solution of this scattering problem of two weakly bound dimers, using a diagrammatic approach in the resonance approximation, which can be seen as a bridge between the approach of Pieri and Strinati [9] and the exact result of Petrov, Salomon, and Shlyapnikov [10,11].

In order to show the strength and the versatility of our approach, we make use of it to obtain results for various systems, in the two-dimensional (2D) case which is of interest not only for cold gases, but also for high T_c superconductivity. Specifically we consider first a system of resonantly interacting bosons. First we calculate exactly the three bosons bbb and four bosons $bbbb$ bound state energies. For these cases the results are already known from the works of Bruch and Tjon [12] and of Platter *et al.* [13] and we are in very good agreement with their results. We also make use of our approach for the study of 2D bosons interacting resonantly with fermions. In this case we calculate exactly the bound-state energies of two bosons plus one fermion bbf, two bosons plus two fermions $bf_\uparrow bf_\downarrow$, and three bosons plus one fermion $bbbf$. In this respect the present paper is in the line with previous results obtained by some of us. Indeed the possibility of two-fermion [14,15] ff and two-boson [16] bb pairing was predicted, as well as the creation [17] of a composite fermion bf in resonantly interacting ($a \gg r_0$) 2D Fermi-Bose mixtures.

II. THREE-PARTICLE SCATTERING

As a preliminary exercise we will rederive the result of Skorniakov and Ter-Martirosian for the dimer-fermion scattering length a_3 using the diagrammatic method [18]. Following Skorniakov and Ter-Martirosian, in the presence of the weakly bound resonance level $-E_b$ (with $E_b > 0$), we can limit ourselves to the zero-range interaction potential between fermions in the scattering of these two particles. The two-fermion vertex can be approximated by a simple one-pole structure, which reflects the presence of the s-wave resonance level in the spin-singlet state and is essentially given by the scattering amplitude, namely,

$$T_{2\alpha\beta;\gamma\delta}(P) = T_2(P)(\delta_{\alpha,\gamma}\delta_{\beta,\delta} - \delta_{\alpha,\delta}\delta_{\beta,\gamma})(\delta_{\alpha,\uparrow}\delta_{\beta,\downarrow} + \delta_{\alpha,\downarrow}\delta_{\beta,\uparrow})$$
$$= T_2(P)\chi(\alpha,\beta)\chi(\gamma,\delta), \quad (1)$$

$$T_2(P) = \frac{4\pi}{m^{3/2}} \frac{\sqrt{E_b} + \sqrt{\mathbf{P}^2/4m - E}}{E - \mathbf{P}^2/4m + E_b},$$
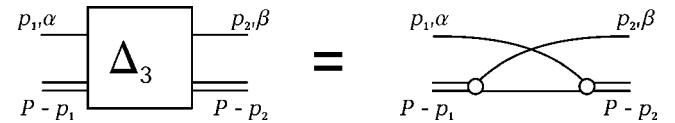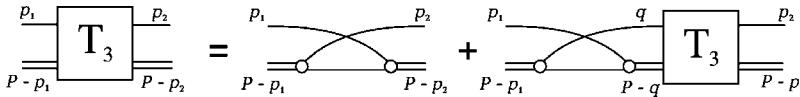

FIG. 2. The graphic representation of the simplest dimer-fermion scattering process Δ_3 (the two external fermion propagators and the two external dimer propagators do not belong to Δ_3).

$$\chi(\alpha,\beta) = \delta_{\alpha,\uparrow}\delta_{\beta,\downarrow} - \delta_{\alpha,\downarrow}\delta_{\beta,\uparrow}, \quad (2)$$

where $P = \{\mathbf{P}, E\}$, E is the total frequency, $\mathbf{P}$ is the total momentum of incoming particles, m is the fermionic mass, and $E_b = 1/ma_F^2$. The indices α, β and γ, δ denote the spin states of incoming and outgoing particles. The function $\chi(\alpha,\beta)$ stands for the spin-singlet state. We will draw this vertex in the way, shown in Fig. 1, where the double line can be regarded as a propagating dimer.

The simplest process that contributes to the dimer-fermion interaction is the exchange of a fermion. We denote the corresponding vertex as Δ_3, and it is described by the diagram in Fig. 2. Its analytical expression reads

$$\Delta_{3\alpha,\beta}(p_1,p_2;P) = -\delta_{\alpha,\beta}G(P - p_1 - p_2), \quad (3)$$

where $G(p) = 1/(\omega - \mathbf{p}^2/2m + i0_+)$ is the bare fermion Green's function. The minus sign on the right-hand side of Eq. (3) comes from the permutation of the two fermions. In order to obtain the full dimer-fermion scattering vertex T_3 we need to sum up all possible diagrams with an indefinite number of Δ_3 blocks. In the present case these diagrams have a ladder structure. It is obvious that the spin projection is conserved in every order in Δ_3 and thus $T_{3\alpha,\beta} = \delta_{\alpha,\beta}T_3$. An equation for T_3 will have the diagrammatic representation shown in Fig. 3. It is obtained by writing that either the simplest exchange process occurs alone or it is followed by any other process. In analytical form it reads

$$T_3(p_1,p_2;P) = -G(P - p_1 - p_2)$$
$$- \sum_q G(P - p_1 - q)G(q)T_2(P - q)T_3(q,p_2;P),$$
$$(4)$$

where $\Sigma_q \equiv i \int d^3q \, d\Omega/(2\pi)^4$. We can integrate out the frequency Ω in Eq. (4) by closing the integration contour in the lower half-plane, since both $T_2(P-q)$ and $T_3(q,p_2;P)$ are analytical functions of Ω in this region [this property for $T_3(p_1,p_2;P)$ results from Eq. (4) itself]. Hence only the "on-the-shell" value $T_3(\{\mathbf{q},q^2/2m\},p_2;P)$ comes on the right-hand side of Eq. (4). Moreover, if we are interested in the low-energy s-wave dimer-fermion scattering length a_3, we have to put $P = \{\mathbf{P},E\} = \{\mathbf{0},-E_b\}$ and $p_2 = 0$. Hence Eq. (4) reduces to an equation for the on-the-shell value of
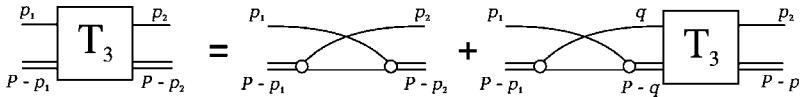
FIG. 3. The diagrammatic representation of the equation for the full dimer-fermion scattering vertex T_3.

$T_3(p_1, p_2; P)$. Taking into account the standard relation between the T matrix and scattering amplitude (with reduced mass) and the fact that, from Eq. (1), T_2 has an additional factor $8\pi/(m^2 a_F)$ compared to a standard boson propagator, we find that the full vertex T_3 is connected with a_3 by the following relation:

$$\left(\frac{8\pi}{m^2 a_F}\right) T_3(0,0;\{\mathbf{0}, -E_b\}) = \frac{3\pi}{m} a_3. \tag{5}$$

This leads to introduce a function $a_3(\mathbf{k})$ defined by

$$a_3(\mathbf{k}) = \frac{4}{3m}\left(\sqrt{mE_b} + \sqrt{3k^2/4 + mE_b}\right)$$
$$\times T_3(\{\mathbf{k}, k^2/2m\}, 0; \{\mathbf{0}, -E_b\}), \tag{6}$$

and substituting it into Eq. (4), we obtain the Skorniakov-Ter-Martirosian equation for the scattering amplitude:

$$\frac{(3/4)a_3(\mathbf{k})}{\sqrt{mE_b} + \sqrt{3k^2/4 + mE_b}} = \frac{1}{k^2 + mE_b} - 4\pi \int \frac{d\mathbf{q}}{(2\pi)^3} \frac{a_3(\mathbf{q})}{q^2(k^2 + q^2 + \mathbf{k} \cdot \mathbf{q} + mE_b)}. \tag{7}$$

Solving this equation one obtains the well-known result [6] for the dimer-fermion scattering length $a_3 = a_3(0) = 1.18 a_F$.

III. DIMER-DIMER SCATTERING

By now we can proceed to the problem of dimer-dimer scattering. This problem was previously solved by Petrov *et al.* [10,11] by studying the Schrödinger equation for a four-fermion wave function. Our diagrammatic approach is conceptually close to that of Petrov *et al.* Its basic point is that it requires the introduction of a special vertex which describes an interaction of one dimer as a single object with the two fermions constituting the other dimer.

Let us investigate all the possible types of diagrams that contribute to the dimer-dimer scattering vertex T_4. In this process both dimers are temporarily "broken" in their fermionic components, which means that the fermions of one dimer exchange and/or interact with the fermions of the other dimer. The simplest process is an exchange of fermions by two dimers shown in Fig. 4(a). More complicated diagrams are composed by introducing intermediate interactions between exchanging fermions [see Figs. 4(b) and 4(c)]. As long as one of the fermions does not interact or exchange with the other ones, all these complications can be summed up in the T_3 block [see Fig. 4(d)] which describes, as we have seen in the preceding section, the scattering of a fermion on a dimer. Furthermore, we may exchange bachelor fermions participating in the T_3 scattering. The resulting series has the diagrammatic structure shown in Fig. 4(e). This series describes a

"bare" interaction between dimers. The last obvious step is to compose ladder-type diagrams from this bare interaction. A typical ladder diagram is shown in Fig. 4(f). These general ladder diagrams describe all possible processes which contribute to the dimer-dimer scattering.

The fact that the T_4 vertex should be expressed in terms of T_3 was first noticed by Weinberg in his work on multiparticle scattering problems [19]. Note that a calculation of the diagrams shown in Figs. 4(e) and 4(f) requires information about an off-shell matrix T_3, which is about a matrix with arbitrary relation between frequencies and momenta of incoming and outgoing particles. On the other hand, for the calculation of the dimer-fermion scattering length a_3 in Eq. (7), only the simpler on-shell structure of T_3 is required as we have seen in the preceding section. Luckily, as we will see now, we can exclude T_3 from our considerations and express T_4 only in terms of T_2. By doing this we reduce the number of integral equations required for the calculation of the dimer-dimer scattering length a_4.

Since, as we have just seen, it is impossible to construct a closed equation for the dimer-dimer scattering vertex T_4, we wish to find an alternative way for taking into account in one equation all the diagrams contributing to dimer-dimer scattering. Inspired by the work of Petrov *et al.* [10,11] and looking at the diagrams we have considered above, we are naturally led to look for a special vertex that describes the interaction of two fermions, constituting the first dimer, with the second dimer taken as a single object. This vertex would be the sum of all diagrams with two fermions and one dimer as incoming lines. It would be natural to suppose that these diagrams should have the same set of outgoing—two fermi-
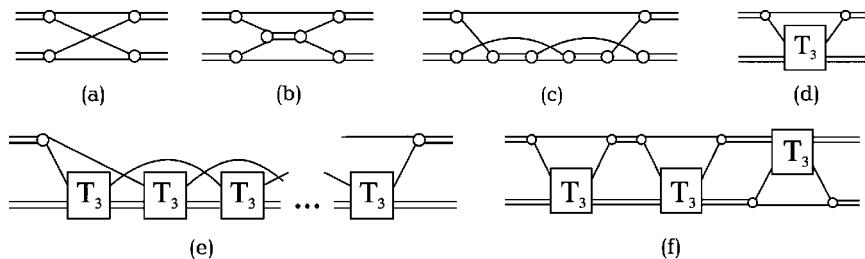

FIG. 4. The graphic representation of the dimer-dimer scattering processes contributing to T_4.
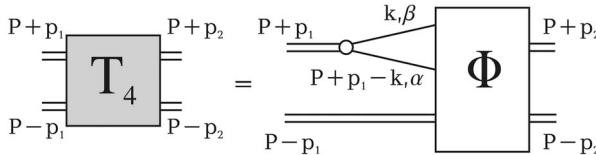
FIG. 5. Diagrammatic representation of the relation between the full dimer-dimer scattering matrix T_4 and the vertex Φ.

onic and one dimer—lines. However, in this case there will be a whole set of disconnected diagrams contributing to our sum that describe interaction of a dimer with only one fermion. As was pointed out by Weinberg [19], one can construct a good integral equation of Lippmann-Schwinger type only for connected class of diagrams. Thus we are forced to pay our attention to the vertex $\Phi_{\alpha\beta}(q_1,q_2;p_2,P)$ corresponding to the sum of all diagrams with one incoming dimer, two incoming fermionic lines and two outgoing dimer lines (see Fig. 5). This is also quite natural from our view point since, in our scattering problem we are interested in a final state with two outcoming dimers. Indeed, once this vertex $\Phi_{\alpha\beta}(q_1,q_2;p_2,P)$ is known, it is straightforward to calculate the dimer-dimer scattering vertex $T_4(p_1,p_2;P)$ which is given by

The corresponding diagrammatic representation is given in Fig. 5. One can readily verify that, in any order of interaction, Φ contains only connected diagrams.

The spin part of the vertex $\Phi_{\alpha,\beta}$ has the simple form $\Phi_{\alpha,\beta}(q_1,q_2;P,p_2)=\chi(\alpha,\beta)\Phi(q_1,q_2;P,p_2)$. The diagrammatic representation of the equation for Φ is given in Fig. 6. One can assign some "physical meaning" to the processes described by these diagrams. The diagram of Fig. 6(a) represents the simplest exchange process in a dimer-dimer interaction. The diagram of Fig. 6(b) accounts for a more complicated nature of a bare dimer-dimer interaction. Finally the diagram of Fig. 6(c) allows for a multiple dimer-dimer scattering via a bare interaction [it generates ladder-type diagrams analogous to those of Fig. 4(f)]. The last term in Fig. 6 means that we should add another set of three diagrams analogous to those of Figs. 6(a)–6(c) but with the two incoming fermions (q_1 and q_2) exchanged. The diagrammatic representation translates into the following analytical equation for the vertex Φ:

$$T_4(p_1,p_2;P) = \frac{1}{2}\sum_{k;\alpha,\beta} \chi(\alpha,\beta)G(P+p_1-k)G(k)$$
$$\times\Phi_{\alpha\beta}(P+p_1-k,k;p_2,P). \qquad (8)$$

$$\Phi(q_1,q_2;p_2,P) = -G(P-q_1+p_2)G(P-q_2-p_2) - \sum_k G(k)G(2P-q_1-q_2-k)T_2(2P-q_1-k)\Phi(q_1,k;p_2,P)$$

$$-\frac{1}{2}\sum_{Q,k} G(Q-q_1)G(2P-Q-q_2)T_2(2P-Q)T_2(Q)G(k)G(Q-k)\Phi(k,Q-k;p_2,P) + (q_1\leftrightarrow q_2). \qquad (9)$$

Finally let us also indicate that it is possible to rederive the same set of equations, purely algebraically, by taking a complementary point of view. Instead of focusing, as we have done, on the free fermions lines as soon as a dimer is "broken," we can rather keep track of the fermions which make up a dimer. This leads again automatically to introduce the vertex $\Phi(q_1,q_2;p_2,P)$. Then Eq. (9) is recovered when one keeps in mind that, after breaking dimers, one may have

propagation of a single dimer and two free fermions before another break [this corresponds to the second term on the right-hand side of Eq. (9)]. Alternatively one may also have the propagation of two dimers, which leads to the third term in Eq. (9).

Coming back now more specifically to our problem, we can put $p_2=0$ and $P=\{0,-E_b\}$ since we are looking for an s-wave scattering length. At this point we have a single


FIG. 6. The diagrammatic representation of the integral equation for the function Φ introduced by dimer-dimer scattering.

closed equation for the vertex Φ in momentum representation, which we believe is analogous to the equation of Petrov *et al.* in coordinate representation. To make this analogy more prominent we have to exclude frequencies from the equation by integrating them out. However, this exclusion requires some more technical mathematics and we leave it out for Appendix A.

The dimer-dimer scattering length is directly related to the full symmetrized vertex $T_4(p_1, p_2; P)$. Just as in the preceding section, taking also statistics into account, we have

$$\left(\frac{8\pi}{m^2 a_F}\right)^2 T_4(0, 0; \{\mathbf{0} - E_b\}, 0) = \frac{2\pi(2a_B)}{m}. \qquad (10)$$

If one skips the second term in Eq. (9)—i.e., one omits the diagram in Fig. 6(b) one will arrive at the ladder approximation of Pieri and Strinati [9]. The exact equation (9) corresponds to the summation of all diagrams. We have calculated the scattering length in the ladder approximation and the scattering length derived from the exact equation and obtained $0.78a_F$ and $0.60a_F$, respectively. Some details of our actual procedure are given in the next section. Thus our results in the ladder approximation are in agreement with the results of Pieri and Strinati [9] and, in the general form, with the results of Petrov *et al.* [10,11]. Note also that our approach allows one to find the dimer-dimer scattering length in the 2D case (this problem was previously solved by Petrov *et al.* [20]).

Finally we would like to mention that our results allows one to find a fermionic Green's function, chemical potential, and sound velocity as a function of a_F in the case of dilute superfluid Bose gas of dimers at low temperatures. The problem of dilute superfluid Bose gas of difermionic molecules was solved by Popov [21] and later deeply investigated by Keldysh and Kozlov [22]. Those authors managed to reduce the gas problem to a dimer-dimer scattering problem in vacuum, but were unable to express the dimer-dimer scattering amplitude in a single two-fermion parameter. A direct combination of our results with those ones of Popov and Keldysh and Kozlov allows one to get all the thermodynamical values of a dilute superfluid resonance gas of composite bosons. Another interesting subject for the application of our results will be a high-temperature expansion for the thermodynamical potential and sound velocity in the temperature region $T \sim T_* \sim E_b$, where the composite bosons begin to appear.

IV. PRACTICAL IMPLEMENTATION

Let us give now some details on the way in which we have solved effectively the above equations. Actually we have dealt with two problems: the scattering-length calculation discussed above and the bound-state problem to be discussed below. Our two problems are quite closely related since, for the scattering-length problem, we look for the scattering amplitude at zero outgoing wave vectors and energy for two dimers, while for the bound states we look for divergences of this same scattering amplitude at negative energy. As already indicated, in both cases the situation is somewhat simplified with respect to the variables we have to consider, due to the specific problem we handle. First, with respect to $P = \{\mathbf{P}, E\}$, we have $\mathbf{P} = \mathbf{0}$ since we work naturally in the rest frame of the four particles. Moreover, with respect to the total energy, $E = -\epsilon E_b$ is negative. Specifically $\epsilon = 1$ when we look for the scattering length. Or when we consider bound states ϵ gives the energy of the bound states we are looking for. Next, with respect to parameter $p_2 \equiv \{\mathbf{p}_2, \bar{p}_2\}$ which characterizes the outgoing dimers, we will have naturally $\mathbf{p}_2 = \mathbf{0}$ as we have said since we consider zero outgoing wave vectors. Since we will evaluate $\bar{p}_2$ on the shell, we have merely $\bar{p}_2 = 0$, and this parameter drops out. Hence in the following we do not write anymore explicitly the value of parameter P. For both the scattering-length problem and the bound-state problem, we have followed two main routes.

In our first route, we have written a specific integral equation for $T_4(p_1, p_2)$, which is then solved numerically. The details of our derivation for this integral equation are given in Appendix B. The kernel for this equation is itself obtained from a vertex Γ. The defining integral equation (B2) for this vertex has been solved numerically by calculating the inverse matrix to obtain the vertex $\Gamma(q_1, q_2; p_2)$. We have used [23] LU factorization and Gauss quadrature. The result has then been substituted into Eq. (B1) which gives the kernel $\Delta_4(p_1, p_2)$ coming in the integral equation (B3). The solution of this last equation is naturally also handled numerically—for example, by finding the eigenvalues of the kernel for the bound-state problem.

In our second route we have kept both functions T_4 and Φ. In the following we do not write anymore the parameter p_2 which takes always the trivial value $p_2 = 0$, as explained above. Hence we are left with $T_4(p_1)$ which, because of rotational invariance, depends only on the energy $\bar{p}_1$ and the modulus $|\mathbf{p}_1|$ of the momentum. For brevity we denote this quantity $t_4(|\mathbf{p}_1|, \bar{p}_1)$. On the other hand, it is shown in Appendix A that, in order to evaluate the second term on the right-hand side of Eq. (9), we need only the evaluation of $\Phi(q_1, q_2)$ on the shell, which we denote as $\phi(\mathbf{q}_1, \mathbf{q}_2)$. It depends only on the three variables $|\mathbf{q}_1|$, $|\mathbf{q}_2|$ and the angle between these two vectors. Hence it is enough to write Eq. (9) only for q_1 and q_2 taking on the shell values. From Eq. (9) this leads for $\phi(\mathbf{q}_1, \mathbf{q}_2)$ to the following more convenient equation:

$$\phi(\mathbf{q}_1, \mathbf{q}_2) = -\frac{1}{(|E| + \mathbf{q}_1^2/m)(|E| + \mathbf{q}_2^2/m)} + \int \frac{d^D \mathbf{k}}{(2\pi)^D} \frac{2mt_2(2|E| + [2\mathbf{k}^2 + 2\mathbf{q}_1^2 + (\mathbf{k} + \mathbf{q}_1)^2]/4m)\phi(\mathbf{q}_1, \mathbf{k})}{4m|E| + \mathbf{k}^2 + \mathbf{q}_1^2 + \mathbf{q}_2^2 + (\mathbf{k} + \mathbf{q}_1 + \mathbf{q}_2)^2}$$

$$-\frac{1}{2}\sum_Q \frac{(2m)^2 t_2(|E| + \bar{Q} + Q^2/4m)t_2(|E| - \bar{Q} + Q^2/4m)t_4(|\mathbf{Q}|, \bar{Q})}{[2m(|E| - \bar{Q}) + \mathbf{q}_1^2 + (\mathbf{Q} + \mathbf{q}_1)^2][2m(|E| + \bar{Q}) + \mathbf{q}_2^2 + (\mathbf{Q} + \mathbf{q}_2)^2]} + (\mathbf{q}_1 \leftrightarrow \mathbf{q}_2), \qquad (11)$$

where the dimer propagator $t_2(x)$ depends on the space dimension D. For $D=3$ it is given from Eq. (1) by $t_2(x) \equiv -4\pi/[m^{3/2}(\sqrt{x}-\sqrt{E_b})]$, while for $D=2$ according to Eq. (21) we have $t_2(x) \equiv -4\pi/[m\ln(x/E_b)]$. In the third term the angular integration can be performed analytically, and one is left with double integrals for the last two terms, for the 3D as well as for the 2D case. It is actually quite convenient, in the last term, to deform the $\bar{Q}$ contour from $]-\infty,\infty[$ to $]-i\infty,i\infty[$ by rotating it by $\pi/2$.

No singularity is met in this deformation, and one is left to deal only with real quantities.

The above equation has to be supplemented by a corresponding equation for $t_4(|\mathbf{q}|,\bar{q})$ obtained from the definition (8). The important point is that the additional integrations can be performed analytically, owing to the various invariances under rotations found in the resulting terms. We just give here as an intermediate step the structure of the resulting equation:

$$t_4(k,iz) = S(k,z) + \int_0^\infty dp_1 \int_0^\infty dp_2 \int_0^{2\pi} d\alpha\, I(k,z,p_1,p_2,\alpha) t_2\big(2|E| + [3p_1^2 + 3p_2^2 + 2\mathbf{p}_1\cdot\mathbf{p}_2]/4m\big)\phi(\mathbf{p}_1,\mathbf{p}_2)$$

$$+ \int_0^\infty dK \int_0^\infty dZ\, J(k,z,K,Z)|t_2(|E| + iZ + K^2/4m)|^2 t_4(K,iZ), \tag{12}$$

where α is the angle between $\mathbf{p}_1$ and $\mathbf{p}_2$. Here $S(k,z)$, $I(k,z,p_1,p_2,\alpha)$, and $J(k,z,K,Z)$ are analytically known functions of the variables (except that J requires one to perform numerically a simple integration to be obtained; see below). In this equation and in particular in its last term, we have already gone to the purely imaginary frequency variable for t_4. The resulting $t_4(x,iz)$ turns out to be real and even with respect to z.

To be fully specific let us now give the actual self-contained integral equations which we have solved. We restrict ourselves to the 3D case and to the *bfbf* case (implying $\alpha=1$), corresponding to the dimer scattering problem treated by Petrov *et al.* [10,11]. The only generalization is that we keep $E=-\epsilon|E_b|$, instead of setting $\epsilon=1$ as we should if we considered only the scattering length problem. For clarity we write the resulting equations with dimensionless quantities, where $1/a$ has been taken as unit wave vector and $|E_b|=1/ma^2$ as the energy unit. For simplicity we keep basically the same notation for the various variables. We just indicate by a bar over the function name that they are expressed in reduced units, with reduced variables [actually we write $\bar{t}_4(k,z)$ instead of $\bar{t}_4(k,iz)$, and there is a change of sign between $\phi(\mathbf{q}_1,\mathbf{q}_2)$ and $\bar{\phi}(\mathbf{p}_1,\mathbf{p}_2)$]. The equations for other cases and dimensions are completely similar with only a few changes in coefficients, signs (for the particle statistics), for the expression of $\bar{t}_2(x)$ and for the explicit functions coming from analytical angular integrations.

We obtain

$$\bar{\phi}(\mathbf{p}_1,\mathbf{p}_2) = \frac{1}{(\epsilon+p_1^2)(\epsilon+p_2^2)} + \frac{1}{\pi}\int_0^\infty k^2 dk \int_0^\pi \sin\theta\, d\theta\, \frac{\bar{\phi}(\mathbf{p}_1,\mathbf{k})\bar{t}_2\big(2\epsilon + [3p_1^2 + 3k^2 + 2kp_1\cos\theta]/4\big)}{\sqrt{A_+ A_-}} + (\mathbf{p}_1 \leftrightarrow \mathbf{p}_2)$$

$$+ \frac{8}{\pi p_1 p_2} \int_0^\infty dz \int_0^\infty dk\, \bar{t}_4(k,z)|\bar{t}_2(\epsilon + k^2/4 + iz)|^2 I(B_1,B_2,\alpha), \tag{13}$$

with

$A_\pm = 2\epsilon + p_1^2 + p_2^2 + k^2 + p_1 p_2 \cos\alpha + kp_1 \cos\theta + kp_2 \cos(\alpha \pm \theta)$

and α is the angle between $\mathbf{p}_1$ and $\mathbf{p}_2$, while θ is the polar angle of $\mathbf{k}$ with $\mathbf{p}_1$. We have simply set now $\bar{t}_2(x) = [1-\sqrt{x}]^{-1}$. Here we have also defined the function

$$I(B_1,B_2,\alpha) = \mathrm{Re}\,\frac{1}{2\sqrt{E}}\ln\frac{B_1 B_2^* + \cos\alpha + \sqrt{E}}{B_1 B_2^* + \cos\alpha - \sqrt{E}}, \tag{14}$$

$$E = B_1^2 + B_2^{*2} + 2B_1 B_2^* \cos\alpha - \sin^2\alpha, \tag{15}$$

$$B(p,k,z) = \frac{1}{kp}\left[\epsilon + p^2 + \frac{k^2}{2} - iz\right], \tag{16}$$

$$B_i \equiv B(p_i,k,z). \tag{17}$$

The corresponding equation for $\bar{t}_4(k,z)$ is

$$\bar{t}_4(k,z) = -\frac{1}{4\pi kz}\ln\frac{1+\cos\gamma+2\sqrt{\cos\gamma}\cos(\varphi-\gamma/2)}{1+\cos\gamma+2\sqrt{\cos\gamma}\cos(\varphi+\gamma/2)} - \frac{1}{\pi^3 k^2}\int_0^\infty p_1 dp_1\int_0^\infty p_2 dp_2\int_0^\pi \sin\alpha\, d\alpha\, \bar{\phi}(\mathbf{p}_1,\mathbf{p}_2)\bar{t}_2\left(2\epsilon+[3p_1^2+3p_2^2\right.$$

$$\left. +2p_1 p_2\cos\alpha]/4\right)I(B_1,B_2,\alpha) - \frac{1}{2\pi^3 k}\int_0^\infty KdK\int_0^\infty dZ\, \bar{t}_4(K,Z)|\bar{t}_2(\epsilon+K^2/4+iZ)|^2\bar{J}(k,z,K,Z), \qquad (18)$$

with $\varphi=\arctan(k/2)$ and $\gamma=\arctan[4z/(4+k^2)]$, and we have defined the function

$$\bar{J}(k,z,K,Z) = \int_0^\infty dx\, \frac{1}{\epsilon+x^2+\dfrac{k^2+K^2}{4}}$$

$$\times\ln\frac{C(x,k,K,Z)}{C(x,-k,K,Z)}\ln\frac{C(x,K,k,z)}{C(x,-K,k,z)}, \quad (19)$$

$$C(x,k,K,Z) = \left[\epsilon+\left(x+\frac{k}{2}\right)^2+\frac{K^2}{4}\right]^2+Z^2. \qquad (20)$$

It is seen in these integral equations for our two unknown functions $\bar{t}_4(x,z)$ and $\bar{\phi}(\mathbf{p}_1,\mathbf{p}_2)$ that they require only at most triple integrals to be performed numerically. In this sense they are not numerically more complicated than the work involved in solving directly for the corresponding Schrödinger equation, as has been done by Petrov *et al.* [10,11]. Indeed these integrals require only a few appropriate changes of variables to take care of singular behaviors occurring on some boundaries. Otherwise they have been performed with an unsophisticated integration routine.

In the case of the scattering length a mere iteration algorithm has been found to lead rapidly to the solution (provided an appropriate exact algebraic manipulation is made to make the iteration convergent). In this way we have been able to handle $45\times45\times45$ matrices [for the three variables entering $\bar{\phi}(\mathbf{p}_1,\mathbf{p}_2)$]. This size is large enough to allow improved precision by extrapolation to infinite size, although we have not done it in the present case, but rather for the ground state of the *bbbb* complex discussed below. This leads to the result $a_B=0.60a_F$ in full agreement with Petrov *et al.* [10,11] within a quite reasonable computing time on a (nowadays) unsophisticated computer. We have not tried to improve on the accuracy of the result, since there is no basic interest. In the case of the bound states, to be described below, we have proceeded to a straight diagonalization of the matrix equivalent to the right-hand sides of Eqs. (13) and (18) with the LAPACK library algorithm. In the 2D case, it is worth noticing that, because of the logarithmic dependence of $\bar{t}_2(x)$ on x, it is quite an improvement to make the change of variables $K=\epsilon^{1/2}K'$ and $Z=\epsilon Z'$, and so on, since the more appropriate variable turns out to be $\ln\epsilon$ rather than ϵ itself.

V. RESULTS IN A 2D CASE

We will now apply the diagrammatic approach developed in the previous sections (see also Appendix A) to rederive some known results and to obtain some new ones for the systems of resonantly interacting particles in a 2D case.

As was first shown by Danilov [24] (see also the paper by Minlos and Fadeev [25]) in the 3D case, the problem of three resonantly interacting bosons could not be solved in the resonance approximation. This statement stems from the fact that in the case of identical bosons the homogeneous part of Skorniakov-Ter-Martirosian equation (7) has a nonzero solution at any energies. The physical meaning of this mathematical feature was elucidated by Efimov [26], who showed that a two-particle interaction leads to the appearance of an attractive $1/r^2$ interaction in a three-body system. Since in the attractive $1/r^2$ potential a particle can fall into the center, the short-range physics is important and one cannot replace the exact pair interaction by its resonance approximation.

On the contrary in the case of the 2D problem the phenomenon of the particle falling into the center is absent and one can utilize the resonant approximation [12,27]. Therefore it is possible to describe three- and four-particle processes in terms of the two-particle binding energy $E_b=1/ma^2$ only (below, for simplicity, we will assume that all particles under consideration have the same mass m). We will leave aside the problem of composite-particle scattering and will concentrate on the problem of the binding energies of complexes of three and four particles.

As well as in the case of the 3D problem, the cornerstone in the diagrammatic technique is the two-particle resonance scattering vertex T_2 (see Fig. 1). For two resonantly interacting particles with total mass $2m$ it reads, in 2D,

$$T_2(P) = -\frac{4\pi}{m}\frac{\alpha}{\ln(\{\mathbf{P}^2/4m-E\}/|E_B|)}, \qquad (21)$$

where we introduce a factor $\alpha=\{1,2\}$ in order to take into account whether two particles are indistinguishable or not—that is, $\alpha=2$ for the case of a resonance interaction between identical bosons, while $\alpha=1$ for the case of a resonance interaction between fermion and boson or for the case of two distinguishable fermions.

A. Three particles in 2D

We start with a system of three resonantly interacting identical bosons (*bbb*) in 2D. An equation for the dimer-boson scattering vertex T_3 which describes interaction of three bosons has the same diagrammatic form as the one shown in Fig. 3; however, there are small changes in the rules for its analytical evaluation. The resulting equation reads

TABLE I. Bound states of resonantly interacting particles in 2D.

System	Relative[a] interaction	Number of bound states	Energy (in $|E_B|$)[b]	α[c]
bbb	U_{bb}	2	1.27, 16.5	2
fbb	U_{fb}	1	2.39	1
$fbbb$	U_{fb}	1	4.1	1
$bf_\uparrow bf_\downarrow$	U_{fb}	2	2.8, 10.6	1
$bbbb$	U_{bb}	2	22, 197	2

[a]Interaction that yields resonance scattering. All other interactions are negligible.
[b]$m = m_b = m_f$.
[c]The indistinguishability parameter in Eq. (21).

$$T_3(p_1, p_2; P) = G(P - p_1 - p_2)$$
$$+ \sum_q G(P - p_1 - q)G(q)T_2(P - q)T_3(q, p_2; P),$$
$$(22)$$

where we have now $\Sigma_q \equiv i \int d^2q\, d\Omega/(2\pi)^3$, $P = \{\mathbf{0}, E\}$, and one should put $\alpha = 2$ for the two-particle vertex T_2 in Eq. (21). The opposite signs in Eq. (4) for fermions and Eq. (22) for bosons are due to the permutational properties of the involved particles: an exchange of fermions (see Fig. 2) results in a minus sign, while an analogous exchange of bosons brings no extra minus. Finally, as we mentioned above, we note that three-particle s-wave (s-wave channel of a boson-dimer scattering) binding energies E_3 correspond to the poles of $T_3(0, 0; \{\mathbf{0}, -|E_3|\})$ and, consequently, at energies $E = E_3$ the homogeneous part of Eq. (22) has a nonzero solution. Solving Eq. (22) we find that a complex of three identical bosons has two s-wave bound states $E_3 = -16.5E_b$ and $E_3 = -1.27E_b$ in accordance with the previous results of Bruch and Tjon [12,27].

Let us now consider a complex (fbb) consisting of one fermion and two bosons. As noted above we take bosons and fermions with equal masses $m_b = m_f = m$. We assume that a fermion-boson interaction U_{fb}, characterized by the length r_{fb}, yields a resonant two-body bound state with an energy $E = -E_b$. In the same time a boson-boson interaction U_{bb}, characterized by the interaction length r_{bb}, does not yield a resonance. Hence, if we are interested in the low-energy physics, the only relevant interaction is U_{fb}, and we can ignore the boson-boson interaction U_{bb}, the latter would give small corrections of the order $|E_B|mr_{bb}^2 \ll 1$ at low energies. In order to determine three-particle bound states one has to find poles in the dimer-boson scattering vertex T_3. Since we neglect the boson-boson interaction U_{bb} the vertex T_3 is described by the same diagrammatic equation of Fig. 3 as for the problems of three bosons. The analytical form of this equation also coincides with Eq. (22) with the minor differ-
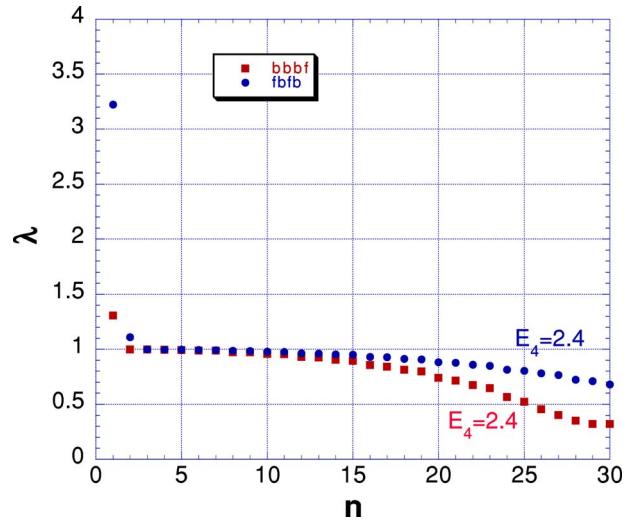

FIG. 7. (Color online) Eigenvalues λ found for $|E_4| = 2.4$, for both the $bbbf$ and $bf_\uparrow bf_\downarrow$ cases. When one of the eigenvalues is equal to 1, E_4 is the energy of a possible eigenstate of the complex. The number n appearing on the x axis is just here to number the first few eigenvalues which are displayed by decreasing order.

ence that the resonance scattering vertex T_2 now corresponds to the interaction between a boson and a fermion, and therefore we should put $\alpha = 1$ in Eq. (21) for T_2. Solving the equation for T_3 we find that the fbb complex has only one s-wave bound state with energy $E_3 = -2.39E_b$. Note that a complex (bff) consisting of a boson and two spinless identical fermions with resonance interaction U_{fb} does not have any three-particle bound states.

B. Four particles in 2D

After solving the above three-particle problems we may proceed to the complexes consisting of four particles. At first we will consider [13] four identical resonantly interacting bosons $bbbb$. Any two bosons would form a stable dimer with binding energy $E = -E_b$. We are going to find a four-particle binding energy as an energy of an s-wave bound state of two dimers. Generally speaking a bound state could emerge in channels with larger orbital moments; however, this question will be a subject of further investigations. Just as in the preceding subsection, in order to find a binding energy we should examine the analytical structure of the dimer-dimer scattering vertex T_4 and find its poles. The set of equations for T_4 has the same diagrammatic structure as those shown in Figs. 5 and 6. The analytical expression for the first equation reads

$$T_4(p_1, p_2; P) = \frac{1}{\alpha} \sum_k G(P + p_1 - k)G(k)\Phi(P + p_1 - k, k; p_2, P),$$
$$(23)$$

and the equation for the vertex Φ is

$$\Phi(q_1,q_2;p_2,P) = G(P-q_1+p_2)G(P-q_2-p_2) + \sum_k G(k)G(2P-q_1-q_2-k)T_2(2P-q_1-k)\Phi(q_1,k;p_2,P)$$

$$+ \frac{1}{2\alpha}\sum_{Q,k} G(Q-q_1)G(2P-Q-q_2)T_2(2P-Q)T_2(Q)G(k)G(Q-k)\Phi(k,Q-k;p_2,P) + (q_1 \leftrightarrow q_2), \quad (24)$$

where T_2 should be taken from Eq. (21) and one should put $\alpha=2$ for the case of identical resonantly interacting bosons. When we look for the poles of T_4 as a function of the variable E, with $P=\{0,E\}$, we have naturally to consider only the homogeneous part of this equation. We have found two bound states for the $bbbb$ complex. The values of the total binding energy $|E_4|=2|E|$ are given in Table I. They are in very good agreement with the results which were first obtained more accurately by Platter, Hammer, and Meißner [13]. We did not try to get very high accuracy for our numerical results, since this is not our main purpose, but it could certainly be improved. Clearly for the validity of our approximation we should have $|E_4| \ll 1/mr_0^2$. For the case of four bosons $bbbb$ it means that $197E_b \ll 1/mr_0^2$ and hence $a/r_0 \gg \sqrt{197}$. This case can still be considered as quite realistic for the Feshbach resonance situation.

The case of a four-particle complex $(bf_\uparrow bf_\downarrow)$ consisting of resonantly interacting bosons and fermions is still described by the same equations (23) and (24) but with parameter $\alpha=1$. In this case we found two bound states and they are also listed in Table I.

In order to obtain bound states of the $fbbb$ complex one has to find energies $P=\{0,E\}$ corresponding to nontrivial solutions of the following homogeneous equation
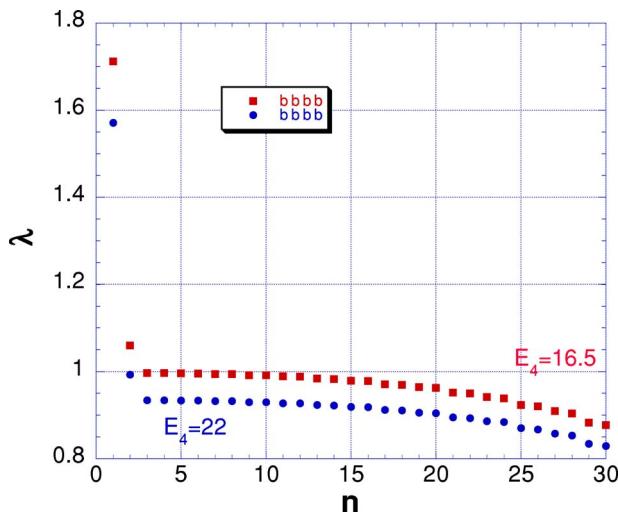

FIG. 8. (Color online) Eigenvalues λ found for $|E_4|=16.5$ and $|E_4|=22$, for the $bbbb$ case. When one of the eigenvalues is equal to 1, E_4 is the energy of a possible eigenstate of the complex. The number n appearing on the x axis is just here to number the first few eigenvalues which are displayed by decreasing order.

$$\Phi(q_1,q_2;p_2,P) = \sum_k G(k)G(2P-q_1-q_2-k)$$
$$\times T_2(2P-q_1-k)\Phi(q_1,k;p_2,P) + (q_1 \leftrightarrow q_2). \quad (25)$$

This equation corresponds to the diagram of Fig. 6(b). We have found a single bound state for this $fbbb$ complex. Finally we summarize the results concerning binding energies of three and four resonantly interacting particles in 2D in Table I.

For the $bbbb$ complex we find the beginning of a continuum of states at $|E_4|/E_b=16.5$, as it should be since this is, within our numerical precision, the binding energy of bbb. Similarly we find the beginning of a continuum at $|E_4|/E_b =2.4$ for the $fbbb$ and $bf_\uparrow bf_\downarrow$ complexes, in agreement with the binding energy of fbb. We display our corresponding results in Figs. 7 and 8. In all our calculations we find numerically, as a function of $|E_4|$, the eigenvalues λ corresponding to the matrix on the right-hand side of our equations—for example, Eq. (25). When one of these eigenvalues is equal to 1, this means that the corresponding E_4 is the energy of an eigenstate of our complex. In Fig. 7, we display the first highest eigenvalues for $|E_4|=2.4$, for both the $bf_\uparrow bf_\downarrow$ and $bbbf$ cases. One sees clearly that a fair number of eigenvalues are essentially equal to 1. One could tune them exactly to 1 by changing very slightly $|E_4|$. Hence this corresponds to the beginning of the continuum. By contrast one sees also clearly two isolated eigenvalues larger than 1 for the $bf_\uparrow bf_\downarrow$ case and one eigenvalue larger than 1 for the $bbbf$ case. One can bring them to $\lambda=1$ by increasing $|E_4|$, and therefore they correspond to the bound states that we have found. Similarly we display in Fig. 8 the eigenvalues for the $bbbb$ case, for the value $|E_4|=16.5$ corresponding essentially to the threshold for the continuum. Here again one sees many eigenvalues quite close to 1. In the same figure we also show the results of the same calculations for $|E_4|=22$ in order to display the way in which this whole spectrum evolves with $|E_4|$. In particular one sees clearly the two isolated eigenvalues, corresponding to the two bound states found in this case. In particular, since one of them is equal to 1, this means that the binding energy of one of the bound states is equal to $22E_b$, within our numerical precision.

Note finally that all our calculations correspond to the case of particles with equal masses $m_f=m_b=m$, although they can be quite easily generalized to the case of different masses.

VI. CONCLUSIONS AND DISCUSSION

For the problem of resonantly interacting fermions in 3D we have developed a diagrammatic approach that allows to find the dimer-dimer scattering length $a_B = 0.60a_F$ in perfect agreement with known results. This exact diagrammatic solution of the dimer-dimer scattering length problem in 3D opens new horizons for the extension of the self-consistent mean-field schemes of Leggett, and of Nozières and Schmitt-Rink, to the inclusion of the quite essential three- and four-particle physics in the two-particle variational wave functions of the BCS type. This in turn will help us to get diagrammatically exact results for T_c, the pseudogap, and the sound velocity in the dilute BEC limit and to develop a more sophisticated interpolation scheme for these quantities toward the unitarity limit. Work on this very exciting project is now in progress.

We have applied the developed approach to the 2D case. Namely, we have calculated exactly the binding energies of the following complexes: three bosons *bbb*, two bosons plus one fermion *bbf*, three bosons plus one fermion *bbbf*, two bosons plus two fermions $bf_\uparrow bf_\downarrow$, and four bosons *bbbb*. Note that for the case of three bosons *bbb* and four bosons *bbbb* we have effectively rederived the results which were first obtained by Bruch and Tjon [12,27] for three particles and by Platter, Hammer, and Meißner [13] for four particles. We did not try to get a very high accuracy of our numerical results for binding energies, since we were more interested in similarities between our results and the results of Refs. [12,13,27] for various situations. We would like to emphasize once more that our results for the three-particle complex *fbb* and the four-particle complexes $f_\uparrow bf_\downarrow b$ and *fbbb* are new. These results are important for the construction of the phase diagram of a Fermi-Bose mixture with resonance interaction between fermions and bosons considered in our recent paper [17]. They can be also useful for 2D Fermi-Bose mixtures of spinons and holons in the framework of slave-boson (slave-fermion) approaches to the phase diagram of underdoped high-T_c superconductors. Finally our results for the binding energies of the three-particle complex and the four-particle complex in 2D are important to complete the phase diagram of the Bose gas with two kinds of resonantly interacting bosons considered in Ref. [8].

Our investigations enrich the phase diagram for ultracold Fermi-Bose gases with resonant interaction. They serve as an important step for future calculations of the thermodynamical properties and the spectrum of collective excitations in different temperature and density regimes, in particular in the superfluid domain. Note that in purely bosonic models in 2D or in the Fermi-Bose mixtures in the case of the prevailing density of bosons $n_B > n_F$ a creation of larger complexes consisting of five, six, and so on particles is also possible. In fact here we are dealing with the macroscopic phase separation (with the creation of large droplets). The radius of this droplet R_N and the binding energy E_N for N-bosons in 2D has been estimated by Hammer and Son [28] on the basis of a variational approach. Their calculation represents the leading-order in a $1/N$ expansion and becomes exact when N goes to infinity. Note that the authors used the renormalization-group philosophy to evaluate the effective (running) cou-

pling constant $g(R)$ of boson-boson interaction. After that they applied a standard variational procedure based on the minimization of the total energy of the N-particle droplet radius R_N. It is interesting that they got a qualitative agreement with the exact result of Platter *et al.* [13] already for $N=4$ (see also the review article by Braaten and Hammer [7] for the discussion of this result based on the universality concept). Note that for $N \geq 5$ the exact calculations of the binding energies requires huge computational capability, but it would be interesting to see precisely how this would appear within our approach and how it would compare with the variational results [7,28]. Note also that the concept of macroscopic phase separation (corresponding to the formation of large droplets) is very popular nowadays in different strongly interacting electron systems such as high-T_C superconductors, systems with colossal magnetoresistance, and excitonic systems. In connection with ultracold quantum Fermi-Bose gases the problem of large droplets formation has been experimentally investigated by Roati and co-workers [29,30] for the Fermi-Bose mixture of ^{40}K-^{87}Rb in the case of a prevaling density of bosons $n_B > n_F$.

APPENDIX A: DIMER-DIMER SCATTERING EQUATION—FREQUENCY INTEGRATION

In this appendix we will show how one can integrate explicitly over the frequency dependence in the dimer-dimer scattering equation (9) (we consider only this case; the other ones considered in Sec. IV would require trivial modifications). To simplify further computations we slightly change the notation and introduce a chemical potential $\mu = -E_b/2$ and the single-fermion energy $\xi_\mathbf{p} = \mathbf{p}^2/2m - \mu = \mathbf{p}^2/2m + E_b/2$, with the modified fermion Green's function $\mathcal{G}(p) = 1/(\omega - \xi_\mathbf{p})$. In expression (1) for $\mathcal{T}_2(Q)$ we have similarly to replace E by $E - E_b$.

The integral equation (9) reads more, explicitly (with $k = \{\mathbf{k}, \omega\}$ and $Q = \{\mathbf{Q}, \Omega\}$),

$$\Phi(q_1,q_2) = -\mathcal{G}(-q_1)\mathcal{G}(-q_2) - i\int_{-\infty}^{\infty} \frac{d\omega}{2\pi} \int \frac{d^3\mathbf{k}}{(2\pi)^3} \mathcal{G}(k)\mathcal{G}(-q_1-q_2-k)\mathcal{T}_2(-q_1-k)\Phi(q_1,k)$$

$$+ \frac{1}{2}\int \frac{d^4Q}{(2\pi)^4}\frac{d^4k}{(2\pi)^4} \mathcal{G}(Q-q_1)\mathcal{G}(-Q-q_2)\mathcal{T}_2(-Q)\mathcal{T}_2(Q)\mathcal{G}(k)\mathcal{G}(Q-k)\Phi(k,Q-k) + (q_1 \leftrightarrow q_2). \qquad (A1)$$

From this equation $\Phi(q_1,q_2)=\Phi(q_2,q_1)$, as is obvious physically. Note also that the third term is already explicitly symmetrical in $q_1 \leftrightarrow q_2$.

First we note that, from Eq. (A1) itself, $\Phi(q_1,q_2)$ is analytical with respect to the frequency variables ω_1 and ω_2 of the four-vectors q_1 and q_2 in the lower half-planes Im $\omega_1 < 0$ and Im $\omega_2 < 0$. This can be seen by assuming this property self-consistently on the right-hand side and checking that the three terms are then indeed analytical, or equivalently one can proceed to a perturbative expansion. Then, if we make the "on-the-shell" calculation of $\Phi(q_1,q_2)$ from Eq. (A1)—that is, for $\omega_1=\xi_{\mathbf{q}_1}$ and $\omega_2=\xi_{\mathbf{q}_2}$—we see that, for second term on the right-hand side, the only singularity in the lower complex plane Im $\omega<0$ is the pole of $\mathcal{G}(k)$ at $\omega=\xi_{\mathbf{k}}$. Hence the integration contour can be closed in the lower half-plane, leading to

$$i\int_{-\infty}^{\infty} \frac{d\omega}{2\pi} \mathcal{G}(k)\mathcal{G}(-q_1-q_2-k)\mathcal{T}_2(-q_1-k)\Phi(q_1,k)$$

$$= -\frac{\mathcal{T}_2(-\xi_{\mathbf{q}_1}-\xi_{\mathbf{k}},\mathbf{q}_1+\mathbf{k})}{\xi_{\mathbf{q}_1}+\xi_{\mathbf{q}_2}+\xi_{\mathbf{k}}+\xi_{\mathbf{q}_1+\mathbf{q}_2+\mathbf{k}}} \Phi(\mathbf{q}_1,\mathbf{k}). \qquad (A2)$$
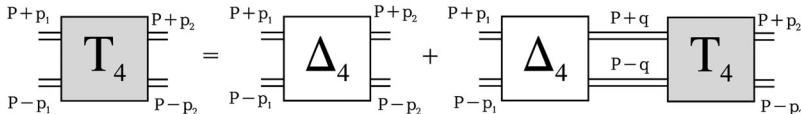
Here we denote $\Phi(\mathbf{q}_1,\mathbf{q}_2)=\Phi(\{\mathbf{q}_1,\xi_{\mathbf{q}_1}\},\{\mathbf{q}_2,\xi_{\mathbf{q}_2}\})$.

The frequency integration of the third term in Eq. (A1) over the frequencies Ω and ω is more difficult because singularities are not essentially located in one-half of the complex plane, as was the case for the second term. For example, $\Phi(k,Q-k)$ has singularities in both half planes, with respect to ω, and similarly for $\mathcal{T}_2(-Q)\mathcal{T}_2(Q)$ with respect to Ω. We solve this problem by splitting the involved functions as the sum of two parts: one analytical in the upper complex plane and the other one in the lower complex plane.

First we write $F(\Omega,\mathbf{Q},\mathbf{q}_1,\mathbf{q}_2) \equiv \mathcal{G}(Q-q_1)\mathcal{G}(-Q-q_2)\mathcal{T}_2(-Q)\mathcal{T}_2(Q)+(q_1 \leftrightarrow q_2)$ [we take into account that we want to calculate $\Phi(q_1,q_2)$ "on the shell"] as

$$F(\Omega,\mathbf{Q},\mathbf{q}_1,\mathbf{q}_2) = U_+(\Omega,\mathbf{Q},\mathbf{q}_1,\mathbf{q}_2) + U_-(\Omega,\mathbf{Q},\mathbf{q}_1,\mathbf{q}_2),$$

$$(A3)$$

where U_+ and U_- are, respectively, analytical in the upper and lower complex planes of Ω. This is done by making use of the Cauchy formula $f(\Omega)=(1/2i\pi)\int_C dz f(z)/(z-\Omega)$ for a contour C which encircles the real axis (on which F has no

singularity) and is infinitesimally near of it. This gives

$$U_+(\Omega,\mathbf{Q},\mathbf{q}_1,\mathbf{q}_2) = \frac{1}{2i\pi}\int_{-\infty}^{\infty} dz \frac{F(z,\mathbf{Q},\mathbf{q}_1,\mathbf{q}_2)}{z - i\epsilon - \Omega}, \qquad (A4)$$

with $\epsilon=0_+$. Making use of $F(-\Omega)=F(\Omega)$, we find $U_-(\Omega,\mathbf{Q},\mathbf{q}_1,\mathbf{q}_2)=U_+(-\Omega,\mathbf{Q},\mathbf{q}_1,\mathbf{q}_2)$.

On the other hand, the last part of the third term $\bar{T}_4(Q') \equiv \int d^4k'\mathcal{G}(k')\mathcal{G}(Q'-k')\Phi(k',Q'-k') = \int d^4k'\mathcal{G}(Q'/2+k')\mathcal{G}(Q'/2-k')\Phi(Q'/2+k',Q'/2-k')$ satisfies $\bar{T}_4(-Q')=\bar{T}_4(Q')$. This can be seen by substituting Eq. (A1) for $\Phi(Q'/2+k',Q'/2-k')$ in this last expression for $\bar{T}_4(Q')$. For the first-term contribution, the result is trivial. For the second term, one has to make the shift $k \to k-Q'/2$ and then $k \leftrightarrow k'$. In the third term one has to make the shift $k' \to k'+Q/2$ and then $k' \to -k'$. Then, when we make the change $Q \to -Q$ in the third term of Eq. (A1) and use $\bar{T}_4(-Q)=\bar{T}_4(Q)$, we see that the U_- contribution is exactly identical to the U_+ contribution and we are left with a single contribution from U_- to evaluate.

In order to perform the ω integration in $\bar{T}_4(Q)= \int d^4k\mathcal{G}(Q/2+k)\mathcal{G}(Q/2-k)\Phi(Q/2+k,Q/2-k)$, we split

$$\Phi(Q/2 + k, Q/2 - k) = \Phi_+(Q/2+k,Q/2-k)$$
$$+ \Phi_-(Q/2+k,Q/2-k) \qquad (A5)$$

into the sum of two functions, with Φ_+ analytical in the upper complex plane with respect to ω and Φ_- analytical in the lower complex plane. That this can be done is immediately seen from Eq. (A1) itself. For the first term we just have to write the product of Green's functions as $\mathcal{G}(k-Q/2)\mathcal{G}(-k-Q/2)=-[\mathcal{G}(k-Q/2)+\mathcal{G}(-k-Q/2)]/(\Omega+\xi_{\mathbf{k}+\mathbf{Q}/2}+\xi_{\mathbf{k}-\mathbf{Q}/2}-i\epsilon)$, which has explicitly the required property. In the third term we can handle the product of the first two Green's functions in the same way. Finally, in the second term, after performing the ω integration as indicated above (but without taking the on-the-shell values for the frequencies), one sees that the result for the term written explicitly above in Eq. (A1) is analytical in the lower complex plane with respect to ω. The corresponding term obtained by $(q_1 \leftrightarrow q_2)$ is analytic in the upper complex plane. In each case one checks that the functions analytical in the upper and lower complex planes are related by $k \leftrightarrow -k$, so that


FIG. 9. The diagrammatic representation of the equation for the full dimer-dimer scattering vertex $T_4(p_1,p_2;P)$.
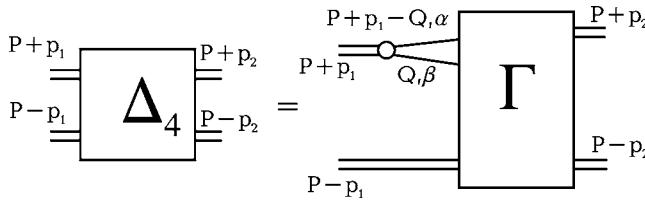
FIG. 10. The diagrammatic representation of the sum of all irreducible diagrams $\Delta_4(p_1, p_2; P)$.

$\Phi_-(Q/2+k, Q/2-k) = \Phi_+(Q/2-k, Q/2+k)$. Hence, by the change of variable $k \leftrightarrow -k$, the contributions of Φ_+ and Φ_- are equal.

Then we have arrived, for the calculation of $\bar{T}_4(Q)$, at a situation which is similar to the one we met for three particles. Since $\Phi_+(Q/2-k, Q/2+k)$ and $\mathcal{G}(Q/2-k)$ are analytical in the lower complex plane, we can close the integration contour at infinity in this lower half plane and the only contribution comes from the pole of $\mathcal{G}(Q/2+k)$. This leads to

$$\bar{T}_4(Q) = -2i \int \frac{d\mathbf{k}}{(2\pi)^3} \frac{\mathcal{F}(\Omega, \mathbf{k}, \mathbf{Q})}{\Omega - \xi_{\mathbf{k}+\mathbf{Q}/2} - \xi_{\mathbf{k}-\mathbf{Q}/2} + i\epsilon}, \quad (A6)$$

where $\mathcal{F}(\Omega, \mathbf{k}, \mathbf{Q})$ is $\Phi_+(Q/2-k, Q/2+k)$ evaluated for $\omega = \xi_{\mathbf{k}+\mathbf{Q}/2} - \Omega/2$. An important property, which can be checked on each term contributing to $\Phi_+(Q/2-k, Q/2+k)$, is that $\mathcal{F}(\Omega, \mathbf{k}, \mathbf{Q})$ is analytical in the lower complex plane with respect to Ω. Hence the integration of $U_-(\Omega, \mathbf{Q}, \mathbf{q}_1, \mathbf{q}_2)\bar{T}_4(Q)$ over Ω can also be performed by closing the contour in the lower half plane, since the only singularity in this half plane is the pole due to the denominator in Eq. (A6). The contribution of this pole leads to the evaluation of $\mathcal{F}(\Omega, \mathbf{k}, \mathbf{Q})$ for $\Omega = \xi_{\mathbf{k}+\mathbf{Q}/2} + \xi_{\mathbf{k}-\mathbf{Q}/2}$. Taken with the above definition of $\mathcal{F}$ this means that we have calculated $\Phi_+(Q/2-k, Q/2+k)$ for $\Omega/2 - \omega = \xi_{\mathbf{k}-\mathbf{Q}/2}$ and $\Omega/2 + \omega = \xi_{\mathbf{k}+\mathbf{Q}/2}$, which is just an evaluation "on the shell." Because of the simple relation between Φ_+ and Φ_-, the result can be expressed in terms of $\Phi(\mathbf{k}+\mathbf{Q}/2, -\mathbf{k}+\mathbf{Q}/2)$ itself.

Gathering all the above results we end up with the following complete equation for $\Phi(\mathbf{q}_1, \mathbf{q}_2)$:

$$\Phi(\mathbf{q}_1, \mathbf{q}_2) = -\frac{1}{4\xi_{\mathbf{q}_1}\xi_{\mathbf{q}_2}}$$
$$+ \int \frac{d^3\mathbf{k}}{(2\pi)^3} \frac{\mathcal{T}_2(-\xi_{\mathbf{q}_1} - \xi_{\mathbf{k}}, \mathbf{q}_1 + \mathbf{k})}{\xi_{\mathbf{q}_1} + \xi_{\mathbf{q}_2} + \xi_{\mathbf{k}} + \xi_{\mathbf{q}_1+\mathbf{q}_2+\mathbf{k}}} \Phi(\mathbf{q}_1, \mathbf{k})$$
$$- \int \frac{d^3\mathbf{Q}}{(2\pi)^3} \frac{d^3\mathbf{k}}{(2\pi)^3} U(\xi_{\mathbf{k}+\mathbf{Q}/2} + \xi_{\mathbf{k}-\mathbf{Q}/2}, \mathbf{Q}, \mathbf{q}_1, \mathbf{q}_2)$$
$$\times \Phi(\mathbf{k} + \mathbf{Q}/2, -\mathbf{k} + \mathbf{Q}/2) + (q_1 \leftrightarrow q_2). \quad (A7)$$

In this equation we have modified the integration contour in the definition of U_- to have it running on the imaginary axis rather than on the real axis, and we have used the symmetry property of $F(z, \mathbf{Q}, \mathbf{q}_1, \mathbf{q}_2)$ with respect to z, together with symmetry properties of $\Phi(\mathbf{q}_1, \mathbf{q}_2)$, to rewrite the result in terms of the real function

$$U(\Omega, \mathbf{Q}, \mathbf{q}_1, \mathbf{q}_2) = \frac{\Omega}{\pi} \int_0^\infty dy \frac{F(iy, \mathbf{Q}, \mathbf{q}_1, \mathbf{q}_2)}{y^2 + \Omega^2}, \quad (A8)$$

which shows that $\Phi(\mathbf{q}_1, \mathbf{q}_2)$ itself is real.

We have made practical numerical use of Eq. (A7) to find for example the ground-state energy. Although this turned out to be quite feasible, this equation appears finally less convenient than what we have described in Sec. IV. This was expected since the solution implies quadruple integrals, instead of the triple integrals we had only to deal with in Sec. IV.

APPENDIX B: MODIFIED DIMER-DIMER SCATTERING EQUATION

This appendix is devoted to an alternative description of the dimer-dimer scattering process. The purpose is to obtain a direct integral equation for $T_4(p_1, p_2; P)$, in a way convenient for numerical calculations. Below we derive such a set of equations, which were used for practical computations as indicated in Sec. IV.

The first step is to construct for two dimers a "bare" interaction potential, or vertex, Δ_4, which is the sum of all irreducible diagrams, and then to build ladder diagrams from this vertex, in order to obtain an integral equation (see Fig. 9). These irreducible diagrams are those ones which cannot be divided by a vertical line into two parts connected by two dimer lines. As was pointed above the vertex Δ_4 is
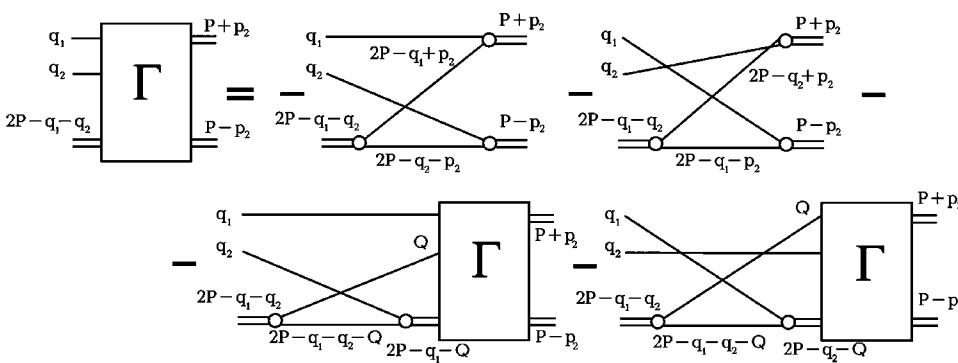

FIG. 11. The graphic representation of the equation on the full vertex $\Gamma(q_1, q_2; p_2, P)$.

given by the series shown in Fig. 4(e), since the diagrams in Fig. 4(f) are by contrast reducible. Again we can eliminate T_3 from our considerations and express Δ_4 only in terms of T_2. For this purpose we have to introduce a special vertex with two fermionic and one dimer incoming lines and two dimer outgoing lines $\Gamma_{\alpha\beta}(q_1,q_2;p_2,P)$ (see Fig. 10). This vertex $\Gamma_{\alpha\beta}(q_1,q_2;p_2,P)$ corresponds to the vertex Δ_4 with one incoming dimer line being removed, in much the same way as $\Phi(q_1,q_2;p_2,P)$ and $T_4(p_1,p_2;P)$ are related in Eq. (8). The difference is that $\Gamma_{\alpha\beta}(q_1,q_2;p_2,P)$ is irreducible with respect to two dimer lines while $\Phi(q_1,q_2;p_2,P)$ is not, just in the same way as $T_4(p_1,p_2;P)$ and $\Delta_4(p_1,p_2;P)$ are related. The corresponding equation relating $\Gamma_{\alpha\beta}(q_1,q_2;p_2,P)$ and

$\Delta_4(p_1,p_2;P)$ is

$$\Delta_4(p_1,p_2;P) = \frac{1}{2}\sum_{Q;\alpha,\beta}\chi(\alpha,\beta)G(P+p_1-Q)G(Q)$$
$$\times\Gamma_{\alpha\beta}(P+p_1-Q,Q;p_2,P). \quad \text{(B1)}$$

One can readily verify that the diagrammatic expansion for Γ shown in Fig. 11 yields the same series as the one shown in Fig. 4(e) for the vertex Δ_4. The spin part of $\Gamma_{\alpha,\beta}$ has again the simple form $\Gamma_{\alpha,\beta}(q_1,q_2;P,p_2) = \chi(\alpha,\beta)\Gamma(q_1,q_2;p_2,P)$, and the function $\Gamma(q_1,q_2;p_2,P)$ obeys the following equation:

$$\Gamma(q_1,q_2;p_2,P) = -G(P-q_1+p_2)G(P-q_2-p_2) - G(P-q_2+p_2)G(P-q_1-p_2)$$
$$-\sum_Q G(Q)G(2P-q_1-q_2-Q)[T_2(2P-q_1-Q)\Gamma(q_1,Q;p_2,P) + T_2(2P-q_2-Q)\Gamma(Q,q_2;p_2,P)]. \quad \text{(B2)}$$

The sign minus in Eq. (B2) is a consequence of the anticommutativity of Fermi operators. It is clear that Eqs. (B1) and (B2) can be analytically integrated over the variable Ω. Thus the s-wave component of the vertex $\Gamma(q_1,q_2;p_2,P)$ is a function of the absolute values of vectors $|\mathbf{q}_1|$ and $|\mathbf{q}_2|$, the angle between them, the absolute value of vector $|\mathbf{p}_2|$, and the frequency ω_2. The s-wave component of the sum of all irreducible diagrams $\Delta_4(p_1,p_2;P)$ is a function of the absolute values of the vectors $|\mathbf{p}_1|$ and $|\mathbf{p}_2|$ and the frequencies ω_1 and ω_2.

The fully symmetrized vertex $T_4(p_1,p_2;P)$ of two-dimer scattering can be found from the solution of the following equation (see Fig. 9):

$$T_4(p_1,p_2;P) = \Delta_4(p_1,p_2;P) + \frac{1}{2}\sum_q \Delta_4(p_1,q;P)$$
$$\times T_2(P+q)T_2(P-q)T_4(q,p_2;P), \quad \text{(B3)}$$

where $\Delta_4(p_1,p_2;P)$ is the sum of all irreducible diagrams, $P\pm p_{1,2} = \{-E_b\pm\omega_{1,2},\pm\mathbf{p}_{1,2}\}$ are four-vectors of incoming (1) and outgoing (2) dimers in the center-of-mass system.

Let us finally note that, equivalently to our above derivation, Eqs. (B1)–(B3) can be also related to Eqs. (8) and (9) algebraically by simple formal operator manipulations.

[1] Workshop on ultracold fermi gases, 2004 (Levico), http://bec.science.unitn.it/fermi04/

[2] M. Greiner, C. Regal, and D. Jin, Nature (London) **426**, 537 (2003).

[3] S. Jochim, M. Bartenstein, A. Altmeyer, G. Hendl, S. Riedl, C. Chin, J. H. Denschlag, and R. Grimm, Science **302**, 2101 (2003).

[4] M. W. Zwierlein, C. A. Stan, C. H. Schunck, S. M. F. Raupach, S. Gupta, Z. Hadzibabic, and W. Ketterle, Phys. Rev. Lett. **91**, 250401 (2003).

[5] T. Bourdel, L. Khaykovich, J. Cubizolles, J. Zhang, F. Chevy, M. Teichmann, L. Tarruell, S. J. J. M. F. Kokkelmans, and C. Salomon, Phys. Rev. Lett. **93**, 050401 (2004).

[6] G. V. Skorniakov and K. A. Ter-Martirosian, Zh. Eksp. Teor. Fiz. **31**, 775 (1956) [Sov. Phys. JETP **4**, 648 (1957)].

[7] E. Braaten and H. W. Hammer, e-print cond-mat/0410417.

[8] R. Haussmann, Z. Phys. B: Condens. Matter **91**, 291 (1993).

[9] P. Pieri and G. C. Strinati, Phys. Rev. B **61**, 15370 (2000).

[10] D. S. Petrov, C. Salomon, and G. V. Shlyapnikov, Phys. Rev. Lett. **93**, 090404 (2004).

[11] D. S. Petrov, C. Salomon, and G. V. Shlyapnikov, Phys. Rev. A **71**, 012708 (2005).

[12] L. W. Bruch and J. A. Tjon, Phys. Rev. A **19**, 425 (1979).

[13] L. Platter, H. W. Hammer, and U. Meißner, Few-Body Syst. **35**, 169 (2004).

[14] M. Yu. Kagan and T. M. Rice, J. Phys.: Condens. Matter **6**, 3771 (1994).

[15] M. Yu. Kagan, R. Fresard, M. Capezzali, and H. Beck, Phys. Rev. B **57**, 5995 (1998).

[16] M. Yu. Kagan and D. V. Efremov, Phys. Rev. B **65**, 195103 (2002).

[17] M. Yu. Kagan, I. V. Brodsky, D. V. Efremov, and A. V.

Klaptsov, Phys. Rev. A **70**, 023607 (2004).

[18] P. F. Bedaque and U. van Kolck, Phys. Lett. B **428**, 221 (1998).

[19] S. Weinberg, Phys. Rev. **133**, B232 (1964).

[20] D. S. Petrov, M. A. Baranov, and G. V. Shlyapnikov, Phys. Rev. A **67**, 031601(R) (2003).

[21] V. N. Popov, Zh. Eksp. Teor. Fiz. **50**, 1550 (1966) [Sov. Phys. JETP **23**, 1034 (1966)].

[22] L. V. Keldysh and A. N. Kozlov, Zh. Eksp. Teor. Fiz. **54**, 978 (1968) [Sov. Phys. JETP **27**, 521 (1968)].

[23] W. H. Press, S. A. Teukolsky, W. T. Vetterling, and B. P. Flannery, *Numerical Recipes: The Art of Scientific Computing* (Cambridge University Press, Cambridge, England, 1996).

[24] G. S. Danilov, Zh. Eksp. Teor. Fiz. **40**, 498 (1961) [Sov. Phys.

JETP **13**, 349 (1961)].

[25] R. Minlos and L. D. Fadeev, Zh. Eksp. Teor. Fiz. **41**, 1850 (1961) [Sov. Phys. JETP **14**, 1315 (1962)].

[26] V. N. Efimov, Yad. Fiz. **12**, 1080 (1970) [Sov. J. Nucl. Phys. **12**, 589 (1971)].

[27] A. S. Jensen, K. Riisager, D. V. Fedorov, and E. Garrido, Rev. Mod. Phys. **76**, 215 (2004).

[28] H. W. Hammer and D. T. Son, Phys. Rev. Lett. **93**, 250408 (2004).

[29] G. Roati, F. Riboli, G. Modugno, and M. Inguscio, Phys. Rev. Lett. **89**, 150403 (2002).

[30] G. Modugno, G. Roati, F. Riboli, F. Ferlatino, R. Brecha, and M. Inguscio, Science **297**, 2240 (2002).

Superfluid Equation of State of Dilute Composite Bosons

X. Leyronas and R. Combescot

Laboratoire de Physique Statistique, Ecole Normale Supérieure, 24 rue Lhomond, 75231 Paris Cedex 05, France
(Received 28 June 2007; published 23 October 2007)

We present an exact theory of the BEC-BCS crossover in the Bose-Einstein-condensate (BEC) regime, which treats explicitly dimers as made of two fermions. We apply our framework, at zero temperature, to the calculation of the equation of state. We find that, when expanding the chemical potential in powers of the density n up to the Lee-Huang-Yang order, proportional to $n^{3/2}$, the result is identical to the one of elementary bosons in terms of the dimer-dimer scattering length a_M, the composite nature of the dimers appearing only in the next order term proportional to n^2.

The BEC-BCS crossover first considered by Leggett [1], and the recent experimental realization of Bose-Einstein condensates (BEC) of molecules made of fermionic atoms [2–5] have motivated a number of theoretical works. Indeed, thanks to Feshbach resonances, it is experimentally possible, with two fermions of mass m (^{6}Li or ^{40}K) in different hyperfine states (we denote them as "spin" $\uparrow$ and $\downarrow$), with scattering length a, to realize weakly bound molecules, or dimers, with binding energy $E_b = 1/ma^2$ (we take $\hbar = 1$ in this Letter). In particular one can obtain a dilute condensate of molecules. A crucial quantity controlling the physics of the condensate is the dimer-dimer scattering length a_M. This is, however, a highly nontrivial quantity to calculate, since one has to solve a four-body problem to find it. In the case of a broad resonance, one finds $a_M = 0.6a$ by solving the Schrödinger equation [6] or resumming the diagrammatic series [7]. The study of a Bose-Einstein condensate of composite bosons, where all the theory is formulated in terms of fermions only, was started a long time ago [8,9]. Quite recently, Pieri and Strinati [10] derived the Gross-Pitaevskii equation from the Bogoliubov–de Gennes equations. However, because of their approximate scheme, they ended up with the Born approximation $2a$ for the dimer scattering length a_M instead of the exact result.

In this Letter, we present an exact fermionic theory of a BEC superfluid of composite bosons in the low density range. Our framework is completely general. Our present work is a first step toward going to higher orders, which will be clearly more complex to handle. Here we restrict ourselves to the $T = 0$ thermodynamics. We obtain for the expansion of the chemical potential μ of our fermions of single spin density n in the BEC regime:

$$\mu = -\frac{E_b}{2} + \frac{\pi a_M}{m} n \left[1 + \frac{32}{3\sqrt{\pi}} (na_M^3)^{1/2} \right]. \quad (1)$$

Except for the obvious first term (which implies $\mu < 0$), this is exactly the result found, for $\mu_{\text{Bose}} = 2\mu$, by Lee, Huang, and Yang (LHY) [11] for elementary bosons with density n, mass $m_B = 2m$, and scattering length $a_B = a_M$. The identity of the mean field term is somewhat expected.

However, even if it is reasonable to expect in our case a correction of the LHY type, it is not at all obvious that the coefficient is the same. We will see that our derivation is quite involved and has no systematic mapping on a purely bosonic formulation. In other terms one expects the composite nature of our bosons to enter at some stage in the theory. We find indeed that this happens, but only at the level of the n^2 term in Eq. (1). Hence we prove that, for our composite bosons, the LHY term is unchanged with respect to elementary bosons [12]. In calculations of collective mode frequencies, this result has been previously assumed to be correct [13], in agreement with Monte Carlo calculations, and this has been supported by recent experiments [14].

In order to perform a low density expansion, we need a "small parameter" in our theory. The most convenient one turns out to be the anomalous self-energy $\Delta(k)$ which, together with the anomalous (or off-diagonal) Green's function $F(k)$, is the hallmark of the superfluid state in the diagrammatic technique [15]. We will indeed see that at low density $\Delta(k)$ is of order $n^{1/2}$, which could be anticipated from the standard BCS calculation [1,8]. Hence by performing an expansion in powers of $\Delta(k)$ in Feynman diagrams, we actually perform a low density expansion. The full Green's function $G(k)$ and self-energies are related by the completely general standard equations:

$$G(k) = \mathcal{G}_0(k) - F(k)\Delta^*(k)\mathcal{G}_0(k), \quad (2)$$

$$F(k) = G(k)\Delta(k)\mathcal{G}_0(-k), \quad (3)$$

where we have set $[\mathcal{G}_0(k)]^{-1} = G_0^{-1}(k) - \Sigma(k)$, with $\Sigma(k)$ the normal self-energy, $G_0^{-1}(k) = \omega - k^2/2m + \mu$ and $k \equiv \{\mathbf{k}, \omega\}$.

We proceed in a natural way by finding the expansion of the Green's function G and F in powers of Δ at fixed μ. The single spin density gives the "number equation":

$$n = -\sum_k e^{i\omega 0_+} G(k) \quad (4)$$

with $\sum_k \equiv i \int \frac{d^3\mathbf{k}}{(2\pi)^3} \int_{-\infty}^{+\infty} \frac{d\omega}{2\pi}$. At zeroth order in $\Delta(k)$ the result is obviously $n = 0$ since, without condensate, there

are no fermions at $T = 0$, $\mu < 0$. From particle conservation, the lowest order is given by the second order term:

$$n_2 = -|\Delta|^2 \sum_k e^{i\omega 0_+} T_3(k, k; k)[G_0(k)]^2 \qquad (5)$$

where T_3, depicted in Fig. 1(a), has been discussed in Ref. [7,16] and contains all the normal state diagrams describing the scattering of a single atom by a dimer (actually in the involved vacuum Green's functions we have to shift the frequencies by the chemical potential μ). This includes, in particular, a term $-G_0(-k)$ which is just the Born approximation for T_3. In writing Eq. (5) we have made use of the fact that, at this order, the k dependence of $\Delta(k)$ can be neglected as will be shown below, and we have just denoted the resulting constant by Δ. The frequency integral in Eq. (5) can be calculated by closing the contour in the upper-half complex plane Im$\omega > 0$, where $G_0(k)$ is analytic. It can be proved that, except for the Born term, $T_3(k, k; k)$ is also analytic in this half-plane. Hence the only contribution in Eq. (5) comes from the Born term. However, this term is the only one considered in the standard BCS theory on this BEC side. We end up with the very surprising conclusion that, at this order, all the detailed physics involved in the atom-dimer scattering is irrelevant and that the result is merely given by the standard BCS calculation, namely $n_2 = m^2|\Delta|^2/(8\pi[2m|\mu|]^{1/2})$. This shows that Δ is indeed of order $n^{1/2}$.

We consider now the anomalous self-energy $\Delta(k)$, in order to obtain our equivalent of the "gap equation" [12]. $\Delta(k)$ describes two atoms $(k\uparrow, -k\downarrow)$ which go in the condensate. Quite generally the contributions to $\Delta(k)$ are divided in two classes, so we have $\Delta(k) = \delta_1(k) + \delta_2(k)$. The first class, the only one found in BCS theory, gathers diagrams where these two fermions *first* interact through the bare two-body potential, with Fourier transform $V(\mathbf{q})$, the second class containing all the other possibilities. In full generality the contribution of the first class, shown diagrammatically in Fig. 1(b), can be written:

$$\delta_1(\mathbf{k}) = \sum_{k_1} V(\mathbf{k} - \mathbf{k_1})F(k_1) \qquad (6)$$

from the very definition of the *full* Green's function F. Note that $\delta_1(\mathbf{k})$ is independent of ω and, since the potential is very short-ranged, it depends on $\mathbf{k}$ only for very high momenta.
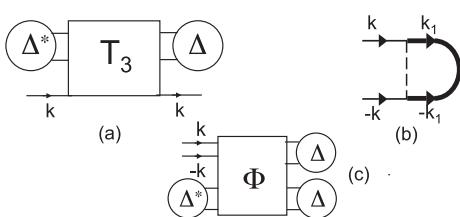

FIG. 1. (a) Structure of the lowest order normal self-energy (b) BCS-like contribution $\delta_1(k)$ (c) The diagram for $\delta_2(k)$.

In the second class, where the two incoming fermions $(k\uparrow, -k\downarrow)$ do *not first* interact, we proceed to a Δ expansion. The first order term is already included in δ_1 and particle conservation implies that the next order contains $\Delta\Delta^*\Delta$, the rest of the diagrams being made only of any number of normal state propagators $G_0(k)$ with any number of interactions, as shown schematically in Fig. 1(c). Moreover these diagrams cannot contain loops of normal state propagators, since this would correspond, in time representation, to the creation of particle-hole pairs. Such processes are impossible in the normal state at $T = 0$ and $\mu < 0$, where the free particle propagator is *retarded*.

When these constraints are taken into account, including the "no first interaction" condition, one ends up with the conclusion that these normal state diagrams have exactly been considered in Ref. [7] [with again a trivial shift of all the frequencies by μ, as for $G_0(k)$], and denoted by Φ, except for a subtle point which we discuss below and is accounted for by the slightly different notation Φ'. Hence,

$$\delta_2(k) = \frac{1}{2}|\Delta|^2 \Delta\Phi'(k, -k; 0, 0). \qquad (7)$$

In writing Eq. (7) we have taken advantage of the idea that, to lowest order [see Eq. (6)], $\Delta(k)$ is a constant independent of k. Hence in this third order term, we can take $\Delta(k)$ as constant. On the other hand, it is clear from Eq. (7) itself that $\Delta(k)$ depends in general on k. The factor $1/2$ is required to avoid double counting which arises from the presence of two factors Δ.

The difference between Φ and Φ' stems from the fact that Φ is reducible, while Φ' is not since it is a contribution to the anomalous self-energy. Specifically Φ contains the contribution $-G_0(k)G_0(-k)$ (this is the Born term) and also a term arising from the normal self-energy $\Sigma(k)$. Hence, in order to obtain Φ', one has to subtract from Φ these reducible diagrams. However, exactly these same reducible diagrams appear automatically if we write from Eq. (2) and (3) the series expansion for $G_0^{-1}(k)F(k)\times G_0^{-1}(-k)$ in terms of the (irreducible) self-energies $\Delta(k)$ and $\Sigma(k)$. Hence it is more convenient to add these reducible contributions on both sides of the equation for $\Delta(k)$, in which case we have $-G_0(k)^{-1}F(k)G_0^{-1}(-k)$ in the left-hand side and Φ appears in the right-hand side, instead of Φ' (note that this manipulation is actually valid to any order in our expansion). This leads to

$$F(k) = G_0(k)\delta_1(\mathbf{k})G_0(-k)$$
$$+ \frac{1}{2}|\Delta|^2 \Delta G_0(k)G_0(-k)\Phi(k, -k; 0, 0). \qquad (8)$$

We then eliminate $F(k)$ in favor of δ_1 by making use of Eq. (6). The summation of the last term over k introduces [7] the dimer-dimer scattering vertex $T_4(0, 0; 0) = \sum_k G_0(k)G_0(-k)\Phi(k, -k; 0, 0)$ evaluated at zero dimer energy. It is directly related [7] to the dimer scattering length by $(8\pi/am^2)^2 T_4(0, 0; 0) = 4\pi a_M/m$. The last step in our procedure is the standard elimination of the interaction

potential in favor of the scattering amplitude [17]. In our case this quantity has to be evaluated at the energy μ, because of our shift in frequency. After this step, $\delta_1(\mathbf{k})$ can be taken as a constant δ_1, since all the momentum integrals are rapidly convergent. We end up with

$$a^{-1} - \sqrt{2m|\mu|} = \frac{m^2 a^2}{8} a_M |\Delta|^2 \qquad (9)$$

where we have simplified by δ_1 and made $\delta_1 \simeq \Delta$ in the right-hand side. When we substitute for $|\Delta|^2$ its lowest order expression found above in terms of n_2, we find for μ the mean field part of Eq. (1), with the appropriate dimer scattering length a_M.

The above is only the first step in our derivation. The natural continuation would be to go to next order in Δ, i.e., to order Δ^4 in Eq. (4) and order Δ^5 in Eq. (8). This would lead to a contribution of order n^2 in Eq. (1). However, this expansion is not regular, as it would be the case if we had a gap between the ground state and the first excited state. Indeed there is, in our neutral superfluid, a branch of the excitation spectrum which goes to zero energy when momentum is zero. This is the collective mode, physically identical to sound waves in the low energy range, which is known as the Bogoliubov mode for Bose-Einstein condensates of elementary bosons. Naturally its existence is a fundamental property of the condensate [18]. In the following we include only the contributions coming from this low energy collective mode.

The propagator of this collective mode is a two-particle vertex and it is the generalization to the superfluid state of $T_2(P)$. It enters our formalism in the following way. In Figs. 1(a) and 1(c), the terms Δ^* and Δ act as "source" and "sink" of fermions. They are required since, at $T = 0$, $\mu < 0$, no fermions are present except coming from the superfluid. However, we can in general well think of having a dimer propagator going from Δ to Δ^* (and replacing them) as shown in Fig. 3. This plays the same role for source and sink, and gives diagrams which must be considered. It is easy to see that, in the normal state, they give a zero contribution (since there are no dimers in the normal state). But in the superfluid state, this dimer propagator has to be replaced by the collective mode and the result is nonzero. The terms we have to retain are just the modifications, with respect to the previous results, coming from this substitution. Actually we do not proceed immediately to a Δ expansion and our procedure is equivalent to series resummation to avoid singularities.

To proceed we have to find in our framework the collective mode propagator, more specifically in the low energy, low momentum range. It has a normal part $\Gamma(P)$ and an anomalous part $\Gamma^a(P)$, which depend only on the total energy-momentum $P \equiv \{\mathbf{P}, \Omega\}$. We write for them the equivalent of Eq. (2) and (3), i.e., the Bethe-Salpeter equations:

$$\Gamma = T_2 + T_2 \Gamma_{\mathrm{irr}} \Gamma + T_2 \Gamma^a_{\mathrm{irr}} \Gamma^a, \qquad (10)$$

$$\Gamma^a = T_{2-} \Gamma_{\mathrm{irr}-} \Gamma^a + T_{2-} \bar{\Gamma}^a_{\mathrm{irr}} \Gamma, \qquad (11)$$

where we did not write explicitly the arguments which are P or $-P$: for instance T_2 stands for $T_2(P)$ and T_{2-} for $T_2(-P)$. The normal (Γ_{irr}) and anomalous (Γ^a_{irr} and $\bar{\Gamma}^a_{\mathrm{irr}}$) irreducible vertices are analogous to self-energies.

Then we expand these irreducible vertices in powers of Δ. Again from particle conservation the lowest order terms are second order. The result for Eq. (10) is depicted in Fig. 2. The "normal part" (i.e., without the Δ factors) of the irreducible vertices involves clearly the normal state dimer-dimer scattering vertex T_4 considered above, since all "in" and "out" lines are dimer lines. Again, at this lowest order, Δ can be taken as constant. In this way Eqs. (10) and (11) become

$$\Gamma = T_2 + T_2 |\Delta|^2 \tilde{T}_4 \Gamma + T_2 \Delta^2 \bar{T}_4 \Gamma^a, \qquad (12)$$

$$\Gamma^a = T_{2-} |\Delta|^2 \tilde{T}_{4-} \Gamma^a + T_{2-} \Delta^{*2} \hat{T}_4 \Gamma, \qquad (13)$$

where $\tilde{T}_4 = T_4(P/2, P/2; P/2)$, $\bar{T}_4 = (1/2) T_4(P, 0; 0)$, and $\hat{T}_4 = \frac{1}{2} T_4(0, P; 0)$, the factor $\frac{1}{2}$ being again topological.

We can now solve for Γ and Γ^a. In the low energy limit $|\mathbf{P}| \ll 1/a$ and $|\Omega| \ll 1/ma^2$, we find easily $\Gamma(P) = -8\pi(\Omega + \mu_B + \mathbf{P}^2/4m)/(m^2 aD)$ and $\Gamma^a(P) = 8\pi\mu_B/(m^2 aD)$, where $D = (\mathbf{P}^2/4m)^2 + 2\mu_B \mathbf{P}^2/4m - \Omega^2$. We have set $\mu_B \equiv |\Delta|^2 maa_M/4$ and evaluated the factor of Δ to zeroth order by taking $2|\mu| = 1/ma^2$. The collective mode frequency is obtained by setting $D = 0$ and we recover as expected the Bogoliubov dispersion relation.

We now consider the additional contributions to the self-energies coming from the collective mode. For the normal self-energy we have to add the left diagram in Fig. 3, which gives an additional contribution n_{cm} to our lowest order result Eq. (5):

$$n_{\mathrm{cm}} = -\sum_{k,P} e^{i\omega 0_+} T_3(k, k; k + P) \Gamma(P) [G_0(k)]^2. \qquad (14)$$

Actually we should have subtracted from $\Gamma(P)$ its zeroth and second order terms in the series expansion in powers of Δ (this is indicated in Fig. 3 by the slash in the mode propagator), since they are in principle taken into account in Eq. (5). However it is easily seen that they are zero since they contain normal state propagator loops. In Eq. (14) we can first perform the integration over the frequency variable ω of k, by closing the contour in the upper half-plane. Just as above in Eq. (4), it can be proved that the only contribution comes from the Born term of $T_3(k, k; k + P)$. Then the $\mathbf{k}$ integration is easily performed and we are left
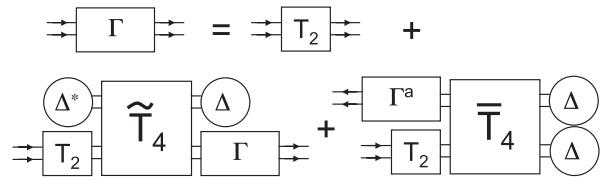

FIG. 2.   Diagrammatic representation for Eq. (12) for Γ.
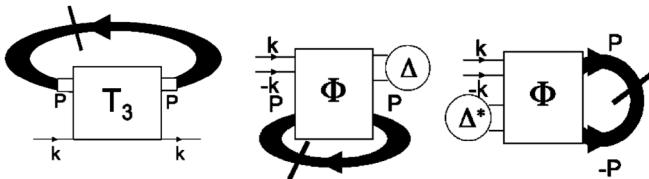
FIG. 3.   Collective mode contributions to the self-energies.

with $n_{cm} = (m^{3/2}/8\pi)\sum_P \Gamma(P)/[2|\mu| + \mathbf{P}^2/4m - \Omega]^{1/2}$. The Ω integration can be transformed over a contour which encloses all the singularities of $\Gamma(P)$ on the real negative axis. The high energy contributions to n_{cm} coming from $|\Omega| \gtrsim 1/ma^2$ (physically linked to breaking dimers) will give negligible regular terms of order Δ^4, as discussed above. On the other hand, the contribution of the low frequency collective mode is easily calculated with the low energy expression of $\Gamma(P)$ given above. We find

$$n_{cm} = \frac{1}{3\pi^2}(2m\mu_B)^{3/2} \qquad (15)$$

where we have used the zeroth order expression $E_b/2$ for $|\mu|$. When we use for μ_B its lowest order expression, we find that n_{cm} coincide with the "depletion of the condensate," known for elementary boson superfluids.

We proceed now in the same way for the collective mode contributions to the anomalous self-energy. Corresponding to the diagram Fig. 1(c), we have to add the two bottom diagrams in Fig. 3. Just as in Eq. (7) we should take only irreducible diagrams into account. But handling this problem in the same way by adding the reducible contributions on both sides of the equation, we end up with Eq. (8) except, in the right-hand side, for the additional contribution $\Delta G_0(k)G_0(-k)\Phi(k, -k; 0, 0)[\sum_P \Gamma(P) + (1/2)\sum_P \Gamma^a(P)]$. As in Eq. (7) the factor $1/2$ is topological. Then we follow the same procedure as after Eq. (8). As in the calculation of n_{cm}, we retain only in the summation over P the low energy contribution, the other ones giving higher order terms. The summation $\sum_P \Gamma(P)$ has already been found in the above calculation of n_{cm}. The summation $\sum_P \Gamma^a(P)$ is more involved since, as we mentioned below Eq. (14), we have to subtract from $\Gamma^a(P)$ the lower order terms already taken into account in our lowest order calculation, leading to Eq. (9). In contrast with the case of $\Gamma(P)$, the term we subtract is not zero, but acts to regularize the remaining integral over momentum $\mathbf{P}$, which would otherwise have a high momentum divergence [19]. We obtain for the slashed contribution, which takes into account this subtraction, $\sum_P \slashed{\Gamma}^a(P) = 3\sum_P \Gamma(P) = 24\pi n_{cm}(2m|\mu|)^{1/2}/m^2$.

If we gather all the contributions, we have for the single spin density $n = n_2 + n_{cm}$ while the gap equation [Eq. (9)] is changed into the simple form:

$$a^{-1} - \sqrt{2m|\mu|} = \frac{m^2 a^2}{8} a_M |\Delta|^2 + 5\pi a a_M n_{cm}. \qquad (16)$$

When $|\Delta|^2$ is eliminated between the gap and the number equations, the consistently expanded result for μ is indeed found to be Eq. (1).

In conclusion, we have shown how an exact purely fermionic framework can be used in the BEC regime of the BEC-BCS crossover, and we have demonstrated that the Lee-Huang-Yang result for the chemical potential remains valid for the corresponding composite bosons.

We are very grateful to M. Yu. Kagan for stimulating discussions at the beginning of this work.

[1] A. J. Leggett, J. Phys. (Paris), Colloq. **41,** C7-19 (1980).
[2] M. Greiner, C. Regal, and D. Jin, Nature (London) **426,** 537 (2003).
[3] S. Jochim *et al.*, Science **302,** 2101 (2003).
[4] M. W. Zwierlein *et al.*, Phys. Rev. Lett. **91,** 250401 (2003).
[5] T. Bourdel *et al.*, Phys. Rev. Lett. **93,** 050401 (2004).
[6] D. S. Petrov, C. Salomon, and G. V. Shlyapnikov, Phys. Rev. Lett. **93,** 090404 (2004).
[7] I. V. Brodsky *et al.*, Phys. Rev. A **73,** 032724 (2006).
[8] V. N. Popov, Sov. Phys. JETP **23,** 1034 (1966).
[9] L. V. Keldysh and A. N. Kozlov, Sov. Phys. JETP **27,** 521 (1968).
[10] P. Pieri and G. C. Strinati, Phys. Rev. Lett. **91,** 030401 (2003), and references therein for earlier work; in Phys. Rev. Lett. **96,** 150404 (2006) on polarized gases these authors included formally the 3-body and 4-body vertices in their gap equation to obtain the correct scattering lengths in the mean field terms.
[11] T. D. Lee and C. N. Yang, Phys. Rev. **105,** 1119 (1957); T. D. Lee, K. Huang, and C. N. Yang, Phys. Rev. **106,** 1135 (1957).
[12] Here we sketch the derivations. Details will be given in an extended version, in preparation.
[13] S. Stringari, Europhys. Lett. **65,** 749 (2004); Astrakharchik *et al.*, Phys. Rev. Lett. **95,** 030404 (2005); By contrast the LHY term was omitted for convenience by R. Combescot and X. Leyronas, Europhys. Lett. **68,** 762 (2004) since it was not yet firmly established.
[14] A. Altmeyer *et al.*, Phys. Rev. Lett. **98,** 040401 (2007).
[15] A. A. Abrikosov, L. P. Gorkov, and I. E. Dzyaloshinski, *Methods of Quantum Field Theory in Statistical Physics* (Dover, New York, 1975).
[16] J. Levinsen and V. Gurarie, Phys. Rev. A **73,** 053607 (2006).
[17] V. M. Galitskii, Sov. Phys. JETP **7,** 104 (1958).
[18] See R. Combescot, M. Yu. Kagan, and S. Stringari, Phys. Rev. A **74,** 042717 (2006) for a study of this mode, within the dynamical BCS theory (which gives $a_M = 2a$).
[19] This subtraction also removes an (imaginary) contribution arising from $T_4(0, 0; 0)$, due to the fact that it has to be evaluated at the chemical potential μ, which is not exactly half the bound state energy of the molecule. A similar feature is present in the approach of S. T. Beliaev, Sov. Phys. JETP **7,** 289 (1958) for elementary bosons. More generally there are necessarily, in our handling of the collective mode, clear links with Beliaev's work since this mode corresponds physically to the elementary boson excitations handled by Beliaev.